AWARD NUMBER: W81XWH18-1-0443

TITLE: The Role of Astrocytes and Microglia in Exercise-Induced Neuroplasticity in Parkinson's Disease

PRINCIPAL INVESTIGATOR: Michael W. Jakowec, PhD,

CONTRACTING ORGANIZATION: University of Southern California, Los Angeles, CA

REPORT DATE: October 2022

TYPE OF REPORT: Annual

PREPARED FOR: U.S. Army Medical Research and Development Command
Fort Detrick, Maryland, 21702-5012

REPORT DOCUMENTATION PAGE	*Form Approved OMB No. 0704-0188*

1. REPORT DATE	**2. REPORT TYPE**	**3. DATES COVERED**
October 2022	Annual	01Sep2021-31Aug2022

4. TITLE AND SUBTITLE

The Role of Astrocytes and Microglia in Exercise-Induced Neuroplasticity in Parkinson's Disease

5a. CONTRACT NUMBER

5b. GRANT NUMBER
W81XH-19-1-0443

5c. PROGRAM ELEMENT NUMBER

6. AUTHOR(S)
Michael W. Jakowec, PhD (PI)

E-Mail: mjakowec@surgery.usc.edu

5d. PROJECT NUMBER
PD180100

5e. TASK NUMBER

5f. WORK UNIT NUMBER

7. PERFORMING ORGANIZATION NAME(S) AND ADDRESS(ES)

1333 San Pablo St. MCA-241
Department of Neurology
University of Southern California,
LA, CA, 90033

8. PERFORMING ORGANIZATION REPORT NUMBER

9. SPONSORING / MONITORING AGENCY NAME(S) AND ADDRESS(ES)

U.S. Army Medical Research and Development Command
Fort Detrick, Maryland, 21702-5012

10. SPONSOR/MONITOR'S ACRONYM(S)

11. SPONSOR/MONITOR'S REPORTNUMBER(S)

12. DISTRIBUTION / AVAILABILITY STATEMENT

Approved for Public Release; Distribution Unlimited

13. SUPPLEMENTARY NOTES

14. ABSTRACT

Recent studies in our labs have implicated a role for glial cells (astrocytes and microglia) in exercise- induced synaptogenesis and synaptic repair. The primary goal of this application is to investigate the role of astrocytes, microglia and peripheral monocytes in regulating exercise induced synaptogenesis and behavioral recovery in Parkinson's disease. Studies in this application will explore region specific metabolic changes mediatedby exercise, using imaging tools and molecular biology approaches to determine the mechanistic roles of glial cells,metabolism and immune processes associated with exercise induced neuroplasticity and potential disease modification. **Specific Aim 1** will test the hypothesis that exercise induced astrocytic activation and elevated lactatemetabolism regulates synaptogenesis and behavioral recovery in an animal model of PD. **Specific Aim 2** will test the hypothesis that activation of anti-inflammatory resident microglia and infiltrating peripheral mononuclear cells regulate synaptogenesis in the striatum and Prefrontal cortex of exercised 6-OHDA mice. We will further test the hypothesis that anti- vs. pro-inflammatory serum immune soluble factors (cytokines and BDNF) are associated withexercise benefits in PD.

15. SUBJECT TERMS None listed.					
16. SECURITY CLASSIFICATION OF:			**17. LIMITATION OF ABSTRACT**	**18. NUMBER OF PAGES**	**19a. NAME OF RESPONSIBLE PERSON** USAMRDC
a. REPORT	**b. ABSTRACT**	**c. THIS PAGE**			**19b. TELEPHONE NUMBER** *(include area code)*
Unclassified	Unclassified	Unclassified	Unclassified	63	

Standard Form 298 (Rev. 8-98)
Prescribed by ANSI Std. Z39.18

TABLE OF CONTENTS

1. Introduction

Parkinson' disease (PD) is characterized by motor and non-motor (cognitive) impairments that lead to a progressive decline in quality of life (QoL) and increased morbidity. While there is no cure, research from our labs and others have demonstrated a role for exercise in improving motor/nonmotor features, QoL and repair of corticostriatal synaptic circuits). Recent studies in our labs have implicated a role for glial cells (astrocytes and microglia) in exercise-induced synaptogenesis and synaptic repair. It has long been known that activated glial cells accompany tissue damage in PD and contribute to an inflammatory cascade responsible for persistent injury that results in onset and progression of clinical disease. Astrocytes are essential for metabolic processes in the brain and are important in synaptic transmission. They couple multiple neurons and synapses into functional assemblies. Astrocytes also respond to increased synaptic neurotransmission via ability to sense extracellular concentrations of K^+ and glutamate. Neurons and astrocytes are metabolically coupled such that, even in the presence of cellular oxygen, astrocytes generate high levels of lactate through aerobic glycolysis and shuttle high-energy metabolites to neurons engaged in elevated synaptic activity. Astrocytes are also tightly associated with blood vessels and contribute to the blood brain barrier. In addition, synaptic loss and dysfunction, cell death, and neurite loss occurs in the presence of activated microglia, secretion of pro-inflammatory cytokines and chemokines, and recruitment of monocytes from the periphery. However, published studies and recent preliminary data from our lab have demonstrated that mechanisms capable of controlling pro-inflammatory activities in the CNS are induced by intensive exercise and involve production of anti-inflammatory cytokines (including the trophic factor BDNF), regional activation of microglia, and recruitment of monocytes with a "regulatory" phenotype to sites of synaptogenesis.

The primary goal of this application is to investigate the role of astrocytes, microglia and peripheral monocytes in regulating exercise induced synaptogenesis and behavioral recovery in PD. Studies in this application will explore region specific metabolic changes mediated by exercise, using imaging tools and molecular biology approaches to determine the mechanistic roles of glial cells, metabolism and immune processes associated with exercise induced neuroplasticity and potential disease modification.

Specific Aim 1 will test the hypothesis that exercise induced astrocytic activation and elevated lactate metabolism regulates synaptogenesis and behavioral recovery in an animal model of PD. This hypothesis is based on our preliminary data and recent reports demonstrating the importance of astrocytes and lactate metabolism in synaptic transmission, synaptogenesis and learning. We will also test whether exercise-induced changes in astrocytic activation and lactate metabolism is associated with increases in regional cerebral glucose uptake (rCGU) due to exercise. Studies will utilize a novel transgenic mouse model, established in our lab, which expresses astrocyte-specific red fluorescent protein tdTomato (ACT mouse) to isolate astrocytes. We have also developed a shRNA viral vector to selectively knock-down MCT-4, which we hypothesize to be critical for establishing the metabolic relationship between astrocytes and activated neuronal circuits through the ANLS.

Specific Aim 2 will test the hypothesis that activation of anti-inflammatory resident microglia and infiltrating peripheral mononuclear cells regulate synaptogenesis in the striatum and PFC of exercised 6-OHDA mice. We will further test the hypothesis that anti- vs. pro-inflammatory serum immune soluble factors (cytokines and BDNF) are associated with exercise benefits in PD. Our preliminary experiments in animals and pilot clinical study support this hypothesis. The CNS mononuclear cell population was more responsive to activation, which when cultured in the presence of stimuli secreted significantly higher amounts of IL-10, TGFβ, and BDNF suggesting enhancement of synaptic plasticity in these regions. processes are related to exercise benefits of cognitive function in physically (exercise) active PD subjects.

Impact: Studies from this application will (i) elucidate the role of glia in mediating exercise-induced neuroplasticity in PD and its models, (ii) support that changes in neuronal metabolism in conjunction with activation of astrocytes and microglia support improved synaptogenesis, leading to improved motor andcognitive behavior, and (iii) demonstrate how small energetic molecules like glucose and lactate in conjunction with components of the peripheral immune system (monocytes) link region-specific neuronal activation in the brain with non-neuronal cells (glia) at sites of circuitry activation. Understanding the mechanisms of exercise- induced neuroplasticity are critical to the development of strategies to treat patients suffering from degenerative brain disorders such as PD. Indeed, our studies in both animal models of PD and in patients with PD have led to widespread adoption of exercise and physical therapy as standard of care. The immediate impact of the studies in this application will shed additional mechanistic light on the benefits of exercise to reveal region specificity, allowing refinement of neurological physical therapy approaches. The long-term clinical impact will provide a framework for future clinical studies to determine if exercise (i) can modify diseaseprogression, (ii) can impact immune components to promote synaptogenesis and restoration of motor and cognitive circuits, and (iii) whether benefits can be enhanced by including additional components of a healthy

lifestyle, including diet, mindfulness, and stress management. Finally, it is possible that the data will reveal potential for the addition of supplemental pharmacological interventions designed to target astrocytes, microglia and components of the peripheral immune system), and interventions that modify metabolism.

2. KEYWORDS

Parkinson's disease, exercise, metabolism, astrocytes, immune system, microglia, 6-OHDA, cognition, neuroplasticity, synaptogenesis.

3. ACCOMPLISHMENTS IN YEAR 1

3.1. Major Goals

The Following Section 3.1. outlines the major scientific goals achieved during Year 1, 2 and 3. The Figure below highlights graphically the progress of the overall study. The Following Table lists the Statement of Word (SOW) with achievements in Year 1 to 3 highlighted in yellow. Following the Table are bullet points of major achievement and goals reached in Year 1 and Year 2.

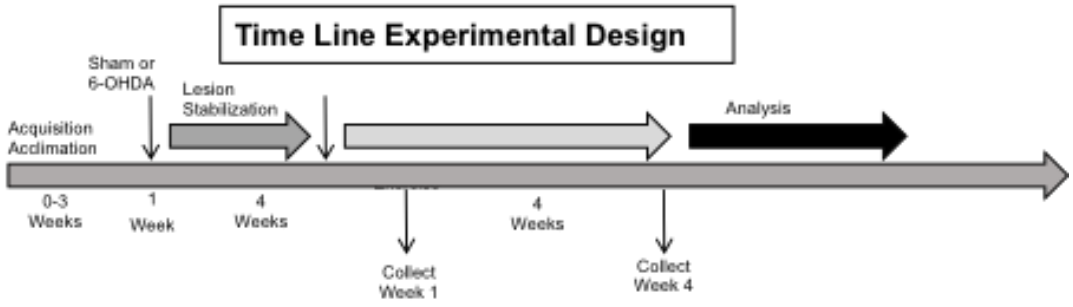

Specific Aim 1a	2DG/GFAP Analysis of Metabolism and Astrocyte Activation	Year 1-1.5
Specific Aim 1b	FACS Astrocytes/Gene Expression	Year 1.5 – 2.5
Specific Aim 1c	shRNA KD MCT-4 impact on Block of Exercise Benefits	Year 2 - 3
Specific Aim 2a	FACS Monocytes/Microglia Analysis	Year 1 - 3
Specific Aim 2b	Block Monocyte Infiltration to block Exercise Benefits	Year 2 - 3
Specific Aim 2c	Blood Samples from PD Patients for Cytokine Analysis	Year 1- 3

Lab 1 **University of Southern California**1333 San Pablo St. MCA-241/3/5 Los Angeles, CA 90033

PI: M. Jakowec (MJ)

Lab 2 **University of Southern California**
1333 San Pablo St. MCA-B6/8Los Angeles, CA 90033
Co-I: D. Holschneider/ Zhou Wang (DH/ZW)

Lab 3 **University of Southern California**
1333 San Pablo St., MCA-246Los Angeles, CA 90033

Co-PI: B. Lund (BL)Co-IP: W. Gilmore Co-PI: G. Petzinger

Tasks in Specific Aim 1a	Timeline	Lab

	Month	Group
Hiring and Training of Study Staff	All personnel are currently employed in labs	1, 2, 3
IACUC Approval for entire project (addendum to ongoing approved projects)	1	1, 2, 3
Milestone Achieved	2	1, 2, 3
6-OHDA lesioning of mice, stabilization of lesion, exercise regimen	2-6	1,2
2DG studies in Sham±exercise and 6-OHDA ± exercise mice	4-8	2
Milestone Achieved	8	1,2
GFAP analysis of astrocyte activation by IHC	4-8	1
Analysis of outcome data including correlation studies	8-9	1,2
Milestone Achieved	10	1,2
Analysis of data, completion of Aim 1b, report, publication, data storing	14	1,2
Tasks in Specific Aim 1b		
IACUC Approval for entire project (addendum to ongoing approved projects)	1	1,2
Milestone Achieved	2	1,2
6-OHDA lesioning of mice, stabilization of lesion, exercise regimen, breeding ACT mice	6-12	1,2
Construction and validation of ACT mouse	Completed	2
Milestone Achieved	Completed	2
FACS analysis of ACT mouse astrocytes	9-12 underway	2
Analysis of ACT astrocytes by qRT-PCR and RNAseq	10-14 underway	2
Milestone Achieved	14	2
Tasks in Specific Aim 1c		
Hiring and Training of Study Staff	All personnel are currently employed in labs	2
IACUC Approval for entire project (addendum to ongoing approved projects)	1	2
Milestone Achieved	2	2
6-OHDA lesioning of mice, stabilization of lesion, exercise regimen	14-18	2
Milestone Achieved	18	2
Construction of shRNA vector	Completed	2
Milestone Achieved	Completed	2
Validation of shRNA to KD MCT2 in astrocyte cultures	6	2
Milestone Achieved	8	2
Stereotaxic targeting of vector to mouse brain	14-18	2
Molecular and behavioral outcome measures	18-24	2

Analysis of data	20-24	2
Milestone Achieved	24-28	2
Tasks in Specific Aim 2a		
Hiring and Training of Study Staff	All personnel are currently employed in labs	3
IACUC Approval for entire project (addendum to ongoing approved projects)	1	3
Milestone Achieved	2	3
6-OHDA lesioning of mice, stabilization of lesion, exercise regimen	4-8	1, 3
FACS analysis microglia phenotype/function brain serum	8-18 underway	1, 3
Milestone Achieved	18	1, 3
Tasks in Specific Aim 2b		
Hiring and Training of Study Staff	All personnel are currently employed in labs	1, 3
IACUC Approval for entire project (addendum to ongoing approved projects)	1	1, 3
Milestone Achieved	2	1, 3
6-OHDA lesioning of mice, stabilization of lesion, exercise regimen	18-22	1
Blocking monocyte infiltration, behavioral molecular study of effects	24-28	1, 3

Milestone Achieved	30	1, 3
Tasks in Specific Aim 2c		
IRB approval of addendum to current protocol	1-2	3
Begin subject recruitment	Currently underway as part ofongoing IRB approved project	3
Collection of samples	6-24	3
Analysis of serum cytokines in PD patients at baseline, 9, 18 months	6-24	3
Milestone Achieved	24-30	3
Analysis of data, completion of Aim 2c, report, publication, data storing	36 underway	3
Tasks Overall		
Subtask 1: Coordinate with Data Core for monitoring data collection ratesand data quality	Every 6 months	1, 2, 3
Perform all analyses according to specifications, share output andfindings with all investigators	Every 6 months	1, 2, 3
Work with data core and dissemination of findings (abstracts,presentation, publications, DOD)		1, 2, 3
Completion of Studies	36	1, 2, 3

Major Goals Achieve in Year 1 through Year 3

Specific Aim 1a will test the hypothesis that exercise leads to increase regional Cerebral Glucose Uptake and astrocytic phenotypic activation. We will utilize [^{14}C]-2-deoxyglucose autoradiography mapping to measure glucose uptake in the brain and GFAP IHC as a phenotypic marker of astrocytic activation. This study is supported by our preliminary data showing exercise-related increase in astrocyte morphology consistent with activation. Adjacent brain slices will be used to examine for co-localization/correlation between increase in rCGU and astrocytic GFAP.

- Approval of IACUC for use of vertebrate animals. (Year 1)
- Conducting studies of [^{14}C]-2-deoxyglucose autoradiography mapping to measure glucose uptake in the brains of 6-OHDA mice subjected to exercise or that remain sedentary. All parameters for studies in Aim 1A are validated and currently underway. Brains have been harvested from non-lesioned mice with and without exercise and subjected to [^{14}C]-2-deoxyglucose autoradiography mapping. (Year 1)
- Significant number of 6-OHDA lesioned mice have been established to carryout studies in Aim 1. The site of the lesions in the basal ganglia have been verified with immunohistochemical staining for tyrosine hydroxylase. The impact of the 6-OHDA lesion in the dorsomedial stratum and its impact on motor and cognitive behaviors has been verified using rotarod, novel object recognition, open field, and pole test. (Year 1)
- **Year 2**: We have completed 2DG analysis of mice subjected to dopamine-depletion by 6-OHDA in the dorsal striatum and subjected to exercise training. This manuscript is now in preparation and will be submitted in mid-2022. For this Aim we are also utilizing published literature derived from the connectome analysis of the mouse brain. This allows significant expansion of the regions of interest throughout the basal ganglia, substantia nigra, and thalamus to develop higher resolution of connectivity in order to better evaluate circuit specific changes.
- **Year 3**: A manuscript has been submitted and is currently in review entitled Wang, Z., E. K. Donahue, Y. Guoa, M. Renteln, G. M. Petzinger, M. W. Jakowec, D. P. Holschneider. (2022) Exercise alters cortico-basal ganglia network connectivity: A mesoscopic level functional analysis informed by the mouse brain connectome. eLife, In Review
- Another manuscripts has been now published Wang, Z., A. J. Lundquist, E. Donahue, Y. Guo, D. Phillips, G. M. Petzinger, M. W. Jakowec, and D. P. Holschneider (2022) A mind in motion: Exercise improves cognitive flexibility, impulsivity, and alters dopamine receptor gene expression in a Parkinsonian rat model. Current Research in Neurobiology, In Press.
-

•

Specific Aim 1b will test the hypothesis that exercise leads to an increase of lactate metabolism of activated astrocytes in brain regions identified in SA1a and including PFC, dSTR, ERC, and vCB. Using our ACT transgenic mouse, FACS enrichment of astrocytes from these regions will be examined for expression of mRNA transcripts and proteins of interest including MCT-4 and LDHa and GLUT1 using qRT-PCR and WIB. We will also examine for astrocyte phenotype (S100A10, thrombospondin-1/2). (Year 1)

- Construction of the ART mouse expressing the red fluorescent protein tdTomato has been completed and validated using immunohistochemistry and microscopy. Currently these mice are continuing to be bred to achieve enough numbers to be used in studies as outlined in Year 2 of the research proposal. (Year 1)
- **Year 2**: Construction of the ART mouse has been achieved. Breeding continues to provide mice for subsequent Aims in Year 2 indicated below.
- **Year 2.5**: Adult mice of 10 weeks of age are now available for isolation of red fluorescent astrocytes. Our next upcoming phase will involve analysis of the RNA examining transcripts of interests that are astrocyte specific (GFAP, S100B, BDNF, Thrombospondin). These samples will then be subjected to RNASeq analysis to search for other transcript changes. These analyses will involve mice that have also been subjected to treadmill exercise. We will determine the efficiency of region-specific astrocytes comparing striatal (region of motor circuit activation) to cortical regions not involved in motor circuitry.
- **Year 3**: A major setback of the covid-19 pandemic was the shutdown of all research activity and loss of existing mouse inventory. We were forced to re-obtain starting mouse strains for the construction of the ART mouse expressing ref fluorescent protein exclusively in astrocytes. We initially attempted to re-establish this strain from our existing colony but due to aging they were not able to successfully breed to establish the needed transgenic lines. Over the summer of 2022 new mice have been breeding with success. We carried out a FACS analysis of red fluorescent astrocyte in mice to isolate astrocytes exclusively from the striatum. Cells were obtained and analyzed for astrocyte specific markers (GFAP, S100) and did not display markers or neurons or microglia using qRT-PCR. This approach was validated and will be utilized to complete the studies proposed in these Aims.

Specific Aim 1c will test the hypothesis that astrocyte mediated lactate transport is important in exercise-induced synaptogenesis. For these studies we have designed shRNA viral vector to selectively knock-down MCT-4 expression in astrocytes within the dSTR. Behavioral analysis will be conducted to examine recovery of motor and cognition. Molecular analysis will be used to quantitate synaptogenesis using IHC and Golgi. We will also test whether knock-down of MCT-4 leads to decreased expression of GLUT-1, and LDHa using qRT-PCR and WIB in the PFC and dSTR.

- Construction of the shRNA vector to knockdown MCT4 expression has been constructed and validated in both in vitro (astrocyte cell cultures) and in vivo (injections into the mouse striatum). (Year 1)
- Studies have been carried out addressing Aim 1B where ACT mice have been administered L-lactate and the activation of genes of interest involve in metabolism and neurotrophic factor expression have been evaluated. These studies have been complemented with in vitro studies in astrocyte cultures. A manuscript describing these outcome measures is currently in review. (Year 1)
- **Year 2:** We have carried out 2 studies targeting the knock-down of the L-lactate transporter MCT4. In the first study we injected the lentiviral vector carrying shRNA to knock-down MCT4 to the M1 of the motor cortex. Overall findings indicated no impact on MCT1 expression, astrocyte cell death, or neuronal cell death. However, we did observe changes in neuronal dendritic spine density in M1, reduced uptake of the glucose transport ligand 2-deoxyglucose, and deficits in motor learning (but no deficit in motor performance). These findings are described in a manuscript (Lundquist et al, 2022) that is in review following its initial review in the journal Molecular Neurobiology. The second study utilized the approach described in the first study except the lentiviral vector was injected into the dorsolateral striatum. Studies have shown similar findings to the targeting studies in the motor cortex in terms of gene expression and cell viability. Interestingly, we found that knock-down of MCT4 results in enhanced sensitivity to the neurotoxin MPTP where a mild lesion (a single injection of MPTP) shows increased dopamine depletion, and increased loss of tyrosine hydroxylase expression, the hallmark of basal ganglia integrity, at the site of MCT4 knock-down.
- **Year 3**: A manuscript reporting the impact of astrocyte Specific knockdown of MCT4 in the motor cortex has been published Lundquist, A. J., S. H. Kishi, G. N. Llewellyn, N. A. Jakowec, P. M. Cannon, G. M. Petzinger, and **M. W. Jakowec** (2022) Knockdown of astrocyte-specific monocarboxylate transporter-4 in the mouse striatum results in increased striatal dopamine levels and elevated sensitivity to the dopamine depleting neurotoxin 1-methyl-4-phenyl-1,2,3,6-tetrahydropyridine.

- Two additional manuscripts addressed in this Aim are in preparation and are about to be submitted for review including: Lundquist, A. J., S.H. Kishi, G. N. Llewellyn, N. A. Jakowec, P. M. Cannon, G. M. Petzinger, and M. W. Jakowec (2022) Knockdown of astrocyte-specific monocarboxylate transporter-4 in the mouse striatum results in increased striatal dopamine levels and elevated sensitivity to the dopamine depleting neurotoxin 1-methyl-4-phenyl-1,2,3,6-tetrahydropyridine. And a second Lundquist, A. J., D. Philips, G. N. Llewellyn, N. A. Jakowec, P. M. Cannon, G. M. Petzinger, and M. W. Jakowec (2022) Knock-down of striatal lasctate shuttle MCT4 results in elevated sensitivity to the dopamine depleting neurotoxin 1-methyl-4-phenyl-1,2,3,6-tetrahydropyridine

Specific Aim 2a will test the hypothesis that exercise leads to the activation of anti-inflammatory microglia in the STR and PFC. This Aim will utilize FACS analysis phenotypically identify and examine functional capacity as well as identifying infiltrating cells derived from peripheral blood.

- Mice to be used in this study have been constructed and validated. (Year 1)
- We have validated the FACS approach to be used in these studies. This Aim will be carried out in Year 2. (Year 1)
- **Year 2**: We have bred the ART mouse to now allow us to conduct FACS analysis on a subset of cell. We will compare total brain with samples of tissues from the striatum and cortex. We will examine know genes of interest using qRT-PCR, which requires less starting material, and then test FACS to determine the threshold of sensitivity for determination of changes in gene expression.
- **Year 3**: As indicated above this strain has been re-established and validated for these studies.

Specific Aim 2b will test the hypothesis that peripheral monocyte infiltration to the STR and PFC may regulate exercise-induced synaptogenesis and behavioral recovery. To test this hypothesis, we will block peripheral monocyte infiltration using Natalizumab, an inhibitor of integrin a4β1. We will use Golgi staining for dendritic spine density and IHC for markers of synaptogenesis (PSD95, synaptophysin) at the termination of the exercise intervention. Analysis will be conducted in the STR and PFC. We will conduct behavioral analysis of motor and cognitive function at completion of exercise.

- We have established and validated the 6-OHDA lesioning of mice for this aim. Studies are underway forYear 2 to determine infiltration of peripheral monocytes to the striatum and to determine if blocking the integrin receptor will block exercise-enhanced uptake to the striatum. (Year 1)
- **Year 2:** We pursued the analysis of the integrity of the BBB through several methods to complement the approach to examine the changes in BBB and the ability of cell to cross from the periphery to the brain. Using mice that have been lesioned with the dopamine -depleting neurotoxin MPTP and with the addition of exercise we have examined the patter of expression of proteins involved in tight junctions including occludin, and claudin. In addition, we have initiated studies to examine the integrity of the BBB in terms of its permeability to large molecules including Evans Blue and sodium fluorescein. Methods for these analyses are now in characterization and validation phases.
- **Year 2.5**: We are in the process of writing a manuscript showing infiltration of peripheral macrophages into the striatum of mice subjected to dopamine-depletion and treadmill exercise.
- **Year 3**: We have completed analysis of CNS microglia and infiltrating macrophages in mice subjected to dopamine-depletion with MPTP and exercise. Studies have shown that exercise leads to an increase in peripheral infiltrating macrophages that take on an anti-inflammatory phenotype in the injured brain. This manuscript is now near completion.

Specific Aim 2c will test the hypothesis that an increased level of serum anti-inflammatory (IL-10, TGFβ, and BDNF) vs. pro-inflammatory cytokines (TNFα, IL-1β, IL-6, and IL-2) is associated with higher levels of exercise intensity (average total METS/hr./week) and fitness levels (motor and/or cardiovascular) over an 18-month period in PD subjects. We will also examine whether increase level of serum anti-inflammatory vs. pro- inflammatory cytokines are associated with higher cognitive (executive function, EF) function at baseline, 9 and18 months of follow up.

- Addendum to IRB (PI: Dr. G. M. Petzinger, MD) to conduct blood collection and analysis of samples outlined in Specific Aim 2. (Year 1)
- Blood Samples are being analyzed for the presence of immune markers at the early time point (baseline) and we have completed the analysis of 46 samples (baseline) 20 samples (9 months) and 14 samples (18 months). Data are currently undergoing analyses and statistical validation. (Year 1)

- **Year 2**: Blood samples have been analyzed. A subset of these data are included in a manuscript in preparation Donahue et al 2022 (Listed below in Publications).
- **Year 2.5**: Overall we have examined 26 serum markers in patients with PD and conducted correlation and regression studies against cognition and fitness. We will publish these data as their own manuscript in 2022 that is now in progress. the section below highlights the major findings.
- **Year 3**: All data for analysis has been collected. Final analysis of the relationship between immune markers, cognition, and fitness, are now underway and should be completed in early 2023. A manuscripts describing these findings will be published in early 2023.

Table 1: Bivariate correlations between moderate to vigorous physical activity minutes per day and blood solutes

	r	*p*
IL-1β	-.068	.605
IL-6	-.148	.250
IL-10	.432**	<.001
Leptin	-.395**	.001
MIP-1β	.303*	.017
TNF-α	.070	.588

Legend to Table 1: Correlation table showing the Pearson correlation coefficient and *p*-values of the relationship between moderate to vigorous physical activity (MVPA) and aging, inflammation, and Parkinson's disease associated blood-solute levels (N = 62). Abbreviations: IL-1β: interleukin-1β; IL-6: interleukin-6; IL-10: interleukin-10; MIP1β: macrophage inflammatory protein 1β; MVPA: moderate to vigorous activity (as recorded by wearable device); TNFα: tumor necrosis factor α.

Table 2: Adjusted associated between minutes of moderate to vigorous physical activity per day and blood-solutes

		95% CI	
	β	Lower, Upper	*p*
IL-10	.090**	.039, .141	<.001
Leptin	-.019	-.038, .000	.055
MIP-1β	.023*	.004, .043	.021

Legend to Table 2: Associations between number of minutes engaged in moderate to vigorous physical activity (MVPA) per day and disease-associated blood solute levels that were significant in correlations (N = 62). Adjusted associations represent the effect of one minute increase in moderate to vigorous physical activity on z-score standardized immune factor concentrations, adjusted for age, sex, UPDRS motor score, and average minutes of self-reported structured exercise per day as reported on a seven-day exercise diary. Abbreviations: IL-1β: interleukin-1β; IL-6: interleukin-6; IL-10: interleukin-10; MIP1β: macrophage inflammatory protein 1β; MVPA: moderate to vigorous activity (as recorded by wearable device); TNFα: tumor necrosis factor α.

Methods: Blood was collected from 62 participants and plasma analyzed for Macrophage Inflammatory Protein-1β (MIP-1β), Interleukin-10 (IL-10) (BD Biosciences, San Diego, CA, Cat # 558288, 558274); Interleukin-1β (IL-1β) (BD Biosciences, Cat #561509); Interleukin-6 (IL-6), Leptin, Tumor Necrosis Factor-α (TNFα) (Milliplex, Cat # HBNMAG-51K, Billerica MA), and were assessed as previously described. Concentration determinations were performed using Masterplex software (v2.0.0.62). Results were natural log-transformed to ensure normal distribution of data. Analytes are presented as pg/ml.

Results: Immunological factors examined are shown in **Table 1**. There was a significant positive association between MVPA and IL-10 (r(60) = 0.432, *p* = <0.001) and MIP-1β (r(60) = 0.303, *p* = 0.017). There was a significant negative association between MVPA and Leptin (r(60) = -0.395, *p* = 0.001). After controlling for age, sex, UPDRS motor score, and duration of self-reported exercise, there remained a significant association between MVPA and IL-10 (unstandardized β= 0.090, 95% CI [0.039, 0.141], *p* = <0.001) and MIP-1β (unstandardized β= 0.023, 95% CI [0.004, 0.043], *p* = *0*.021), and a trend for Leptin (unstandardized β= -0.019, 95% CI [-0.038, 0.000], *p* = .055).

Discussion: Examining the effects of PA on immune markers that may promote neuroplasticity, we found that higher time spent in MVPA was associated with increased levels of anti-inflammatory IL-10 and the chemoattractant MIP-1β, and a trend towards decreased levels of pro-inflammatory leptin. Increased serum IL-10 has been associated with milder PD symptoms. IL-10 is a global regulator of inflammation, and in addition to its role suppressing damaging inflammatory processes is thought to exert neuroprotective effects in the CNS.[32] Our findings with Il-10 are consistent with the exercise-associated enhancement of anti-inflammatory response. While less is known about MIP-1b in the context of exercise and PD, it is a chemoattractant molecule that could serve to recruit cells important for injury and repair, particularly CD4+ T cells important in targeted immune response, which are a major source of IL-10. In addition, leptin plays a regulatory role in global inflammation by initiating a pro-inflammatory response, and our observed trend towards MVPA-mediated reduction of leptin may result in decreased inflammation.

3.2. Opportunities for Training and Professional Development Provided by Project

This project has provided the following opportunities for training and development.

- Research electives for 8 undergraduate students.
- Components of this project and data collection will be part of the doctoral thesis work of 3 USC doctoral students in the USC Neuroscience Graduate Program.
- One of the 3 graduate students supported in this project has graduate and he is currently Director of Neuroscience Discovery at BioAge in Alameda CA.
- A new graduate student has been added to this study (Derek Phillips).
- In Year 2.5, three new undergraduate students have been added to the lab to participate in studies in this proposal.
- In Year 3 the two graduate students supported by this research proposal will competed all data collection, analysis, and will participate in the writing and publication of the findings. The graduate students have presented some of their findings at the Society for Neuroscience Annual Meeting in San Diego November 12-17, 2023.

3.3. Results Disseminated to Communities of Interest

Findings from this research study have been disseminated to the scientific research community through published manuscript (listed). In addition, findings on the impact of exercise on brain health are used as a foundation for describing these studies and their translation to the medical and patient community at seminars for patients and support groups.

3.4. Plans During the Next Reporting Period

In Year 2.5 to 3 we will:

- Complete glucose uptake mapping in lesioned and non-lesioned mice with and without exerciseto identify regions of greatest activity and is now reported in a manuscript in preparation.
- Utilizer FACS to identify genes and proteins in astrocytes whose expression is altered with exercise and 6-OHDA-lesioning. At the writing of this report we have generated adult mice expressing astrocyte specific red dTomato fluorescence for sorting.
- Determination the impact of administration of L-lactate on gene and protein expression in our rodent modelof PD has been reported in a manuscript (Lundquist et al., 2021). Cell culture studies are used to validate this approach.
- Determine of blocking lactate transport leads to the attenuation of exercise-enhanced benefits in our mouse model of PD at both the motor cortex and striatum are reported in 2 manuscripts (Lundquist et al., 2022).
- Continue to examine the alterations in infiltrating monocytes observed with exercise in the brain of our mouse model of PD.
- Analyzed the collect blood from patients with PD to conduct analysis of immune components

and correlate them with disease and fitness levels. A subset of these data are reported in Donahue et al, 2022 (in preparation) and the complete analysis will be reported in a manuscript in 2022. In Year 3 we will complete a longitudinal study of blood markers.

- After Year 3 during the no cost extension period we will complete experimental in all Aims and complete analysis. Manuscript will be completed and submitted for peer review. It is expected that all studies and reports will be completed in this time period.

4. IMPACT

This application has immediate and long-term clinical and scientific impact. Studies from this application will (i) elucidate the role of glia in mediating exercise-induced neuroplasticity in PD and its models, (ii) support that changes in neuronal metabolism in conjunction with activation of astrocytes and microglia support improved synaptogenesis, leading to improved motor and cognitive behavior, and (iii) demonstrate how small energetic molecules like glucose and lactate in conjunction with components of the peripheral immune system (monocytes) link region-specific neuronal activation in the brain with non-neuronal cells (glia) at sites of circuitry activation. Understanding the mechanisms of exercise-induced neuroplasticity are critical to thedevelopment of strategies to treat patients suffering from degenerative brain disorders such as PD. Indeed, ourstudies in both animal models of PD and in patients with PD have led to widespread adoption of exercise and physical therapy as standard of care. The immediate impact of the studies in this application will shedadditional mechanistic light on the benefits of exercise to reveal region specificity, allowing refinement of neurological physical therapy approaches. The long-term clinical impact will provide a framework for future clinical studies to determine if exercise (i) can modify disease progression, (ii) can impact immune componentsto promote synaptogenesis and restoration of motor and cognitive circuits, and (iii) whether benefits can be enhanced by including additional components of a healthy lifestyle, including diet, mindfulness, and stress management. Finally, it is possible that the data will reveal potential for the addition of supplemental pharmacological interventions designed to target astrocytes, microglia and components of the peripheral immune system), and interventions that modify metabolism.

Scientific Impact: Animal research over the past decade has shown that exercise and the way it is performed matters to neuro-rehabilitative outcomes, with changes in neuronal sprouting, restructuring of synapses and angiogenesis dependent. The current animal study provides a framework for understanding exercise-induced mechanisms of neuroplasticity at the regional level by examining synaptogenesis and metabolism and their influence on dopaminergic neurotransmission. An exciting aspect of this application is that it begins to investigate underlying mechanisms of exercise in animal models of PD and introduces astrocytes and microglia as important players in these processes including their impact on neuronal circuitry. Studies from thisapplication will (i) elucidate the role of glia in mediating exercise-induced neuroplasticity in PD and its models,

(ii) support that changes in neuronal metabolism in conjunction with activation of astrocytes and microglia support improved synaptogenesis leading to improved motor and cognitive behavior, and (iii) demonstrate how small energetic molecules like glucose and lactate in conjunction with components of the peripheral immune system (monocytes) link region-specific neuronal activation in the brain with non-neuronal cells (glia) at sites of circuitry activation. While the majority of the proposed studies are in young male animals, future studies can be designed to explore the impact of aging and sex in mediating the benefits of exercise in animal models. Also, benefits of exercise seen in our PD models may also show benefits in other models of disease and serve as an avenue to investigate these same phenomena in other human neurodegenerative disorders. Studies outlined in this application will begin to tease apart more specifically how non-neuronal components are impacted by exercise may be driving differential biological changes in brain circuitry, and in doing so also provides needed insights toward biomarkers that may be critical for future clinical studies to monitor exercise benefits.

Clinical Impact on Patients and Health Care Performance: The proposed application has the potential to lead to improvements in the efficacy of care for individuals with cognitive and motor impairment in PD by more specifically identifying mechanisms underlying and impacting the exercise prescription. This application examines exercise in a novel way by recognizing critical gaps that once addressed will greatly improve the efficiency of health care delivery such as (i) defining the patient characteristics (immune health, diet) that will be directly impacted by exercise; (ii) establishing the specific molecular and metabolic characteristics that are critical for improving and evaluating the impact and benefits of exercise in patients with PD, and (iv) may provide a biomarker for disease progression and its modification. Understanding the mechanisms of exercise- induced neuroplasticity is critical to further develop important therapeutic modalities for patients suffering from degenerative brain disorders such as PD. Studies from our labs over the past 16 years in both animal models

of PD and in patients suffering from PD have led to the wide-spread application of exercise and physical therapy as a component of the current standard of care. Improved quality of life with improved cognitive performance will reduce falls, reduce the burden on healthcare providers, and certainly reduce the economic burden. Findings from this application can be leveraged to begin to apply exercise as a viable evidence-based -treatment to modify other disorders of cognitive impairment and/or deficits in EF, including Alzheimer's disease, Huntington disease, schizophrenia, and traumatic brain injury. Studies in this application will provide important evidence-based data to allow neurologists and general internists to be able to prescribe a more precise form of exercise that targets cognition. Currently, physical therapy and exercise are not standard of care, and therefore not supported by most insurance policies. With information from this study, patients will be more empowered to take control of their personal treatment. The knowledge of a non-pharmacological and low-risk intervention falls within each individual's ability to control. Knowing they can truly impact their quality of life and disease progression, this will provide patients with a much-needed sense of self-empowerment and hope.

4.1. Impact on the Development of the Principal Disciplines of the Project

Studies in this research program are all underway. There are no technical or logistic issues to impede it progress. Findings from this program will demonstrate the important link between glia (astrocytes and microglia) and exercise-enhanced neuroplasticity in a rodent model of Parkinson's disease. We intend to demonstrate the important role played by astrocytes to regulate neuroplasticity especially through the transportof L-lactate that can act both as a metabolic substrate and a signaling molecular to strengthen synaptogenesis.We also aim to link microglia and peripheral monocytes as mediators of the immune response in playing a role in enhancing synaptogenesis and repair of neuronal circuits damaged in Parkinson's disease. The outcome measures of synaptic repair are demonstrated by recovery of both cognitive and motor behaviors in our models.

4.2. Impact on Other Disciplines

As pointed out in the Impact statements in this report the findings from this research program will impact our understanding of a wide spectrum of fields including neuroscience, physical therapy, disease progression in Parkinson's disease, and if such approaches can be implicated to alter disease progression. These studies will continue to implicate the importance of immunology in brain function as well as bringing together neuroscience, immunology, physical therapy, and clinical care.

4.3. Impact on Technology Transfer

Nothing to Report

4.4. Impact on Society Beyond Science and Technology

Findings in this research program will help guide our understanding of the role of exercise and physical therapy in treating neurodegenerative disorders including PD. For example, evidence medicine based on our outcome measures will provide additional support to guide clinicians, caregivers, and patients in the utility of exercise as an essential component of the first line of treatment and standard of care. It will also provide rationale for pharmaceutical and biotechnology companies to identify novel important therapeutic targets to enhance our findings and to find approaches for patients for which exercise may be challenging or difficult.

5. CHANGES / PROBLEMS

5.1. Changes in approach

Nothing to Report

5.2. Actual or Anticipated problems or delays and actions or plans to resolve

Due to COVID-19 outbreak the USC campus was closed to research personnel from March 13 to June 10. However, during this time all personnel were able to continue their responsibilities as outlined in the proposal. Breeding was allowed to continue such that there would be no loss of mice dedicated to these studies. However, some mice subjected to 6-OHDA lesioning just prior to the shutdown did not enter studies upon completion. We were able to utilize mice at 3 months post-lesion and match them to aged controls. The labwas allowed to reopen at 50% occupancy June 10^{th,} and this allowed proposed studies to commence. With careful planning and dedication of all researchers in this proposal we do not anticipate a significant delay other than possibly 3 or 4 months in the timeline. During this period, we were able to write and submit several manuscript supported by this application.

As outlined above we have repurchased from JAX laboratories and re-established our colony of mice expressing red fluorescent Tomato in astrocytes. This delay caused by the Covid-19 pandemic has only subjected these studies to a short delay and now studies has resumed without significant loss of time or outcome measures.

5.3. Changes that had a significant impact on Expenditures

Nothing to Report

5.4. Significant Changes in Use or Care of Human Subject, Vertebrate animal, Biohazards, or select Agents.

Nothing to Report

5.4.1. Significant Changes in Use or Care of Human Subjects.

Nothing to Report

5.4.2. Significant Changes in Use or Care of Vertebrate animals.

Nothing to Report

5.4.3. Significant Changes in Biohazards.

Nothing to Report

5.4.4. Significant Changes in Select Agents.

Nothing to Report

6. PRODUCTS

6.1. Journal Publications

Lundquist, A.J., J. Parizher, G.M. Petzinger, and M.W. Jakowec, Exercise induces region-specific remodeling of astrocyte morphology and reactive astrocyte gene expression patterns in male mice. J Neurosci Res, 2019. 97(9): p. 1081-1094. PMID: 31175682

Lundquist, A. J., T. J. Gallagher, G. M. Petzinger, and M. W. Jakowec (2021) Exogenous l-lactate promotes astrocyte plasticity but is not sufficient for enhancing striatal synaptogenesis or motor behavior in mice. Journal of Neuroscience Research. 99(5):1433-1447. doi: 10.1002/jnr.24804. Epub 2021 Feb 25. PMID: 33629362

Wang, Z., I. Flores, E. K. Donahue, A. J. Lundquist, Y. Guo, G. M. Petzinger, M. W. Jakowec, and D. P.

Holschneider (2020) Cognitive Flexibility Deficits in Rats with Dorsomedial Striatal 6-OHDA Lesions Tested Using a 3-Choice Serial Reaction Time Task with Reversal Learning. NeuroReport PMID: 32881776.

Caldwell, C. C, G. M. Petzinger, M. W. Jakowec, and E. Cadenas (2019) Treadmill Exercise Rescues Mitochondrial Function and Motor Behavior in a CAG140 Knock-In Advanced Huntington's Disease Mouse Model. Chem Biol Interact. 2019 Nov 26; 315:108907. doi: 10.1016/j.cbi.2019.108907. [Epub ahead of print] PMID: 31778667

Lundquist, A.J., G. N. Llewellyn, S. H. Kishi, N. A. Jakowec, P. M. Cannon, G. M. Petzinger, and M. W. Jakowec (2022) Knockdown of astrocytic monocarboxylate transporter 4 (MCT4) in the motor cortex leads to loss of dendritic spines and a deficit in motor learning. Molecular Neurobiology, In Resubmission.

Lundquist, A.J., G. N. Llewellyn, S. H. Kishi, N. A. Jakowec, P. M. Cannon, G. M. Petzinger, and M. W. Jakowec (2022) Knockdown of astrocyte-specific monocarboxylate transporter-4 in the mouse striatum results in increased striatal dopamine levels and elevated sensitivity to the dopamine depleting neurotoxin 1-methyl-4-phenyl-1,2,3,6-tetrahydropyridine. Mol Neurobiol. 2022 Feb;59(2):1002-1017. doi: 10.1007/s12035-021-02651-z. Epub 2021 Nov 25. PMID: 34822124.

Donahue, E.K., S. Venkadesh, V. Bui, D. Schiehser, R. Foreman, R. Wang, D. Haase, J. Duran, A. Petkus, B. Lund, D. Wing, M. Higgins, D. Holschneider, M. W. Jakowec, J. D. Van Horn, G. M. Petzinger (2022) Moderate to Vigorous Physical Activity is associated with better Memory, Executive Function, and Global Cognitive Function in Parkinson's Disease: A cross-sectional neuropsychological, immune, and neuroimaging study. In Preparation.

Wang, Z., A. J. Lundquist, E. Donahue, D. Phillips, G. M. Petzinger, M. W. Jakowec, and D. Holschneider (2022) A mind in motion: Exercise improves cognitive flexibility, impulsivity and alters dopamine receptor gene expression in a Parkinsonian rat model. In Press, Current Research in Neurobiology.

Wang, Z., E. K. Donahue, Y. Guoa, M. Renteln, G. M. Petzinger, M. W. Jakowec, D. P. Holschneider. (2022) Exercise alters cortico-basal ganglia network connectivity: A mesoscopic level functional analysis informed by the mouse brain connectome. eLife, In Review

Donahue, E. K., S. Venkadesh, V. Bui, R. Forman A. C. Tuaczon, R. K. Wang, D. Haase, R. J. Forman, J. J. Duran, Petkus, D. Wing, M. Higgins, D. Holschneider, E. Bayram, I. Litvan, **M. W. Jakowec**, J. D. Van Horn, D. M. Schiehser, G. M. Petzinger. (2022) Physical activity intensity is associated with cognition and functional connectivity in Parkinson's disease. Parkinsonism and Related Disorders. 24;104:7-14. doi: 10.1016/j.parkreldis.2022.09.005. PMID: 36191358.

Garbin, A., J. Díaz, V. Bu, J. Morrison, B. E. Fisher, C. Palacios, I. Estrada-Darley, D. Haase, D. Wing, L. Amezcua, M. W. Jakowec, C. Kaplan, G. M. Petzinger (2022) Promoting Physical Activity in a Spanish-Speaking Latina Population of Low Socioeconomic Status with Chronic Neurological Disorders: Proof-of-Concept Study. JMIR Form Res. 20;6(4):e34312. doi: 10.2196/34312. PMID: 35442197.

(1) Donahue, E. K., V. Bui, R. P. Foreman, J. J. Duran, S. Venkadesh, J. Choupan, J. D. Van Horn, J. R. Alger, M. W. Jakowec, G. M. Petzinger, and J. O'Neill. (2022) Magnetic resonance spectroscopy showing the association between neurometabolite levels and perivascular spaces in Parkinson's Disease: A pilot and feasibility study. NeuroReport, 33(7):291-296.doi: 10.1097/WNR.0000000000001781. Epub 2022 Apr 8. PMID: 35594442.

6.2. Conferences and Presentations

Lundquist, A.J., G. N. Llewellyn, S. H. Kishi, N. A. Jakowec, P. M. Cannon, G. M. Petzinger, and M. W. Jakowec (2021) Knockdown of astrocytic monocarboxylate transporter 4 (MCT4) in the motor cortex leads to loss of dendritic spines and a deficit in motor learning. Gordon Research Conference, Astrocytes, April 2021.

Jakowec, M.W., D. Philips, G. Petzinger, P. Cohen, and S. J. Kim (2022) Administration of the small humanin-

like mitochondria proteins SHLP2 and SHLP4-K4R provides neuroprotection and neurorestoration against the dopamine-depleting neurotoxin MPTP. Society for Neuroscience Annual Meeting, San Diego, CA.

Phillips, D., A. J. Lundquist, S. Kishi, G. M. Petzinger, and M. W. Jakowec (2022) Astrocyte regulation of dopamine transmission in the basal ganglia through lactate shuttling. Society for Neuroscience Annual Meeting, San Diego, CA.

Foreman, R., E. K. Donahue, S. Venkadesh, V. Bui, D. Wing, A. Petkus, B. Lund, I. Litvan, E. Bayram, J. Van Horn, M. W. Jakowec, D> Schiehser, and G. M. Petzinger, (2022) Physical activity intensity is associated with cognition, connectivity, and blood solutes in Parkinson's disease. Society for Neuroscience Annual Meeting, San Diego, CA.

Jakowec, M. W., D. Phillips, E. K. Donahue, A. J. Lundquist, Z. Wang, D. P. Holschneider, and G. M. Petzinger (2022) he role of astrocytes and L-lactate in Parkinson's disease and exercise-induced neuroplasticity. Cold Spring Harbor Laboratory Meetings, Neurodegenerative Diseases: Biology and Therapeutics, Cold Spring Harbor, N.Y.

6.3. Technologies or Techniques

Nothing to Report

6.4. Inventions, Patent Application, Licenses

Nothing to Report

6.5. Other Products

Nothing to Report

7. PARTICIPANTS & OTHER COLLABORATING ORGANIZATIONS

7.1. Individuals that Worked on the Project.

Name: Michael Jakowec, Ph.D.
Project Role: PI
Research Identifier: N/A
Nearest person month worked: 2.4 Mo
Contribution to the project: No change. Project design, directing molecular, histology, and neuroanatomic studies.

Name: Daniel P. Holschneider, MD Project
Role: partnering co-I Research Identifier:
N/A
Nearest person month worked: 2.0 Mo
Contribution to the project: No change. Project design, project management, directing functional brain mapping studies, data analysis.

Name: Brett Lund, PhD
Project Role: co-I
Research Identifier: N/A
Nearest person month worked: 2.16 Mo
Contribution to the project: No change. Project design, project management, directing immune components, data analysis.

Name: Zhuo Wang, Ph.D.
Project Role: co-I

Research Identifier: N/A
Nearest person month worked: 4.2 Mo
Contribution to the project: No change. Stereotaxic lesioning, directing operant studies, functional brain mapping, data analysis.

Name: Giselle M. Petzinger, MD
Project Role: co-I Research Identifier: N/A
Nearest person month worked: 0.36 Mo
Contribution to the project: No change. Project design, data analysis, interpretations, alternative approaches.

Name: Yumei Guo, MS
Project Role: Staff
Research Identifier: N/A
Nearest person month worked: 7.0 Mo
Contribution to the project: No change. Skilled and nonskilled exercising of animals, immunohistochemical staining (tyrosine hydroxylase).

Name: Adam Lundquist, BS
Project Role: Graduate Student
Research Identifier:
Nearest person month worked: 5.0 Mo
Contribution to the project: Western blotting, qRT-PCR, brain dissection, data analysis.

Name: Erin Donahue, BS
Project Role: Graduate Student
Research Identifier:
Nearest person month worked: 5.0 Mo
Contribution to the project: Blood analysis, Animal behavior, Western blotting, qRT-PCR, brain dissection, data analysis

Name: Derek Phillips, BS
Project Role: Graduate student
Research Identifier:
Nearest person month worked: 1.5 Mo
Contribution to the project: immunohistochemistry, behavioral testing, brain dissection

Name: Enrique Cadenas, Ph.D.
Project Role: Collaborator
Research Identifier: N/A
Nearest person month worked: 0.12 Mo
Contribution to the project: No change. Advisement on interpretation of molecular biologic studies

Name: Wendy Gilmore, Ph.D.
Project Role: Collaborator
Research Identifier: N/A
Nearest person month worked: 0.12 Mo
Contribution to the project: No change. Advisement on interpretation of immune studies

7.2. Changes in Active Support for PI or Senior Key Personnel

Nothing to Report regarding Key Personnel.

Note: The Graduate Student Derek Phillips has been added to this study. The graduate student Adam Lundquist graduated in summer 2021 and his responsibilities have been taken over by Derek Phillips.

7.3. Other Organizations Involved as Partners

Nothing to Report

8. SPECIAL REPORTING REQUIREMENTS

None

9. APPENDICES

New Manuscript added Annual Report 3
New Abstracts added in Annual Report 3
No New manuscripts added to Annual Report 2.
Four manuscripts were included in Annual Report Year 1.
Two manuscripts are currently in preparation of the Final Publication Proofs will be added to the next annual report.
Four manuscripts in preparation are not included until submitted for review.

Current Research in Neurobiology 3 (2022) 100039

Contents lists available at ScienceDirect

Current Research in Neurobiology

journal homepage: www.sciencedirect.com/journal/current-research-in-neurobiology

A mind in motion: Exercise improves cognitive flexibility, impulsivity and alters dopamine receptor gene expression in a Parkinsonian rat model

Wang Zhuo [c,1], Adam J. Lundquist [b,1], Erin K. Donahue [b], Yumei Guo [c], Derek Phillips [b], Giselle M. Petzinger [a,b], Michael W. Jakowec [a,b,2], Daniel P. Holschneider [a,b,c,*,2]

[a] Department of Neurology, University of Southern California, 1333 San Pablo St., Los Angeles, CA, 90033, USA
[b] Neuroscience Graduate Program, University of Southern California, Los Angeles, CA, 90089, USA
[c] Department of Psychiatry and the Behavioral Sciences, University of Southern California, 1333 San Pablo St., Los Angeles, CA, 90033, USA

A B S T R A C T

Cognitive impairment, particularly deficits in executive function (EF) is common in Parkinson's disease (PD) and may lead to dementia. There are currently no effective treatments for cognitive impairment. Work from our lab and others has shown that physical exercise may improve motor performance in PD but its role in cognitive function remains poorly eludicated. In this study in a rodent model of PD, we sought to examine whether exercise improves cognitive processing and flexibility, important features of EF. Rats received 6-hydroxydopamine lesions of the bilateral striatum (caudate-putamen, CPu), specifically the dorsomedial CPu, a brain region central to EF. Rats were exercised on motorized running wheels or horizontal treadmills for 6–12 weeks. EF-related behaviors including attention and processing, as well as flexibility (inhibition) were evaluated using either an operant 3-choice serial reaction time task (3-CSRT) with rule reversal (3-CSRT-R), or a T-maze task with reversal. Changes in striatal transcript expression of dopamine receptors (*Drd1-4*) and synaptic proteins (*Synaptophysin, PSD-95)* were separately examined following 4 weeks of exercise in a subset of rats. Exercise/Lesion rats showed a modest, yet significant improvement in processing-related response accuracy in the 3-CSRT-R and T-maze, as well as a significant improvement in cognitive flexibility as assessed by inhibitory aptitude in the 3-CSRT-R. By four weeks, exercise also elicited increased expression of *Drd1*, *Drd3*, *Drd4, synaptophysin, and PSD-95* in the dorsomedial and dorsolateral CPu. Our results underscore the observation that exercise, in addition to improving motor function may benefit cognitive performance, specifically EF, and that early changes (by 4 weeks) in CPu dopamine modulation and synaptic connectivity may underlie these benefits.

1. Introduction

Parkinson's disease (PD) is a chronic, progressive neurodegenerative disorder that diminishes the quality of life in over 630,000 people in the USA, which is projected to double by year 2040 as our population ages (Dorsey et al., 2013; Kowal et al., 2013). An early non-motor feature of PD is cognitive impairment, particularly deficits in executive function (EF), which includes processing information and cognitive flexibility (e.g., set-shifting, reversal learning) (Dirnberger and Jahanshahi, 2013; Parker et al., 2013). In PD, deficits in the fronto-striatal circuit represent a common pathophysiology (Robbins and Cools, 2014). The importance of the striatum in EF, also termed the basal ganglia (BG) or caudate nucleus-putamen (CPu), is based on a large rodent and human literature (see review (Macdonald and Monchi, 2011)). For example, in individuals with PD, resting state functional magnetic resonance imaging, as well as positron emission tomographic neuroimaging, have demonstrated hypo-activation in a number of cortical and sub-cortical (basal ganglia) regions impacting the EF network (Kim et al., 2019; Apostolova et al., 2020; Stögbauer et al., 2020; Hirano, 2021).

Rodent studies have specifically implicated the role of the dorsomedial CPu (dmCPu) in EF, and its importance in set shifting and reversal learning (O'Neill and Brown, 2007; Baker and Ragozzino, 2014; Grospe et al., 2018), particularly when selection requires competing responses and discounting more salient stimuli (Cools, 2006; Thoma et al., 2008; Yehene et al., 2008; van Schouwenburg et al., 2010). It has been proposed that deficits in reversal learning may be due to prominent projection fibers to the dmCPu from the medial prefrontal cortex, including anterior cingulate and prelimbic cortices (Voorn et al., 2004), as well as a broader cortico-striatal-thalamic circuit (Chudasama et al., 2001; Brown et al., 2010; Wang et al., 2019). Although the pathophysiological changes in the dmCPu that underlie EF changes in PD are complex, loss of synaptic integrity, including synaptophysin and PSD95, and dopamine (DA) neurotransmission, including DA loss and altered

* Corresponding author. Department of Psychiatry and the Behavioral Sciences, University of Southern California, 1975 Zonal Ave., KAM 400, MC9037, Los Angeles, CA, 90089-9037, USA.
E-mail address: holschne@usc.edu (D.P. Holschneider).
[1] These authors contributed equally.
[2] Co-senior authors.

https://doi.org/10.1016/j.crneur.2022.100039
Received 18 September 2021; Received in revised form 6 February 2022; Accepted 24 April 2022
Available online 1 May 2022

Abbreviations:

Actb	Actin-beta
ANOVA	Analysis of variance
AP	anterior-posterior
BG	Basal ganglia
CPu	Caudate putamen (striatum)
DA	Dopamine
DAR-D1-4	Dopamine receptors 1-4
dlCPu	Dorsolateral striatum
Dlg4	Gene coding for discs large MAGUK scaffold protein 4, also known as PSD-95
dmCPu	Dorsomedial striatum
Drd1-4	Genes for dopamine receptors 1-4
DT	Dual task
EDTA	ethylenediaminetetraacetic acid
EF	Executive function
Fisher's LSD	fisher's Least Significant Difference test
HPLC	High-performance liquid chromatography
ITI	Intertrial interval
L1-L3	3-CSRT learning levels 1-3
L1R-L3R	3-CSRT-R reversal learning levels 1-3
ML	Medial-lateral
MPTP	1-methyl-4-phenyl-1,2,3,6-tetrahydropyridine
NaOH	Sodium hydroxide
ns	nonsignificant
PD	Parkinson's disease
PFA/PBS	Paraformaldehyde/phosphate buffered saline
PSD-95	Postsynaptic density protein
RT-PCR	Reverse transcription polymerase chain reaction
SEM	standard error of the mean
SNC	Substantia nigra compacta
SNR	Substantia nigra reticulata
Syp	Synaptophysin
TH	Tyrosine hydroxylase
TO	Time out
vlCPu	Ventrolateral striatum
vmCPu	Ventromedial striatum
3-CSRT	3-choice serial reaction time task
3-CSRT-R	3-choice serial reaction time task with reversal
6-OHDA	6-hydroxydopamine

DA receptor expression, are reported to have a certain contribution (Salame et al., 2016). Dopamine receptors, comprised of D1-like receptors (DAR-D1 and D5R), D2-like receptors (DAR-D2, DAR-D3, and DAR-D4) play a central role in learning and EF-related cognitive processing and flexibility (Wang et al., 2019; Sala-Bayo et al., 2020).

A public health priority is to identify cost-effective therapies to combat progressive cognitive impairment in PD, which is not addressed by current therapies (Burn et al., 2014). There is significant evidence utilizing short-term clinical studies showing that different types of exercise may improve motor performance in PD, including aerobic exercise (treadmill walking, cycling), resistance exercise (strength or weight training), balance training (yoga, stepping), and multifaceted exercise (Tai Chi, dancing) (Alberts et al., 2011; Intzandt et al., 2018). Fewer studies have examined the impact of exercise on long-term cognitive function in PD patients. Even less is known regarding the molecular underpinnings of exercise-related benefits in PD-related EF impairment. Indeed, the long-term effects of chronic exercise on cognition remains controversial (Sanders et al., 2020; Schootemeijer et al., 2020; Brown et al., 2021). There is a need for research into the causality of the relationship between physical activity, cognitive performance and insights regarding exercise-induced repair mechanisms. Using the 6-hydroxydopamine (6-OHDA) lesioned model of PD, targeting specifically the dmCPu, this study sought to test the hypothesis that daily exercise improves EF-related cognitive processing and flexibility and that these benefits may be due to improved basal ganglia synaptic integrity and DA neurotransmission.

2. Methods

2.1. Animals

Wistar rats (male, 8–9 weeks of age) were purchased from Envigo Corporation (Placentia, CA, USA). Housing was under standard vivarium conditions in pairs on a 12-hr light/12-hr dark cycle (dark cycle 6 p.m. to 6 a.m.). All cages included a plastic pipe (10 cm diameter, 15 cm length) as an enrichment object. Rats had ad libitum access to food and water, except during food restriction as described in the behavioral studies. All experimental protocols were approved by the Institutional Animal Care and Use Committee of the University of Southern California, a facility approved by the Association for Assessment and Accreditation of Laboratory Animal Care, as well as by the Animal Use and Care Review Office of the US Department of the Army, and in compliance with the National Institutes of Health Guide for the Care and Use of Laboratory Animals, 8th Edition, 2011.

2.2. Experimental design overview

Groups included 6-OHDA lesioned (Lesion) or naïve (Non-Lesion) rats. We originally chose the naïve rat control over the sham-lesioned control, as we felt that examining the exercise effects in 'normals' had greater relevance to clinical translation of the effects of exercise in normal human subjects. Rats underwent food restriction as described below, beginning 2 weeks after lesion surgery. Starting 2 weeks after lesion surgery, rats were subjected to exercise in motorized running wheels with either (i) a smooth surface (termed aerobic exercise), (ii) a complex motorized running wheel with alternating rungs removed, (iii) on a horizontal treadmill, or (iv) sedentary (non-exercise). The sections below detail the experimental approaches, including the cognitive testing (Fig. 1) using the operant 3-CSRT with rule reversal (Section 2.6, Experiment 1) and T-maze with rewarded matching-to-sample (Win-Stay) and reversal (Win-Shift) (Section 2.7., Experiment 2) to evaluate executive function, as well as a striatal transcript analysis for dopamine receptors (DAR-) D1 through D4 and the synaptic genes PSD-95 and synaptophysin (Section 2.8., Experiment 3).

2.3. Rat model of bilateral, dorsomedial striatal dopamine-depletion (Wang et al., 2020)

We targeted the dorsomedial quadrant of the striatum (dmCPu) as past work has shown that this region in rodents is critical for reversal learning (O'Neill and Brown, 2007; Baker and Ragozzino, 2014; Grospe et al., 2018), with alterations in the rostromedial striatum presumably resulting in deficits in frontostriatal processing (Voorn et al., 2004). In brief, rats received stereotaxic injection of 6-OHDA at 4 striatal injection sites (2 in each hemisphere) (Sigma-Aldrich Co., St. Louis, MO, USA, 10 μg/site dissolved in 2 μL of 0.1% L-ascorbic acid/saline, 0.4 μL/min) targeting the bilateral dmCPu (AP: + 1.5 mm, ML: ± 2.2 mm, DV: 5.2 mm, and AP: + 0.3 mm, ML: ± 2.8 mm, DV: 5.0 mm, relative to bregma), which is the primary striatal sector targeted by the medial prefrontal cortex (Voorn et al., 2004) and critical for flexible shifting responses (O'Neill and Brown, 2007; Baker and Ragozzino, 2014; Tait et al., 2017; Grospe et al., 2018). After injection, the needle was left in place for 5

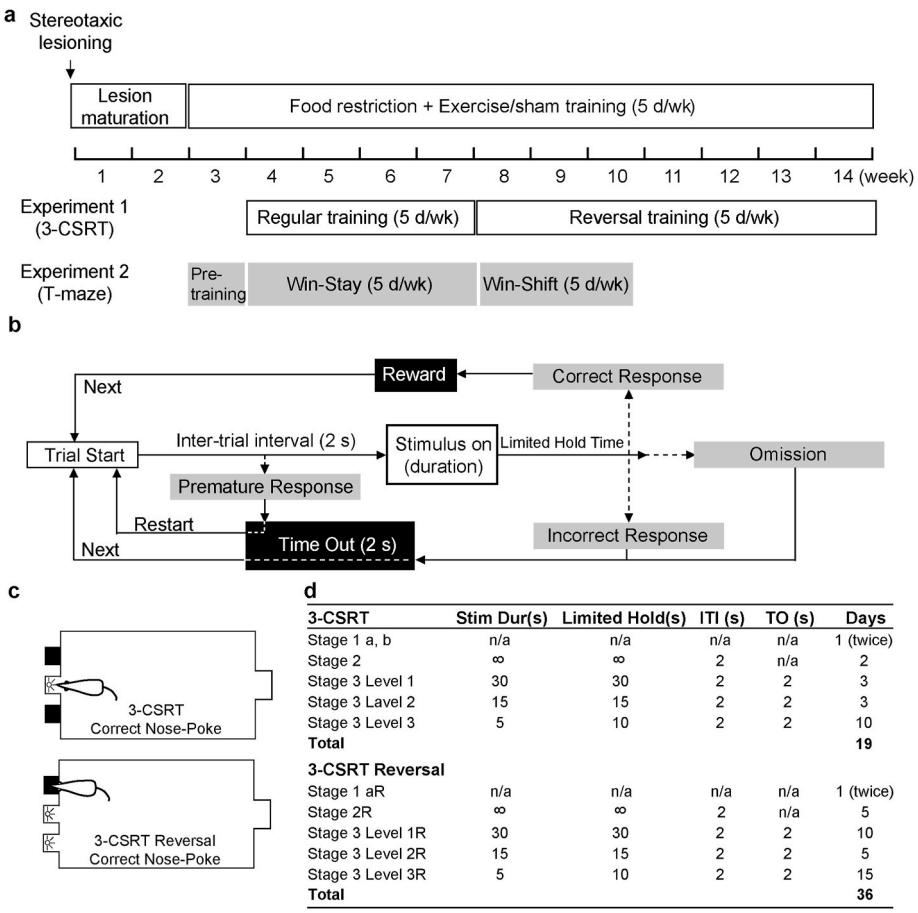

d

3-CSRT	Stim Dur(s)	Limited Hold(s)	ITI (s)	TO (s)	Days
Stage 1 a, b	n/a	n/a	n/a	n/a	1 (twice)
Stage 2	∞	∞	2	n/a	2
Stage 3 Level 1	30	30	2	2	3
Stage 3 Lavel 2	15	15	2	2	3
Stage 3 Level 3	5	10	2	2	10
Total					**19**
3-CSRT Reversal					
Stage 1 aR	n/a	n/a	n/a	n/a	1 (twice)
Stage 2R	∞	∞	2	n/a	5
Stage 3 Level 1R	30	30	2	2	10
Stage 3 Level 2R	15	15	2	2	5
Stage 3 Level 3R	5	10	2	2	15
Total					**36**

Fig. 1. Experimental protocol for operant training, T-maze, and exercise. (a) Timeline of experiments 1 and 2. **(b)** Protocol for the 3-choice serial reaction time task (3-CSRT) and reversal learning (3-CSRT-R). Gray shaded cells depict choices made by the rat. Black shaded cells depict consequences of those choices. Adapted from Asinof and Paine (2014) (Asinof and Paine, 2014)**. (c)** Acquisition of the 3-CSRT and 3-CSRT-R. **(d)** Progressive training schedule.

min before being slowly retracted (1 mm/min). Non-Lesion rats were used for controls. To prevent noradrenergic effects of the toxin, rats received desipramine (Sigma Aldrich, 25 mg/kg i.p.) before surgery (Roberts et al., 1975). Carprofen (2 mg in 5 g tablet, p. o., Bio-Serv, Flemington, NJ, USA) was administered for one day preoperatively and for two days postoperatively for analgesia. Exercise was initiated 2 weeks thereafter when lesion maturation was complete (Sauer and Oertel, 1994; Yuan et al., 2005). To verify the striatal target of 6-OHDA lesion, brains from a subset of rats were collected for immunohistochemical staining for tyrosine hydroxylase protein and HPLC analysis of DA.

2.3.1. *Tyrosine hydroxylase (TH) immunostaining*

TH immunostaining data were collected as previously reported and described quantitatively from lesioned and non-lesioned rats (Wang et al., 2020). Rats were anesthetized, subjected to transcardial perfusion with ice-cold saline followed by ice-cold 4% PFA/PBS. Brains were removed, transferred to the same fixative for 24 h, immersed in 20% sucrose for 48 h, frozen and cryo-sectioned at 25 μm thickness throughout the entire anterior-posterior extent of the brain. Selective sections spanning the 6-OHDA lesion in both the striatum and midbrain were subjected to TH-immunostaining using a primary antibody solution (1:2500 anti-tyrosine hydroxylase, Cat #AB152, Millipore-Sigma, Billerica, MA, USA), then visualized using a secondary antibody solution (1:5000 IRDye 800CW Goat anti-mouse Cat #926–3221, LI-COR, Lincoln, NE, USA). Images of tissues at the levels of the striatum representing the site of the 6-OHDA lesioning targeting the dmCPu and mid-ventral mesencephalon showing the midbrain dopaminergic neurons were obtained using a LI-COR Odyssey CLx (for internal landmarks, please see (Wang et al., 2020)).

2.3.2. *HPLC analysis of striatal dopamine*

Neurotransmitter concentrations in experiments 1 and 2 were determined according to an adaptation of Mayer and Shoup (1983) (Mayer and Shoup, 1983). Striatal tissue sections were dissected and immediately frozen on dry ice and stored at −80 °C until analysis. Tissues were sampled from coronal sections spanning bregma AP +2.00 to 0.00 mm, including tissue bordered ventrally by the anterior commissure, dorsally by the corpus callosum, medially by the lateral ventricle, and ±5.0 mm laterally from the midline) (Kintz et al., 2013; Lundquist et al., 2019). Striatal blocks were further sub-dissected to four quadrants, using the dorsal-ventral and medial-lateral divisions detailed previously (Voorn et al., 2004) to collect tissue from the dorsomedial striatum (dmCPu), dorsolateral striatum (dlCPu), ventromedial (vmCPu), and ventrolateral quadrants (vlCPu). For analysis, tissues were homogenized in 0.4 N perchloric acid, proteins were separated by centrifugation, and the supernatant used for HPLC analysis by electrochemical detection on an ESA HPLC system (ESA, Chelmsford, MA, USA) consisting of an ESA Model 582 pump, ESA Model 542 autosampler, ESA Model 5600 Detector and separation column (MD-150 × 3.2 mm). Data analysis employed the CoulArray for Window Application program (ESA Biosciences, Chelmsford, MA, USA). The protein pellet was resuspended in 0.5 N NaOH and total protein concentration determined using the BCA detection method (Pierce, Rockford, IL, USA). Striatal DA was expressed as nanograms DA per milligram protein.

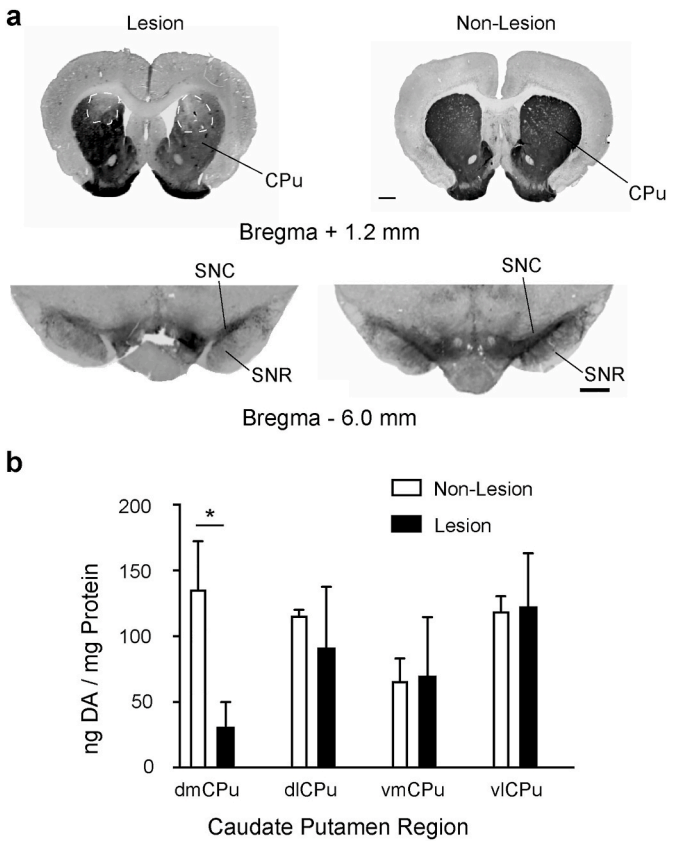

Fig. 2. Immunostaining for tyrosine hydroxylase to determine the degree and anatomical site of lesion. (a) Representative images of coronal sections reveal bilateral loss in tyrosine hydroxylase immunoreactivity in the dorsomedial striatum (bregma AP +1.20 mm anterior to bregma) and midbrain showing immunostaining of the substantia nigra pars compacta (SNC) and substantia nigra reticulata (SNR, bregma AP -6.0 mm). Scale bar = 0.5 mm. (b) HPLC analysis of striatal DA from tissues collected from coronal slice (bregma AP +2.00 to 0.00 mm) from Non-Lesion and Lesion rats in striatal tissue quadrants (dorsomedial dmCPu, dorsolateral dlCPu, ventromedial vmCPu, and ventrolateral vlCPu).

2.4. Food restriction

Food restriction was started 2 weeks after surgery and maintained throughout the 3-CSRT (Experiment 1) and T-maze (Experiment 2) behavioral studies. Rats were brought to 85% of their baseline body weight in one week and allowed to gain 5 g in body weight per week thereafter, with ad libitum access to water. Rats were fed between behavioral testing that took place in the morning and exercise that took place in the afternoon. Body weights were recorded Monday-Friday, with meal size individually adjusted on a daily basis, including weekends.

2.5. Exercise on running wheels and treadmill

2.5.1. Exercise on complex or smooth running wheels

Rats assigned to the skilled exercise group were trained in enclosed, motorized, running wheels (35.6 cm diameter, Lafayette Instrument, Lafayette, IN, USA) with irregularly spaced rungs, termed 'complex' running wheel, which demand the constant adaptation of stride length. A pseudo random pattern of rung spacing was achieved by repeating a pattern OOOOXOX, where O indicates a rung, and X a missing rung, resulting in inter-rung distance of either 1.3 or 2.6 cm). Exercise was initiated 2 weeks after lesion surgery using our prior methods (Wang et al., 2015a,b) and lasted a total of 30 min/day (4 bouts, 5 min/bout, 2-min inter-bout interval), 5 consecutive days/week (Mon - Fri). Starting time point was based on published literature reporting that bilateral striatal 6-OHDA lesions elicits TH losses at the level of the SN that reaches a plateau after 2 weeks (Yuan et al., 2005; Blandini et al., 2007), with DA losses plateauing at 2 weeks (Ben et al., 1999), and with nigral cell losses variably reported as plateauing (Yuan et al., 2005) or decreasing thereafter to 4 weeks post-injury (Blandini et al., 2007). Rats were subjected to 1 week of individually adjusted, performance-based speed adaptation to reach a plateau speed of 5 m/min, a speed achievable by most 6-OHDA lesioned rats in the complex wheel following 1 week of exercise (Wang et al., 2013, 2015). Titration of speed has been described in detail in our prior publication (Wang et al., 2013). Non-Exercise rats were left in a stationary running wheel for 30 min/day. Running speeds for the Non-Lesion, control rats were matched to speeds achievable by lesion rats in the complex wheel (5 m/min maximum). An additional group of lesion rats was trained in motorized running wheels identical to those described above, except that these wheels had regularly placed rungs and an inner plastic 'smooth' floor covering the metal rungs and were termed 'smooth' running wheel as previously reported (Wang et al., 2013, 2015). The modification made foot placement easier for lesioned rats, and therefore minimized the 'motor skill' factor. Speeds for the smooth running wheels were matched to those of the complex running wheels.

2.5.2. Exercise training on horizontal treadmill

A separate group of rats were trained on a motorized, 10-lane horizontal treadmill (lane width 10 cm, length 94 cm, wall height 20 cm, custom made) for 65 min a day, 5 days per week (Mon - Fri) starting two weeks after stereotaxic surgery. Each exercise session consisted of a 15-min warm-up, 15-min running, 5-min break, 15-min running, and 15-min cool-down. The warm-up and cool-down speed started at 4 m/min and went up to 10 m/min by 2 weeks, while the running speed started at 6 m/min and went up to 30 m/min in 4 weeks. The rats were exercised at 10 and 30 m/min for the remaining 10 weeks. A researcher prompted the rats to stay on the treadmill and run by lightly brushing the rear end of any rat that fell back with a brush. After several days of exercise, rats typically will stay on the treadmill running.

2.6. Operant training

2.6.1. Groups

In Experiment 1, rats with bilateral, dmCPu 6-OHDA lesions were exposed to exercise in either: (i) motorized, complex running wheel (Lesion/Complex Wheel, $n = 12$), (ii) motorized smooth running wheel (Lesion/Smooth Wheel, $n = 4$), or (iii) motorized horizontal treadmill (Lesion/Treadmill, $n = 6$). The control group of rats included 6-OHDA lesion, non-exercise rats (Lesion/Non-Exercise, $n = 12$) or Non-Lesion, non-exercise rats (Non-Lesion/Non-Exercise, $n = 12$). The Non-Lesion group consisted of both non-exercise (n = 6) and complex running wheel (n = 6) and since they showed no significant differences in operant training outcomes they were pooled (Supplementary Fig. S1).

Whereas in our original design sample size was balanced across all groups to access modality-specific effects of exercise, we were not able to complete all experiments due to local restrictions and university-mandated euthanasia of rats during the height of the Covid-19 pandemic. These rats were excluded from analysis. Because preliminary analysis showed the exercise effects to be modest (Supplementary Fig. S2), we pooled the three exercise groups to form a single Lesion/Exercise group ($n = 22$) in this report.

2.6.2. Three-choice serial reaction time nose-poke task with reversal (Fig. 1)

We chose a 3-CSRT paradigm with an added rule reversal feature, called 3-CSRT-reversal (3-CSRT-R), to examine cognitive flexibility. Detailed methods are provided in our prior publication (Wang et al., 2020). In brief, rats were food restricted and randomized to receive

complex wheel exercise, simple wheel exercise, treadmill exercise, or no exercise. Exercise was initiated 1 week prior to operant training, during which time they were handled on a daily basis and given 5 sucrose pellets per day in their home cage (45 mg/pellet, chocolate flavor, #F0025, Bio-Serv, Frenchtown, NJ, USA). Exercise was continued for 12 weeks. Each modular test chamber (MedAssociates, St. Albans, VT, USA) was housed in a sound attenuating cubicle, and consisted of grid floor, house light, 3-bay nose-poke wall, pellet trough receptacle, receptacle light, head entry detector, and a PC-controlled smart controller. Rats were trained to associate nose poking into an illuminated aperture with receiving a single sucrose pellet reward. Rats were familiarized with the test chamber and nose-poke and reward retrieval behavior were shaped in pretraining lasting 1 week as previously described (Wang et al., 2020). Thereafter, during the regular phase of 3-CSRT training, the rats were trained following a progressive schedule with a fixed ratio 1 schedule response-reward task (up to 90 trials or 30 min each session per day, 5 days/week, 16 sessions). The walls, nose-poke apertures, food receptacle, and grid floor were wiped with 70% isopropyl alcohol between rats.

For each trial, the light stimulus was turned on in a pseudo-randomly chosen nose-poke aperture (Fig. 1b). The stimulus stayed on for a set duration or until a nose-poke (correct or incorrect) was detected. The rat received a food reward following a correct nose-poke within the set limited hold duration, which was set to be the same as the stimulus duration or slightly longer for short stimulus durations. Following reward retrieval and a 2-s intertrial interval (ITI), the next trial was started. If an incorrect nose-poke was detected, the rat received a 2-s time out (TO), during which the chamber light was turned off. If no nose-poke was detected within the limited hold duration, an omission was recorded, with a 2-s TO. After each TO, the chamber light was turned on, and after a 2-s ITI, the next trial was started. If a nose-poke was detected during the ITI, a premature response was recorded without incrementing the trial number, and the rat received a 2-s TO. Any nose-pokes following a correct response and before reward retrieval were recorded as repetitive responses. Rats were trained through 3 difficulty levels with progressively shortened stimulus durations. We chose to control the number of training days for each level across rats to facilitate between-group comparison. This was selected based on our prior work showing that lesion rats can reach a performance level comparable to that of Non-Lesion rats at this difficulty level (Wang et al., 2020). Differences in reversal learning can thus be interpreted as differences in cognitive flexibility, rather than differences based on incomplete learning. The final stimulus duration was set at 5 s, reflecting a moderate level of difficulty.

During the rule-reversal phase of 3-CSRT-R training (Fig. 1c), the stimulus was switched from a lit aperture among dark apertures to a dark aperture among lit apertures. The animal was trained progressively to learn to nose-poke the dark aperture to receive reward (25 sessions, 1 session/day, 5 days/week).

For 3-CSRT and 3-CSRT-R the following behaviors were captured (Asinof and Paine, 2014): (i) nose-poke accuracy = (number of correct responses)/(number of correct + number of incorrect responses) * 100%, a primary measure of operant learning; to account for modest differences in 3-CSRT acquisition, we normalized nose-poke accuracy during the reversal phase by accuracy at the end of acquisition (L3, Day 10, Fig. 3); (ii) number of omissions, a measure of attention; (iii) premature responses, a measure of impulsivity and response inhibition, (iv) correct nose-poke latency = average time from onset of stimulus to a correct response, a measure of attention and cognitive processing speed; and (v) reward retrieval latency = average time from correct response to retrieval of sugar pellet, a measure of motivation.

2.7. T-maze

2.7.1. Groups

In Experiment 2, rats (n = 7) with 6-OHDA lesions were exercised for 6 ½ weeks in the complex wheel. Controls included lesion, non-exercise rats (Lesion/Non-Exercise, $n = 6$), and Non-Lesion, non-exercise controls (Non-Lesion/Non-Exercise, $n = 9$).

2.7.2. T-maze with rewarded matching-to-Sample and reversal

Cognition testing of EF in rats was adapted from methods from our work (Stefanko et al., 2017) and that of others (Deacon and Rawlins, 2006). Rats were food restricted and randomized to exercise in the complex wheel or non-exercise. One week prior to T-maze training, rats were handled on a daily basis and given 5 dustless, chocolate-flavored sucrose pellets per day in their home cage (45 mg/pellet, #F0025, Bio-Serv, Frenchtown, NJ, USA). The T-maze was constructed as a cross maze of black, opaque Plexiglas. Arms (15.2 cm width, 50.8 cm length, 35.2 cm height) could be sealed off by guillotine doors (15.2 cm width x 35.2 cm height) to prevent entry to an enclosed central platform (15.2 cm width, 15.2 cm length, 35.2 cm height). Two opposing arms were designated as the branch arms, with one of the remaining two arms randomized to be designated the stem arm with its opposite arm sealed during the 'T-maze' testing. A partition extended across the central platform and 6.4 cm into the chosen stem arm, allowing entry into either of the open branch arms. Arm entry was defined as having all four paws in the arm. If a rat failed to mobilize within 90 s, it was removed from the maze, to be exposed again 10 min later. Uneaten sucrose pellets and fecal pellets were removed from the maze between trials, and the maze wiped with 70% isopropyl alcohol solution.

T-Maze acclimatization occurred over 3 days during which time rats were allowed to explore the maze. Initially the floor of the maze was baited with individual sucrose pellets, followed by baiting of both maze arms, followed by baiting of both food cups. Rats were trained for 3 days in a forced trial paradigm, in which food reward was available only in one arm (randomized), with the other branch arm blocked (10 trials with a 5-s intertrial interval in the morning and again in the afternoon). Thereafter, they were trained in a 'Win-Stay' paradigm (sample run→choice trial, 10 trials twice per day, 5-s intertrial interval, x 20 days), in which rats had to choose the same arm during a choice trial (both arms open) that had previously been rewarded on the preceding sample trial (one arm closed). Sample trials were randomized across both arms. Thereafter, during implementation of a rule reversal, rats were exposed to a 'Win-Shift' strategy, in which the rat was only rewarded in the choice run if it entered the branch arm opposite the one chosen in the sample run (sample run→choice trial, 10 sequences twice per day, 5-s intertrial interval, x 13 days). The number of correct entries into the bated choice arm were recorded for each trial.

2.8. Quantitative RT-PCR for striatal dopamine receptor and synaptic gene expression

In Experiment 3, two additional groups of 6-OHDA-lesioned rats were exercised in the complex running wheel (Lesion/Complex Wheel, $n = 6$) or smooth running wheel (Lesion/Smooth Wheel, $n = 6$) for 4 weeks before being euthanized for transcript analysis. Since there were no statistically significant differences in gene expression between the Smooth wheel and the Complex wheel groups, the gene expression data from the two exercise modalities were pooled to form a single composite Exercise group (n = 12), similar to the approach in Experiment 1. Final group analyses included Non-Lesion/Non-Exercise (n = 6), Lesion/Non-Exercise (n = 6), and Lesion/Exercise (n = 12). The pattern of expression of several genes including *Syp* (synaptophysin, Gene ID 24804), *Dlg4* (discs large MAGUK scaffold protein 4, also known as PSD95, Gene ID 29495), *Drd1* (DAR-D1, Gene ID 24316), *Drd2* (DAR-D2, Gene ID 24318), *Drd3* (DAR-D3, Gene ID 29238), and *Drd4* (DAR-D4, Gene ID 25432) were examined. Immediately after the final exercise session, rats were sacrificed via decapitation and whole brains were extracted. Fresh tissue was rapidly micro-dissected in blocks from the CPu (dmCPu, dlCPu, vmCPu, vlCPu as described in section 2.3.2). Tissues were submerged in an RNA stabilization solution (pH 5.2) at 4 °C, containing in

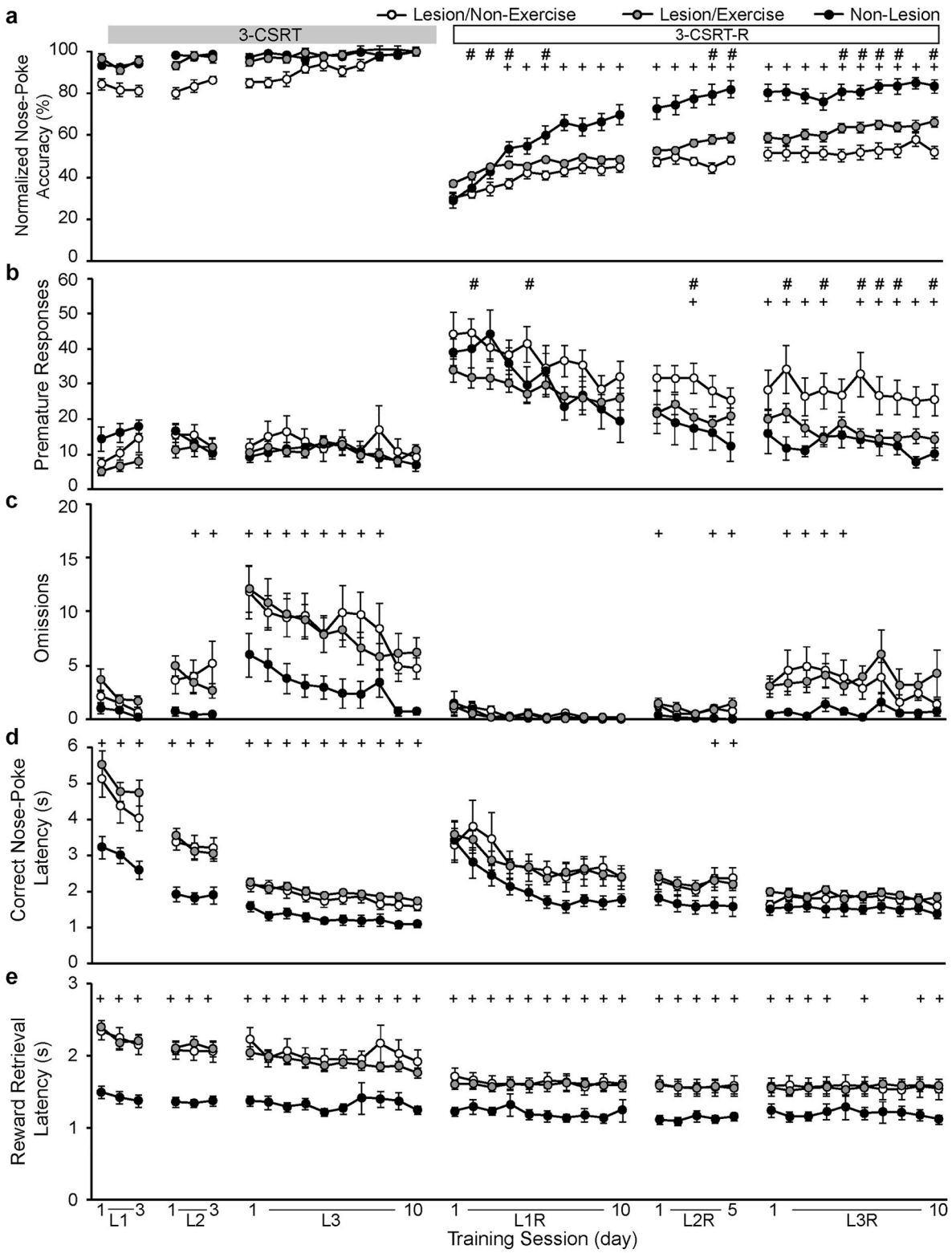

Fig. 3. Effects of exercise and lesion on the 3-choice serial reaction time task (3-CSRT) acquisition and reversal learning (3-CSRT-R). Shown are group mean ± SEM of **(a)** normalized nose-poke accuracy, **(b)** premature responses, **(c)** omissions, **(d)** correct nose-poke latency, and **(e)** reward retrieval latency for Non-Lesion ($n = 12$), Lesion/Non-Exercise ($n = 12$) and Lesion/Exercise group ($n = 22$). Results show that exercise elicits a significant, modest improvement in response accuracy in the 3-CSRT-R, as well as a robust improvement in inhibitory aptitude in the 3-CSRT-R in lesioned rats. #: $p < 0.05$ Lesion/Exercise vs. Lesion/Non-Exercise; +: $p < 0.05$ Lesion/Non-Exercise vs. Non-Lesion, Fisher's LSD multiple comparisons test. Data were also analyzed with two-way ANOVA with repeated measures (results listed in Supplementary Table S1). The Non-Lesion group consisted of both non-exercise (n = 6) and complex running wheel (n = 6), and since they showed no significant differences in operant training outcomes they were pooled (Supplementary Fig. S1).

mM: 3.53 ammonium sulfate, 16.66 sodium citrate, and 13.33 EDTA (ethylenediaminetetraacetic acid), transferred to a sterile tube containing 300 μl TRI-reagent (Cat. No. 11–330T, Genesee Scientific, San Diego, CA, USA), and homogenized with a mechanical pestle before centrifuging at 13,000×*g* for 3 min. Supernatant was removed to a new tube and 250 μl of chloroform was added and tubes vigorously shaken twice for 10 s, followed by 3 min of rest on ice and centrifugation at 13,000×*g* for 18 min at 4 °C. The upper aqueous layer was carefully removed to a new tube, an equal volume of 100% ethanol was added, and the sample was thoroughly mixed before RNA purification using the Zymo Direct-zol RNA Miniprep (Cat. No. 11–330, Genesee Scientific) according to the manufacturer's instructions. RNA was eluted in 35 μl of DNAse/RNAse free water before spectrophotometric analysis of RNA purity and concentration. Complementary DNA (cDNA) was synthesized from 1 μg isolated RNA using the qPCRBIO cDNA Synthesis Kit (Cat. No. PB30.11–10, PCR Biosystems, Wayne, PA, USA) following manufacturer's guidelines before being diluted 1:5 in DNAse/RNAse free water and stored at −20 °C. Gene expression changes were measured with quantitative RT-PCR (qRT-PCR) as previously described (Lundquist et al., 2019, 2021). Briefly, qRT-PCR was run with 2 μl of cDNA and qPCRBIO SyGreen master mix (Cat. No. PB20.11–01, PCR Biosystems) on an Eppendorf Mastercycler Ep Realplex (Eppendorf, Hauppauge, NY, USA) using a program of 15 min at 95 °C, followed by 40 cycles of 15 s at 94 °C, 30 s at 55 °C, and 30 s at 72 °C. Data was collected and normalized on Eppendorf Realplex ep software. Standard delta-CT analysis (Livak and Schmittgen, 2001) was used to quantify fold changes in gene expression in experimental groups normalized to controls, with beta-actin serving as a housekeeping gene. Primer oligonucleotide pairs are listed in Supplementary Table S7.

2.9. Statistical analysis

Data are presented as mean ± S.E.M. and analyzed using GraphPad Prism (version 8.3.0, GraphPad Software, San Diego, CA, USA).

2.9.1. 3-CSRT/3-CSRT-R

3-CSRT data were analyzed using two-way ANOVA with repeated measures for each training level, with lesion and time, or exercise and time as the factors, and with Fisher's LSD multiple comparisons test comparing groups for individual training session. In addition, to control for any possible subtle lesion-related deficits in motor and cognitive functions at the end of the 3-CSRT acquisition phase, we also examined a normalized nose-poke accuracy in which the group average of accuracies during the 3-CSRT-R were normalized by the group mean accuracy on the final day of regular training (L3 of 3-CSRT). All statistical test results for main effect of lesion and exercise are included in Supplementary Table S1.

2.9.2. T-maze with reversal

The lesion effect was analyzed by a mixed model with repeated measures in 'time' and main effect being 'lesion' ($p < 0.05$). Accuracy in the Win-Stay and Win-Shift paradigms was separately analyzed by a two-way ANOVA with repeated measures in 'time' and main effect being 'exercise' ($p < 0.05$). Performance was evaluated as: (i) percent of correct responses per session during initial learning (Win-Stay) and reversal learning (Win-Shift); (ii) the number of trials an individual rat required to reach the learning criterion during the reversal phase, defined as 9 out of 10 correct choices in consecutive trials; and (iii) perseverative or regressive errors made during the reversal learning phase. Perseverative and regressive errors were defined, respectively, as the number of incorrect choices made until or after the rat chose the correct arm for 5 consecutive trials. Perseverative and regressive errors during the Win-Shift phase were separately analyzed by a two-way ANOVA with repeated measures in 'time', and main effect either being 'lesion' or 'exercise' ($p < 0.05$). Fisher's LSD multiple comparisons tests were used to compare groups for individual days.

2.9.3. Transcript and HPLC analysis

All statistical tests were carried out and graphs made in Prism 9.1 (GraphPad, San Diego, CA, USA) with statistical significance set at $p < 0.05$. No sample size calculations were performed prior to the start of the study but are based on previous publications. Unpaired, two-tailed T-tests were used for all qRT-PCR analysis between control and pooled exercise groups (smooth wheel, complex wheel). One-way ANOVA with Tukey's multiple comparisons was used for analysis of gene expression across exercise groups (non-exercise, exercise). Statistical analysis for HPLC data was carried out by using a one-way ANOVA with Dunnett's posttest comparing saline (control) treatment with 6-OHDA-lesioned groups. All statistical test results are included in Supplementary Tables S3–7.

3. Results

3.1. Assessment of 6-OHDA-lesioning on tyrosine hydroxylase expression and dopamine levels

Analysis of TH immunoreactivity demonstrated a significant reduction in TH immunostaining in the dmCPU (the stereotactic target of 6-OHDA) in lesioned rats compared to Non-Lesion rats (Fig. 2a). There were no significant differences in the dlCPu, vmCPu, and vlCPu of lesioned compared to Non-Lesion rats. Examination of TH immunostaining in the midbrain showed reduced staining of the substantia nigra from 6-OHDA-lesioned rats compared to Non-Lesion rats. Analysis of DA levels by HPLC showed a significant difference in only the dmCPu quadrant, the region targeted for stereotaxic delivery of 6-OHDA, compared to Non-Lesion rats (31.2 ± 18.7 ng vs. 136.1 ± 36.1 DA/mg Protein, $p < 0.05$). All other quadrants of CPu tissues did not show a statistically significant difference comparing Non-Lesion with lesioned tissue quadrants (Fig. 2b). These results show that lesions were limited to the dmCPu quadrant, with retrograde bilateral dopaminergic cell losses also apparent at the level of the substantia nigra.

3.2. Experiment 1: Effect of lesion and of exercise on operant training (3-CSRT/3-CSRT-R)

3.2.1. Lesion effects

During the acquisition phase of 3-CSRT (Levels L1, L2, L3), Lesion/Non-Exercise rats compared to Non-Lesion/Non-Exercise showed: (i) statistically significant lower nose-poke accuracy (Supplementary Fig. S2a $p < 0.0001$, two-way ANOVA repeated measures that diminished towards the end of L3 (L3 Day 10: Lesion/Non-Exercise 83.77 ± 2.05% vs. Non-Lesion 91.41 ± 1.10%); (ii) no differences in the number of premature responses ($p > 0.05$. Fig. 3b); (iii) significantly higher number of omissions in L2 and L3 ($p < 0.05$. Fig. 3c); (iv) significantly greater correct nose-poke latency (~0.6 s, $p < 0.005$. Fig. 3d); and (v) significantly greater reward retrieval latency (~0.6 s, $p < 0.001$. Fig. 3e). See Supplementary Table S1 for *F* and *p* values.

A reversal was introduced to evaluate cognitive flexibility. At the start of 3-CSRT-R, when the rule for correct (rewarded) response was switched from nose-poking a lit aperture to nose-poking a dark aperture, both Lesion/Non-Exercise and Non-Lesion/Non-Exercise rats showed a sudden drop in performance with decreased nose-poke accuracy to the same extent, increased correct nose-poke latency, and increased premature responses. Both groups showed improvement in these parameters with continued training. Non-Lesion/Non-Exercise improved nose-poke accuracy rapidly to a plateau of about 75% (L3R Day 10, 76.55 ± 3.21%), while Lesion/Non-Exercise rats only improved accuracy modestly to a plateau of about 40% (L3R Day 10, 43.69 ± 2.95%). Lesion/Non-Exercise rats compared to Non-Lesion controls showed: (i) statistically significant lower nose-poke accuracy ($p < 0.001$. Supplementary Fig. S2a); (ii) significantly higher number of premature responses in L3R ($p = 0.0088$. Fig. 3b); (iii) significantly higher number of omissions in phases L2R and L3R ($p < 0.05$. Fig. 3c); (iv) no differences

in correct nose-poke latency ($p > 0.05$. Fig. 3d); and (v) significantly greater reward retrieval latency (~0.5 s, $p < 0.05$. Fig. 3e).

3.2.2. Exercise effects

Lesion/Complex Wheel, Lesion/Smooth Wheel, and Lesion/Treadmill rats showed similar outcomes in the 3-CSRT task (Supplementary Fig. S2) and were pooled to form a Lesion/Exercise group ($n = 22$). Lesion/Exercise compared to Lesion/Non-Exercise rats showed a statistically significant lower number of premature responses during the reversal phase L3R ($p = 0.018$. Fig. 3b). To account for modest differences in 3-CSRT acquisition, we normalized nose-poke accuracy during the reversal phase by accuracy at the end of acquisition (L3, Day 10). Lesion/Exercise rats showed significantly higher normalized nose-poke accuracy in all reversal levels ($p < 0.05$. Fig. 3a). There were no differences in omission, correct nose-poke latency, and reward retrieval latency between the two groups (Fig. 3c–e).

3.3. Experiment 2: Effect of exercise on T-maze task with reversal

To examine the effect of dmCPu 6-OHDA lesion and exercise on cognitive flexibility, behavior in the T-Maze with reversal was tested. The groups examined were Lesion/Non-Exercise, Non-Lesion/Non-Exercise, and Lesion/Complex Wheel. During the Win-Stay phase, there was a significant effect of lesion ($F_{1,13} = 13.47$, $p = 0.0028$) and a lesion × time interaction ($F_{19,217} = 3.34$, $p < 0.0001$) in response accuracy (Fig. 4a, Supplementary Table S2). Exercise improved accuracy in lesioned rats ($F_{1,11} = 8.063$, $p = 0.016$), without exercise × time interaction. During the rule reversal Win-Shift phase, there were significant effects of lesion ($F_{1,13} = 41.83$, $p < 0.0001$) and lesion × time interaction ($F_{12,142} = 4.76$, $p < 0.0001$. Fig. 4b). Non-Lesion/Non-Exercise compared to Lesion/Non-Exercise rats reached the learning criterion significantly earlier ($p < 0.00001$. Fig. 4c) and showed fewer perseverative errors ($F_{1,13} = 4.69$, $p < 0.05$. Fig. 4d) and fewer regressive errors ($F_{1,13} = 6.76$, $p < 0.05$. Fig. 4e). During the Win-Shift phase, there was a significant effect of exercise ($F_{1,11} = 15.57$, $p = 0.0023$. Fig. 4b), but no significant exercise × time interaction. Lesion/Complex wheel compared to Lesion/Non-Exercise rats reached the learning criterion significantly earlier ($p < 0.002$. Fig. 4c) and showed fewer perseverative errors ($F_{1,11} = 7.29$, $p < 0.02$. Fig. 4d), with no significant differences in regressive errors (Fig. 4e). In summary, the T-maze detected a clear significant lesion effect during the Win-Stay paradigm, a significant difference that was accentuated during the Win-Shift phase. Lesion rats that underwent complex wheel exercise showed a greater number of correct responses compared with Non-Exercise rats. This effect showed a significant difference during the Win-Stay phase and was accentuated during the Win-Shift phase of training.

3.4. Transcript analysis

Following 6-OHDA lesioning of the dmCPu, the effects of 4 weeks of different exercise modalities – aerobic running in a smooth wheel, or skilled running in a complex wheel with irregularly spaced rungs – on synaptic plasticity (*Syp, Dlg4*) and DAR receptor gene (*Drd1, Drd2, Drd3, Drd4*) expression were examined in four quadrants of the striatum using qRT-PCR. There were no statistically significant differences in gene expression between exercise in the Smooth or Complex Running Wheel groups (Supplementary Fig. S3, Tables S3–S6). Therefore, gene expression data from the two exercise modalities were pooled to form a composite Exercise group, in parallel with the approach in Experiment 1 of the behavioral studies. Final group analyses included Non-lesion/Non-Exercise (n = 6), Lesion/Non-Exercise (n = 6), and Lesion/Exercise (n = 12) (Fig. 5). In the dmCPu, there were significant group differences in *Dlg4* (F(2,21) = 4.61, P = 0.02) and *Drd1* (F(2,21) = 10.07, $p < 0.001$), *Drd3* (F(2,21) = 10.07, P = 0.004), and *Drd4* (F(2,21) = 3.69, P = 0.04) but no significant group differences in *Syp* (F(2,21) = 2.35, P = 0.12) or *Drd2* (F(2,21) = 0.73, P = 0.49). Post hoc analysis showed a significant lesion effect on Dlg4 (PSD-95, $P = 0.04$) and an exercise effect on transcript expression of *Dlg4* ($P = 0.03$), *Drd1* ($p < 0.001$), *Drd3* ($p <$

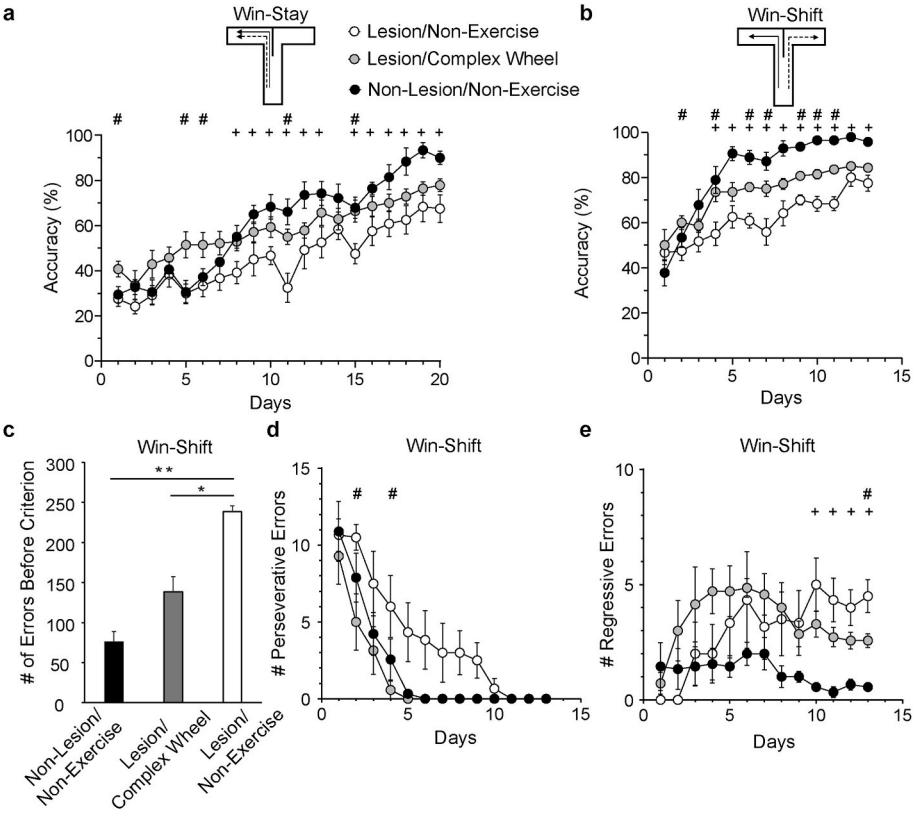

Fig. 4. Effects of lesion and exercise on T-maze learning of rewarded matching-to-sample (Win-Stay) followed by reversal (Win-Shift). **(a)** Rats were trained in a Win-Stay strategy (solid line arrow = sample trial; dashed line arrow = choice trial) for 20 days, followed by training in **(b)** Win-Shift strategy for an additional 13 days. Response accuracy (percentage of correct responses) is shown for Non-Lesion/Non-Exercise ($n = 9$), Lesion/Complex wheel ($n = 7$) and Lesion/Non-Exercise ($n = 6$). **(c)** Total number of incorrect trials performed until criterion (9 correct responses in 10 consecutive trials) was reached during the Win-Shift phase. **(d)** Perseverative errors during the Win-Shift phase. **(e)** Regressive errors during the Win-Shift phase. Mean ± SEM. Exercise improves response accuracy in the T-maze, shortens time until learning, while diminishing perseverative errors following rule reversal (Win-Shift phase). #: $p < 0.05$ Lesion/Complex wheel vs. Lesion/Non-Exercise; +: $p < 0.05$ Lesion/Non-Exercise vs. Non-Lesion/Non-Exercise, Fisher's LSD multiple comparisons test. *: $p < 0.0002$, **: $p < 0.001$ (Student's *t*-test).

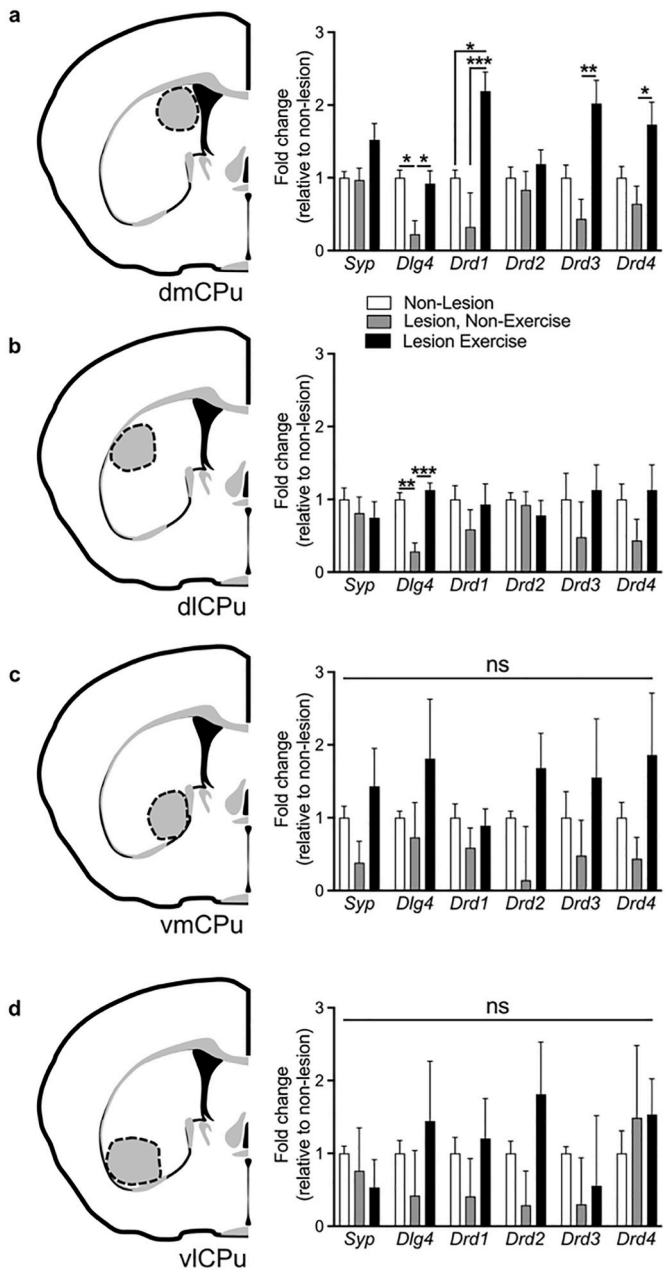

Fig. 5. Dopaminergic signaling and synaptogenic gene expression changes across caudate putamen quadrants following exercise in Lesion rats. Rat caudate putamen was divided into four quadrants for transcript analysis: **(a)** dorsomedial (dmCPu), **(b)** dorsolateral (dlCPu), **(c)** ventromedial (vmCPu), and **(d)** ventrolateral (vlCPu). Corresponding gene expression changes for four DA receptor (*Drd1, Drd2, Drd3, Drd4*) and two synaptic (*Syp, Dlg4*) genes in the exercise group (pooled complex and smooth wheel running, $n = 12$) compared to Non-Exercise controls ($n = 6$). Mean ± SEM. *$p < 0.05$, **$p < 0.01$, ***$p < 0.001$ relative to Non-Exercise control (Student's *t*-test), ns nonsignificant.

0.005), and *Drd4* (P = 0.046) (Fig. 5a). In the dlCPu, there was a significant group difference only in *Dlg*4 ($F(2,21) = 16.57$, $p < 0.001$). Post hoc analysis showed a significant lesion effect on transcript expression of Dlg4 (P = 0.001) and an exercise effect (P = 0.001). (Fig. 5b). In the ventral quadrants of the striatum (vmCPu, vlCPu), there was no statistically significant group difference in transcript expression of *Syp*, *Dlg4*, and *Drd*1, *Drd*2, *Drd*3, and *Drd*4. A complete list of statistical test results can be found in Supplementary Tables S1–S4.

4. Discussion

4.1. Effects of lesions and exercise on cognitive outcomes

Although the rate of acquisition in the 3-CSRT was slower in lesion compared to non-lesion rats, lesion rats were able to acquire a level of accuracy (84%) comparable to that of non-lesion (90%) following 16 days of exercise. This suggests a delay in memory consolidation. There were no significant group differences in premature responses, a measure of impulsive behavior, after 16 days of learning the 3-CSRT. Lesion rats compared to non-lesion rats showed a trend of higher omission rate and a statistically significant greater standard deviation of omissions, suggesting a mild deficit in attention. Consistent with prior work (Hauber and Schmidt, 1994), lesion compared to non-lesion rats had a small but significantly longer reaction time (<1 s) for reward retrieval. This difference was unlikely due to motor deficits as dmCPu lesions do not alter spontaneous locomotor activity, rotarod performance (Wang et al., 2020) or forelimb motor function (Chang et al., 1999). Furthermore, dmCPu lesions do not significantly alter appetitive preference (Wang et al., 2020). Thus, differences in reward retrieval latency (or omissions rate) likely reflect a slowing of cognitive processing and mildly impaired attention, rather than a general motor dysfunction or a lack of motivation.

In contrast to the 3-CSRT, substantial and persistent deficits were unmasked during the 3-CSRT-R phase. During the first day of the 3-CSRT-R, both lesion and non-lesion rats showed an equivalent decrease in nose-poke accuracy. Following 15 days of cognitive training, non-lesion rats rapidly improved (~80% accuracy), while lesion rats showed persistent deficits (~50% accuracy). Performance plateaued thereafter, with an additional 10 days of cognitive training showing little change to the percent accuracy measure (Fig. 3). While a delay in memory consolidation may have contributed, the plateauing of performance beginning at ~15 days for the Lesion/Non-Exercise group suggests that these deficits represent more than simply a slower rate of learning. Lesions also resulted in significant and persistent greater number of premature responses that plateaued at 15 days of cognitive training. We propose that the 3-CSRT-R task unmasked lesion-induced deficits in cognitive flexibility and response inhibition.

Qualitatively, the lesion effect on T-maze learning mirrored those in the operant task. Lesioned rats were slow to learn the Win-Stay task, and never achieved correct response rates above 70%, even after 20 days of cognitive training, while controls achieved a 90% correct response rate by 18 days (Fig. 4). Rule reversal (Win-Shift) enhanced these differences, with the lesioned rats significantly delayed in achieving the learning criterion, and never achieving more than 78% correct after 13 days of cognitive training, at a time when Non-Lesion rats showed 95% correct responses. Perseverative and regressive errors during the reversal phase were significantly greater in Lesion than in Non-Lesion rats as has previously been reported (Grospe et al., 2018).

Our studies showed that exercise in both the operant task and T-maze improved performance in lesioned rats. These results are consistent with earlier work in a rat stroke model showing that running exercise facilitates learning of a subsequent skilled forelimb task (Ploughman et al., 2007). Furthermore, exercise improved nose-poke accuracy during initial learning of the 3-CSRT task. However, as noted above, Lesion/Non-Exercise rats were able to achieve levels of accuracy equivalent to those of the controls and lesioned/exercised rats by days 14–16. The effect of exercise on cognitive improvement was most apparent during the rule shift phase (3-CSRT-R). Here, improvements in accuracy in lesion rats undergoing exercise were progressive, with improvement relative to Lesion/Non-Exercise rats maintained after 25 exercise sessions. Cognitive gains, however, were modest and significant only when exercise of all types was pooled. A greater effect of exercise in lesioned rats was seen on decreases in premature responses, a measure of behavioral impulsivity.

In the T-maze, the effect of exercise on cognitive improvement was

also most apparent during rule reversal (Win-Shift). However, unlike results in the 3-CSRT-R operant task, Lesion/Non-Exercise rats were able to match the performance of lesioned/exercised rats in the T-maze by day 12. The reason likely was that the Win-Shift T-maze task was easier to learn than the 3-CSRT-R operant task as judged by the fewer number of sessions to reach plateau levels in the T-maze. This suggests that exercise can accelerate learning, but for simpler cognitive challenges Lesion/Non-Exercise rats can 'catch up' to the performance of Lesion/Exercise rats. This is in contrast to more challenging tasks such as the 3-CSRT-R, where exercise provided a prolonged performance advantage that extended across 25 test days. Future studies can evaluate this interpretation at longer follow-up periods. Our 6-OHDA PD model assumed that dopaminergic lesions were complete at the 2-week timepoint when exercise was initiated (see section 2.5.1), with exercise-related benefits being understood in the context of neurorestoration. If lesion maturation, however, continued beyond this 2-week timepoint as some have proposed, it is possible that a component of the benefits may have been due to solely neuroprotective rather than neurorestorative mechanisms.

4.2. Changes in dopaminergic receptors and the synaptic marker PSD-95 with lesion and exercise

In these studies, we examined mRNA transcript in striatal tissues and our results showed that by 4 weeks, exercise led to increased transcript expression of both DAR-D1 and the DAR-D2-like receptors 3 and 4 in the dorsal CPu, particularly in the dmCPu, the site with the greatest degree of 6-OHDA-mediated DA-depletion. Dopamine receptors are expressed pre-synaptically within dopaminergic terminals and post-synaptically within medium spiny neurons in the CPu. Since we examined transcripts and most expression is within cell bodies and therefore post-synaptic. Changes in these receptors were concurrent with exercise-induced improvement in cognitive flexibility. In our study, cognitive flexibility was assessed through a reversal learning paradigm in which the learned association of a 'lights-on' cue and its sucrose reward was reversed when a newly presented 'lights-off' cue was associated with the same reward. Cognitive flexibility relies on the interactions of the D1- and D2-like receptors [DAR-D2, DAR-D3, and DAR-D4] (Floresco et al., 2006; Bestmann et al., 2015) at the level of the prefrontal cortex and the striatum. Although the D3-receptor is expressed at a lower level than the D2-receptor within the dorsal striatum, its role and association with the D2-receptor in reversal learning has been well established (Boulougouris et al., 2009; Groman et al., 2016; Clarkson et al., 2017). In addition to the DAR-D3, the DAR-D1 and DAR-D4 also play a role in reversal learning. For example, application of DAR-D1 agonists lead to impairment in the early phase of reversal learning (Izquierdo et al., 2006). The D4-receptor shares a similar modulatory effect on reversal learning to DAR-D1 as demonstrated by the application of a DAR-D4 antagonist and its improvement on reversal learning (Connolly and Gomez-Serrano, 2014). While the importance of the D1-receptor and the D4-receptor signaling in reverse learning has been demonstrated in the prefrontal cortex (Floresco et al., 2006), our study suggests a role of these dopamine receptors in cognitive flexibility also at the level of the dorsomedial striatum. Our results are consistent with recent reports showing that D1-receptors on medium spiny neurons in the dmCPu play an important role in reversal tasks (Wang et al., 2019).

Previous work in our lab using the MPTP model of dopamine depletion, has shown an exercise-induced increase of DAR-D2 in the dorsal CPu (Fisher et al., 2004) after six-weeks of intensive treadmill exercise. In contrast to our previous exercise studies, we found no significant increase in DAR-D2 in the dorsomedial CPu after 4-weeks of wheel running. Possible explanations for this discrepancy include differences in exercise duration, intensity, and choice of toxin and location of DA-depletion. Unlike the dorsal CPU, we found no exercise-induced effects on DA receptor transcript expression in the ventral CPu. In addition, we saw no lesion effect on dopamine receptor transcript expression within the dorsal or ventral striatum. These findings are consistent with the literature which have shown both significant and non-significant changes in the DAR-D1 and DAR-D2 after dopamine depletion, which may due to differences in lesioning paradigms [degree of lesioning, post-lesioning time point, species, toxin and mode of delivery] (Berger et al., 1991; Cadet et al., 1991).

In these studies, using qRT-PCR, we examined mRNA transcript expression in striatal tissues for PSD-95 and synaptophysin. PSD-95 is a major scaffolding protein in the postsynaptic densities of dendritic spines enriched in glutamatergic medium spiny neurons. We found that dopamine depletion in the dorsal CPu was associated with loss of PSD-95 mRNA transcripts and that exercise significantly increased PSD-95 expression in 6-OHDA lesioned rats. This finding likely reflects the increased expression of this transcript in striatal medium spiny neurons, the cells within the striatum that express this synaptic gene and proteins at post-synaptic contacts. This increase in PSD-95 is consistent with synaptogenesis and could be occurring in either or both glutamatergic and dopaminergic terminals at medium spiny neurons. Previous work in non-human primates and mice has demonstrated a significant reduction in dendritic spine density in the striatum of monkeys and mice following dopaminergic deafferentation (Villalba et al., 2009; Toy et al., 2014), with exercise eliciting a significant restoration of spine density, along with increases in synaptophysin and PSD-95 protein expression (Toy et al., 2014). We did not observe changes in synaptophysin mRNA transcripts in striatal tissues which differs in the patterns of change in protein we and others have reported. This may reflect the fact that this protein, expressed in pre-synaptic terminals is transcribes in cell bodies that reside outside of the striatum such as the cerebral cortex or thalamus. The transcriptional and translational mechanisms by which exercise may restore synaptophysin and PSD-95 expression in our model remains unknown. Prior work in the 6-OHDA model has suggested a role for Arc (activity-regulated cytoskeleton-associated protein) (Garcia et al., 2017), acting as a generalized transcription factor that can modulate dendritic spine formation and experience-dependent neuroplasticity (Peebles et al., 2010).

4.3. Translational aspects

Behavioral studies have shown that despite their slower learning-rates, PD subjects retain more or less intact motor learning (Nieuwboer et al., 2009). However, 'task-switching deficits' makes it difficult to translate learning acquired in a rehabilitation session to a real-world situation where responses must be adapted to context (Onla-or and Winstein, 2008). This inflexibility of thought and associated increased cognitive retention rates leads to errors of repetition when transferring between new categories of learning (Steinke and Kopp, 2020). We made a similar observation in our animal model. While the rate of acquisition of the 3-CSRT was delayed, lesioned rats were able to acquire a level of accuracy comparable to that of sham rats within 16 days of exercise (though not in the T-maze task). However, dramatic and persistent deficits were apparent in both the operant and T-maze tasks following the rule shift, such that lesioned rats never improved their performance much above chance levels, even after an extended period of exercise.

4.3.1. Effects of exercise on cognitive flexibility

Prior studies in naïve rodents have shown that exercise can facilitate reversal learning (Van der Borght et al., 2007; Snigdha et al., 2014; O'Leary et al., 2019). Our findings show that exercise-related improvements in cognitive flexibility can also be seen in the 6-OHDA striatal lesion model. Exercise is well known to elicit broad changes in neuroplasticity, including increases in neurogenesis (Ma et al., 2017). Increases in exercise-related neurogenesis have been reported to be associated with lower memory retention, while at the same time facilitating new learning, including reversal learning (Li et al., 2020). It has been proposed that such improved new learning may be the result of a decrease in proactive interference which usually occurs when

consolidated memories inhibit new learning (Epp et al., 2016). While in the current study, exercise effects on nose-poke accuracy of lesioned rats were modest during the reversal phase, greater effects were noted for premature responses, a measure of impulsivity and response inhibition. The decrease in premature responses is consistent with an improved ability of the exercised animal to acquire new learning, either because of a lower exercise-related recall of the prior rule set as previously proposed (Epp et al., 2016; Li et al., 2020), or possibly through facilitated suppression of the prior rule-based learning. The findings of diminished premature responses mirror a report in PD patients where 6 weeks of intermittent aerobic walking elicits significant improvement in cognitive inhibition (Flanker test) but not in set shifting (Wisconsin card sort, Trail Making tests) (Uc et al., 2014). Others have observed improvements in inhibitory aptitude (Stroop test) but not in cognitive flexibility (Trail making test) in PD patients following 3 months of intermittent aerobic cycling (Duchesne et al., 2015).

Improved cognitive flexibility may reflect underlying functional adaptation in cerebral regions of the cortico-striatal-thalamo-cortical and cortical-thalamo-hippocampal circuits (Wang et al., 2013), important in executive function and working memory. It has been suggested that motor rehabilitation programs for PD patients should include a relatively high cognitive demand, such that by engaging patients to practice task-switching, they might be able to overcome their context-dependency (Onla-or and Winstein, 2008; Petzinger et al., 2013). Surprisingly, we did not see a significant difference in cognitive outcomes in comparing different exercise modalities in lesioned rats (see Supplementary Fig. S2). This observation was valid even when exercise was undertaken for two different skill levels at comparable speeds and durations using the same exercise modality (complex versus smooth wheel running, Fig. S2). This was contrary to our expectation which, based on greater functional connectivity of the medial prefrontal-striatal circuit during acute walking in the skilled compared to the smooth wheel, had anticipated a differential cognitive effect of these different exercise modalities (Guo et al., 2017). Our findings differed from those reported in a recent meta-analysis in healthy human subjects, where there appears to be higher benefits after coordinative exercise compared to endurance, resistance and mixed exercise (Ludyga et al., 2020). In contrast, a recent systematic review of randomized controlled trials of physical exercise programs on cognitive function in PD reported that exercise-related improvements in global cognitive function, processing speed, sustained attention and mental flexibility (da Silva et al., 2018) showed the largest effect for intense treadmill exercise, not for skilled exercise (tango or cognitive exercise associated with motor exercise). However, a head-to-head comparison of different exercise modalities on cognitive function has to date not been done in PD patients. In our study, though behavioral outcomes of nose poke accuracy closely tracked across different exercise modalities, our study was insufficiently powered to detect small differences. Furthermore, we did not explore a full range of exercise durations and intensities, variables that in prior studies have shown differential efficacy across different exercise modalities (Coetsee and Terblanche, 2017; Ludyga et al., 2020), though this itself remains controversial (Sanders et al., 2020; Brown et al., 2021). Exercise was maintained for up to 12 weeks during the acquisition and testing phases of our cognitive testing. Future studies may wish to explore the effects of a broader range of exercise intensities and durations across different exercise modalities (da Costa Daniele et al., 2020).

5. Conclusion

In summary, our data adds to the expanding research reports showing the beneficial cognitive effects of physical exercise. Our prospective study demonstrates that following dopaminergic deafferentation, moderate exercise is able to provide improvements in cognitive flexibility and inhibitory aptitude, while eliciting increased expression of Drd1, Drd3, Drd4, synaptophysin, and PSD-95 in the associative and sensorimotor dorsal regions of the striatum.

Funding sources

Don Roberto Gonzalez Family Foundation (GP); Parkinson's Foundation (GP); US Army Medical Research and Materiel Command Parkinson Research Program (USAMRMC) Congressionally Directed Medical Research Programs (CDMRP), Grant/Award Numbers: W81XWH18-0665 (GMP), W81XWH18-00443 (MWJ), W81XWH18-1-0666 (DPH).

Credit authorship contribution statement

Wang Zhuo: contributed to the conception and design of the study, contributed to data acquisition, was responsible for data analysis, were responsible for statistical analyses. **Adam J. Lundquist:** contributed to the conception and design of the study, contributed to data acquisition; were responsible for data analysis, was responsible for statistical analyses. **Erin K. Donahue:** contributed to the conception and design of the study, contributed to data acquisition; was responsible for data analysis. **Yumei Guo:** contributed to the conception and design of the study, contributed to data acquisition, was responsible for data analysis, were responsible for writing and editing the manuscript. **Derek Phillips:** contributed to data acquisition. **Giselle M. Petzinger:** contributed to the conception and design of the study, was responsible for data analysis, were responsible for writing and editing the manuscript, were responsible for acquisition of funding support. **Michael W. Jakowec:** contributed to the conception and design of the study. **Daniel P. Holschneider:** contributed to the conception and design of the study, contributed to data acquisition, was responsible for data analysis, was responsible for writing and editing the manuscript, was responsible for acquisition of funding support.

Declaration of competing interest

The authors declare the following financial interests/personal relationships which may be considered as potential competing interests: Daniel Holschneider, Giselle Petzinger, Michael Jakowec reports financial support was provided by Department of Defense and by the US Army Medical Research and Materiel Command Parkinson Research Program. Giselle Petzinger reports financial support was provided by Don Roberto Gonzalez Family Foundation.

Acknowledgements

The authors would like to thank the contributions of friends of the PD Research Program at USC. Special thanks to lab members for their helpful discussions. Thank you to Dan Haase, Ryan Wang, Susan Kishi, Tyler Gallagher, and Ilse Flores who participated in the exercising of animals.

Appendix A. Supplementary data

Supplementary data to this article can be found online at https://doi.org/10.1016/j.crneur.2022.100039.

References

Alberts, J.L., Linder, S.M., Penko, A.L., Lowe, M.J., Phillips, M., 2011. It is not about the bike, it is about the pedaling: forced exercise and Parkinson's disease. Exerc. Sport Sci. Rev. 39 (4), 177–186.

Apostolova, I., Lange, C., Frings, L., Klutmann, S., Meyer, P.T., Buchert, R., 2020. Nigrostriatal degeneration in the cognitive part of the striatum in Parkinson disease is associated with frontomedial hypometabolism. Clin. Nucl. Med. 45 (2), 95–99.

Asinof, S.K., Paine, T.A., 2014. The 5-choice serial reaction time task: a task of attention and impulse control for rodents. JoVE 90, e51574.

Baker, P.M., Ragozzino, M.E., 2014. Contralateral disconnection of the rat prelimbic cortex and dorsomedial striatum impairs cue-guided behavioral switching. Learn. Mem. 21 (8), 368–379.

Ben, V., Blin, O., Bruguerolle, B., 1999. Time-dependent striatal dopamine depletion after injection of 6-hydroxydopamine in the rat. Comparison of single bilateral and double bilateral lesions. J. Pharm. Pharmacol. 51 (12), 1405–1408.
Berger, K., Przedborski, S., Cadet, J.L., 1991. Retrograde degeneration of nigrostriatal neurons induced by intrastriatal 6-hydroxydopamine injection in rats. Brain Res. Bull. 26 (2), 301–307.
Bestmann, S., Ruge, D., Rothwell, J., Galea, J.M., 2015. The role of dopamine in motor flexibility. J. Cognit. Neurosci. 27 (2), 365–376.
Blandini, F., Levandis, G., Bazzini, E., Nappi, G., Armentero, M.T., 2007. Time-course of nigrostriatal damage, basal ganglia metabolic changes and behavioural alterations following intrastriatal injection of 6-hydroxydopamine in the rat: new clues from an old model. Eur. J. Neurosci. 25 (2), 397–405.
Boulougouris, V., Castañé, A., Robbins, T.W., 2009. Dopamine D2/D3 receptor agonist quinpirole impairs spatial reversal learning in rats: investigation of D3 receptor involvement in persistent behavior. Psychopharmacology (Berl) 202 (4), 611–620.
Brown, B.M., Frost, N., Rainey-Smith, S.R., Doecke, J., Markovic, S., Gordon, N., Weinborn, M., Sohrabi, H.R., Laws, S.M., Martins, R.N., Erickson, K.I., Peiffer, J.J., 2021. High-intensity exercise and cognitive function in cognitively normal older adults: a pilot randomised clinical trial. Alzheimer's Res. Ther. 13 (1), 33.
Brown, H.D., Baker, P.M., Ragozzino, M.E., 2010. The parafascicular thalamic nucleus concomitantly influences behavioral flexibility and dorsomedial striatal acetylcholine output in rats. J. Neurosci. 30 (43), 14390–14398.
Burn, D., Weintraub, D., Ravina, B., Litvan, I., 2014. Cognition in movement disorders: where can we hope to be in ten years? Mov. Disord. 29 (5), 704–711.
Cadet, J.L., Last, R., Kostic, V., Przedborski, S., Jackson-Lewis, V., 1991. Long-term behavioral and biochemical effects of 6-hydroxydopamine injections in rat caudate-putamen. Brain Res. Bull. 26 (5), 707–713.
Chang, J.W., Wachtel, S.R., Young, D., Kang, U.J., 1999. Biochemical and anatomical characterization of forepaw adjusting steps in rat models of Parkinson's disease: studies on medial forebrain bundle and striatal lesions. Neuroscience 88 (2), 617–628.
Chudasama, Y., Bussey, T.J., Muir, J.L., 2001. Effects of selective thalamic and prelimbic cortex lesions on two types of visual discrimination and reversal learning. Eur. J. Neurosci. 14 (6), 1009–1020.
Clarkson, R.L., Liptak, A.T., Gee, S.M., Sohal, V.S., Bender, K.J., 2017. D3 receptors regulate excitability in a unique class of prefrontal pyramidal cells. J. Neurosci. 37 (24), 5846–5860.
Coetsee, C., Terblanche, E., 2017. The effect of three different exercise training modalities on cognitive and physical function in a healthy older population. Eur. Rev. Aging Phys. Act. 14, 13.
Connolly, N.P., Gomez-Serrano, M., 2014. D4 dopamine receptor-specific antagonist improves reversal learning impairment in amphetamine-treated male rats. Exp. Clin. Psychopharmacol 22 (6), 557–564.
Cools, R., 2006. Dopaminergic modulation of cognitive function-implications for L-DOPA treatment in Parkinson's disease. Neurosci. Biobehav. Rev. 30 (1), 1–23.
da Costa Daniele, T.M., de Bruin, P.F.C., de Matos, R.S., de Bruin, G.S., Maia Chaves, C.J., de Bruin, V.M.S., 2020. Exercise effects on brain and behavior in healthy mice, Alzheimer's disease and Parkinson's disease model-A systematic review and meta-analysis. Behav. Brain Res. 383, 112488.
da Silva, F.C., Iop, R.D.R., de Oliveira, L.C., Boll, A.M., de Alvarenga, J.G.S., Gutierres Filho, P.J.B., de Melo, L., Xavier, A.J., da Silva, R., 2018. Effects of physical exercise programs on cognitive function in Parkinson's disease patients: a systematic review of randomized controlled trials of the last 10 years. PLoS One 13 (2), e0193113.
Deacon, R.M., Rawlins, J.N., 2006. T-maze alternation in the rodent. Nat. Protoc. 1 (1), 7–12.
Dirnberger, G., Jahanshahi, M., 2013. Executive dysfunction in Parkinson's disease: a review. J. Neuropsychol. 7 (2), 193–224.
Dorsey, E.R., George, B.P., Leff, B., Willis, A.W., 2013. The coming crisis: obtaining care for the growing burden of neurodegenerative conditions. Neurology 80 (21), 1989–1996.
Duchesne, C., Lungu, O., Nadeau, A., Robillard, M.E., Bore, A., Bobeuf, F., Lafontaine, A. L., Gheysen, F., Bherer, L., Doyon, J., 2015. Enhancing both motor and cognitive functioning in Parkinson's disease: aerobic exercise as a rehabilitative intervention. Brain Cognit. 99, 68–77.
Epp, J.R., Silva Mera, R., Köhler, S., Josselyn, S.A., Frankland, P.W., 2016. Neurogenesis-mediated forgetting minimizes proactive interference. Nat. Commun. 7, 10838.
Fisher, B.E., Petzinger, G.M., Nixon, K., Hogg, E., Bremmer, S., Meshul, C.K., Jakowec, M. W., 2004. Exercise-induced behavioral recovery and neuroplasticity in the 1-methyl-4-phenyl-1,2,3,6-tetrahydropyridine-lesioned mouse basal ganglia. J. Neurosci. Res. 77 (3), 378–390.
Floresco, S.B., Magyar, O., Ghods-Sharifi, S., Vexelman, C., Tse, M.T., 2006. Multiple dopamine receptor subtypes in the medial prefrontal cortex of the rat regulate set-shifting. Neuropsychopharmacology 31 (2), 297–309.
Garcia, P.C., Real, C.C., Britto, L.R., 2017. The impact of short and long-term exercise on the expression of arc and AMPARs during evolution of the 6-hydroxy-dopamine animal model of Parkinson's disease. J. Mol. Neurosci. 61 (4), 542–552.
Groman, S.M., Smith, N.J., Petrullli, J.R., Massi, B., Chen, L., Ropchan, J., Huang, Y., Lee, D., Morris, E.D., Taylor, J.R., 2016. Dopamine D3 receptor availability is associated with inflexible decision making. J. Neurosci. 36 (25), 6732–6741.
Grospe, G.M., Baker, P.M., Ragozzino, M.E., 2018. Cognitive flexibility deficits following 6-OHDA lesions of the rat dorsomedial striatum. Neuroscience 374, 80–90.
Guo, Y., Wang, Z., Prathap, S., Holschneider, D.P., 2017. Recruitment of prefrontal-striatal circuit in response to skilled motor challenge. Neuroreport 28 (18), 1187–1194.
Hauber, W., Schmidt, W.J., 1994. Differential effects of lesions of the dorsomedial and dorsolateral caudate-putamen on reaction time performance in rats. Behav. Brain Res. 60 (2), 211–215.
Hirano, S., 2021. Clinical implications for dopaminergic and functional neuroimage research in cognitive symptoms of Parkinson's disease. Mol. Med. 27 (1), 40.
Intzandt, B., Beck, E.N., Silveira, C.R.A., 2018. The effects of exercise on cognition and gait in Parkinson's disease: a scoping review. Neurosci. Biobehav. Rev. 95, 136–169.
Izquierdo, A., Wiedholz, L.M., Millstein, R.A., Yang, R.J., Bussey, T.J., Saksida, L.M., Holmes, A., 2006. Genetic and dopaminergic modulation of reversal learning in a touchscreen-based operant procedure for mice. Behav. Brain Res. 171 (2), 181–188.
Kim, H., Oh, M., Oh, J.S., Moon, H., Chung, S.J., Lee, C.S., Kim, J.S., 2019. Association of striatal dopaminergic neuronal integrity with cognitive dysfunction and cerebral cortical metabolism in Parkinson's disease with mild cognitive impairment. Nucl. Med. Commun. 40 (12), 1216–1223.
Kintz, N., Petzinger, G.M., Akopian, G., Ptasnik, S., Williams, C., Jakowec, M.W., Walsh, J.P., 2013. Exercise modifies alpha-amino-3-hydroxy-5-methyl-4-isoxazolepropionic acid receptor expression in striatopallidal neurons in the 1-methyl-4-phenyl-1,2,3,6-tetrahydropyridine-lesioned mouse. J. Neurosci. Res. 91 (11), 1492–1507.
Kowal, S.L., Dall, T.M., Chakrabarti, R., Storm, M.V., Jain, A., 2013. The current and projected economic burden of Parkinson's disease in the United States. Mov. Disord. 28 (3), 311–318.
Li, C., Li, R., Zhou, C., 2020. Memory traces diminished by exercise affect new learning as proactive facilitation. Front. Neurosci. 14, 189.
Livak, K.J., Schmittgen, T.D., 2001. Analysis of relative gene expression data using real-time quantitative PCR and the 2(-Delta Delta C(T)) Method. Methods 25 (4), 402–408.
Ludyga, S., Gerber, M., Puhse, U., Looser, V.N., Kamijo, K., 2020. Systematic review and meta-analysis investigating moderators of long-term effects of exercise on cognition in healthy individuals. Nat. Human Behav.
Lundquist, A.J., Gallagher, T.J., Petzinger, G.M., Jakowec, M.W., 2021. Exogenous l-lactate promotes astrocyte plasticity but is not sufficient for enhancing striatal synaptogenesis or motor behavior in mice. J. Neurosci. Res. 99 (5), 1433–1447.
Lundquist, A.J., Parizher, J., Petzinger, G.M., Jakowec, M.W., 2019. Exercise induces region-specific remodeling of astrocyte morphology and reactive astrocyte gene expression patterns in male mice. J. Neurosci. Res. 97 (9), 1081–1094.
Ma, C.L., Ma, X.T., Wang, J.J., Liu, H., Chen, Y.F., Yang, Y., 2017. Physical exercise induces hippocampal neurogenesis and prevents cognitive decline. Behav. Brain Res. 317, 332–339.
Macdonald, P.A., Monchi, O., 2011. Differential effects of dopaminergic therapies on dorsal and ventral striatum in Parkinson's disease: implications for cognitive function. Parkinsons Dis 2011, 572743.
Mayer, G.S., Shoup, R.E., 1983. Simultaneous multiple electrode liquid chromatographic-electrochemical assay for catecholamines, indole-amines and metabolites in brain tissue. J. Chromatogr. 255, 533–544.
Nieuwboer, A., Rochester, L., Muncks, L., Swinnen, S.P., 2009. Motor learning in Parkinson's disease: limitations and potential for rehabilitation. Park. Relat. Disord. 15 (Suppl. 3), S53–S58.
O'Leary, J.D., Hoban, A.E., Murphy, A., O'Leary, O.F., Cryan, J.F., Nolan, Y.M., 2019. Differential effects of adolescent and adult-initiated exercise on cognition and hippocampal neurogenesis. Hippocampus 29 (4), 352–365.
O'Neill, M., Brown, V.J., 2007. The effect of striatal dopamine depletion and the adenosine A2A antagonist KW-6002 on reversal learning in rats. Neurobiol. Learn. Mem. 88 (1), 75–81.
Onla-or, S., Winstein, C.J., 2008. Determining the optimal challenge point for motor skill learning in adults with moderately severe Parkinson's disease. Neurorehabilitation Neural Repair 22 (4), 385–395.
Parker, K.L., Lamichhane, D., Caetano, M.S., Narayanan, N.S., 2013. Executive dysfunction in Parkinson's disease and timing deficits. Front. Integr. Neurosci. 7, 75.
Peebles, C.L., Yoo, J., Thwin, M.T., Palop, J.J., Noebels, J.L., Finkbeiner, S., 2010. Arc regulates spine morphology and maintains network stability in vivo. Proc. Natl. Acad. Sci. U. S. A. 107 (42), 18173–18178.
Petzinger, G.M., Fisher, B.E., McEwen, S., Beeler, J.A., Walsh, J.P., Jakowec, M.W., 2013. Exercise-enhanced neuroplasticity targeting motor and cognitive circuitry in Parkinson's disease. Lancet Neurol. 12 (7), 716–726.
Ploughman, M., Attwood, Z., White, N., Dore, J.J., Corbett, D., 2007. Endurance exercise facilitates relearning of forelimb motor skill after focal ischemia. Eur. J. Neurosci. 25 (11), 3453–3460.
Robbins, T.W., Cools, R., 2014. Cognitive deficits in Parkinson's disease: a cognitive neuroscience perspective. Mov. Disord. 29 (5), 597–607.
Roberts, D.C., Zis, A.P., Fibiger, H.C., 1975. Ascending catecholamine pathways and amphetamine-induced locomotor activity: importance of dopamine and apparent non-involvement of norepinephrine. Brain Res. 93 (3), 441–454.
Sala-Bayo, J., Fiddian, L., Nilsson, S.R.O., Hervig, M.E., McKenzie, C., Mareschi, A., Boulos, M., Zhukovsky, P., Nicholson, J., Dalley, J.W., Alsiö, J., Robbins, T.W., 2020. Dorsal and ventral striatal dopamine D1 and D2 receptors differentially modulate distinct phases of serial visual reversal learning. Neuropsychopharmacology 45 (5), 736–744.
Salame, S., Garcia, P.C., Real, C.C., Borborema, J., Mota-Ortiz, S.R., Britto, L.R., Pires, R. S., 2016. Distinct neuroplasticity processes are induced by different periods of acrobatic exercise training. Behav. Brain Res. 308, 64–74.
Sanders, L.M.J., Hortobágyi, T., Karssemeijer, E.G.A., Van der Zee, E.A., Scherder, E.J.A., van Heuvelen, M.J.G., 2020. Effects of low- and high-intensity physical exercise on physical and cognitive function in older persons with dementia: a randomized controlled trial. Alzheimer's Res. Ther. 12 (1), 28.

Sauer, H., Oertel, W.H., 1994. Progressive degeneration of nigrostriatal dopamine neurons following intrastriatal terminal lesions with 6-hydroxydopamine: a combined retrograde tracing and immunocytochemical study in the rat. Neuroscience 59 (2), 401–415.
Schootemeijer, S., van der Kolk, N.M., Bloem, B.R., de Vries, N.M., 2020. Current perspectives on aerobic exercise in people with Parkinson's disease. Neurotherapeutics 17 (4), 1418–1433.
Snigdha, S., de Rivera, C., Milgram, N.W., Cotman, C.W., 2014. Exercise enhances memory consolidation in the aging brain. Front. Aging Neurosci. 6, 3.
Stefanko, D.P., Shah, V.D., Yamasaki, W.K., Petzinger, G.M., Jakowec, M.W., 2017. Treadmill exercise delays the onset of non-motor behaviors and striatal pathology in the CAG140 knock-in mouse model of Huntington's disease. Neurobiol. Dis. 105, 15–32.
Steinke, A., Kopp, B., 2020. Toward a computational neuropsychology of cognitive flexibility. Brain Sci. 10 (12).
Stögbauer, J., Rosar, F., Dillmann, U., Faßbender, K., Ezziddin, S., Spiegel, J., 2020. Striatal dopamine transporters and cognitive function in Parkinson's disease. Acta Neurol. Scand. 142 (4), 385–391.
Tait, D.S., Phillips, J.M., Blackwell, A.D., Brown, V.J., 2017. Effects of lesions of the subthalamic nucleus/zona incerta area and dorsomedial striatum on attentional set-shifting in the rat. Neuroscience 345, 287–296.
Thoma, P., Koch, B., Heyder, K., Schwarz, M., Daum, I., 2008. Subcortical contributions to multitasking and response inhibition. Behav. Brain Res. 194 (2), 214–222.
Toy, W.A., Petzinger, G.M., Leyshon, B.J., Akopian, G.K., Walsh, J.P., Hoffman, M.V., Vučković, M.G., Jakowec, M.W., 2014. Treadmill exercise reverses dendritic spine loss in direct and indirect striatal medium spiny neurons in the 1-methyl-4-phenyl-1,2,3,6-tetrahydropyridine (MPTP) mouse model of Parkinson's disease. Neurobiol. Dis. 63, 201–209.
Uc, E.Y., Doerschug, K.C., Magnotta, V., Dawson, J.D., Thomsen, T.R., Kline, J.N., Rizzo, M., Newman, S.R., Mehta, S., Grabowski, T.J., Bruss, J., Blanchette, D.R., Anderson, S.W., Voss, M.W., Kramer, A.F., Darling, W.G., 2014. Phase I/II randomized trial of aerobic exercise in Parkinson disease in a community setting. Neurology 83 (5), 413–425.
Van der Borght, K., Havekes, R., Bos, T., Eggen, B.J., Van der Zee, E.A., 2007. Exercise improves memory acquisition and retrieval in the Y-maze task: relationship with hippocampal neurogenesis. Behav. Neurosci. 121 (2), 324–334.
van Schouwenburg, M., Aarts, E., Cools, R., 2010. Dopaminergic modulation of cognitive control: distinct roles for the prefrontal cortex and the basal ganglia. Curr. Pharmaceut. Des. 16 (18), 2026–2032.
Villalba, R.M., Lee, H., Smith, Y., 2009. Dopaminergic denervation and spine loss in the striatum of MPTP-treated monkeys. Exp. Neurol. 215 (2), 220–227.
Voorn, P., Vanderschuren, L.J., Groenewegen, H.J., Robbins, T.W., Pennartz, C.M., 2004. Putting a spin on the dorsal-ventral divide of the striatum. Trends Neurosci. 27 (8), 468–474.
Wang, X., Qiao, Y., Dai, Z., Sui, N., Shen, F., Zhang, J., Liang, J., 2019. Medium spiny neurons of the anterior dorsomedial striatum mediate reversal learning in a cell-type-dependent manner. Brain Struct. Funct. 224 (1), 419–434.
Wang, Z., Flores, I., Donahue, E.K., Lundquist, A.J., Guo, Y., Petzinger, G.M., Jakowec, M.W., Holschneider, D.P., 2020. Cognitive flexibility deficits in rats with dorsomedial striatal 6-hydroxydopamine lesions tested using a three-choice serial reaction time task with reversal learning. Neuroreport 31 (15), 1055–1064.
Wang, Z., Guo, Y., Myers, K.G., Heintz, R., Holschneider, D.P., 2015a. Recruitment of the prefrontal cortex and cerebellum in Parkinsonian rats following skilled aerobic exercise. Neurobiol. Dis. 77, 71–87.
Wang, Z., Guo, Y., Myers, K.G., Heintz, R., Peng, Y.H., Maarek, J.M., Holschneider, D.P., 2015b. Exercise alters resting-state functional connectivity of motor circuits in parkinsonian rats. Neurobiol. Aging 36 (1), 536–544.
Wang, Z., Myers, K.G., Guo, Y., Ocampo, M.A., Pang, R.D., Jakowec, M.W., Holschneider, D.P., 2013. Functional reorganization of motor and limbic circuits after exercise training in a rat model of bilateral parkinsonism. PLoS One 8 (11), e80058.
Yehene, E., Meiran, N., Soroker, N., 2008. Basal ganglia play a unique role in task switching within the frontal-subcortical circuits: evidence from patients with focal lesions. J. Cognit. Neurosci. 20 (6), 1079–1093.
Yuan, H., Sarre, S., Ebinger, G., Michotte, Y., 2005. Histological, behavioural and neurochemical evaluation of medial forebrain bundle and striatal 6-OHDA lesions as rat models of Parkinson's disease. J. Neurosci. Methods 144 (1), 35–45.

Molecular Neurobiology
https://doi.org/10.1007/s12035-021-02651-z

Knockdown of Astrocytic Monocarboxylate Transporter 4 in the Motor Cortex Leads to Loss of Dendritic Spines and a Deficit in Motor Learning

Adam J. Lundquist[1,2] · George N. Llewellyn[3] · Susan H. Kishi[2] · Nicolaus A. Jakowec[3,4] · Paula M. Cannon[3] · Giselle M. Petzinger[2] · Michael W. Jakowec[2]

Received: 9 August 2021 / Accepted: 16 November 2021

Abstract

Monocarboxylate transporters (MCTs) shuttle molecules, including L-lactate, involved in metabolism and cell signaling of the central nervous system. Astrocyte-specific MCT4 is a key component of the astrocyte-neuron lactate shuttle (ANLS) and is important for neuroplasticity and learning of the hippocampus. However, the importance of astrocyte-specific MCT4 in neuroplasticity of the M1 primary motor cortex remains unknown. In this study, we investigated astrocyte-specific MCT4 in motor learning and neuroplasticity of the M1 primary motor cortex using a cell-type specific shRNA knockdown of MCT4. Knockdown of astrocyte-specific MCT4 resulted in impaired motor performance and learning on the accelerating rotarod. In addition, MCT4 knockdown was associated with a reduction of neuronal dendritic spine density and spine width and decreased protein expression of PSD95, Arc, and cFos. Using near-infrared–conjugated 2-deoxyglucose uptake as a surrogate marker for neuronal activity, MCT4 knockdown was also associated with decreased neuronal activity in the M1 primary motor cortex and associated motor regions including the dorsal striatum and ventral thalamus. Our study supports a potential role for astrocyte-specific MCT4 and the ANLS in the neuroplasticity of the M1 primary motor cortex. Targeting MCT4 may serve to enhance neuroplasticity and motor repair in several neurological disorders, including Parkinson's disease and stroke.

Keywords Astrocyte · Lactate · Gene knockdown · Motor behavior · Golgi staining

Abbreviations

2DG-IR	Near-infrared–conjugated 2-deoxyglucose
4-OHT	4-Hydroxytamoxifen
ANLS	Astrocyte-neuron lactate shuttle
ANOVA	Analysis of variance
Arc	Activity-regulated cytoskeleton-associated protein
M1	Primary motor cortex
MCT	Monocarboxylate transporter
PSD95	Postsynaptic density protein 95
shRNA	Short-hairpin RNA
SOX9	SRY-box transcription factor 9

✉ Adam J. Lundquist
lundquistaj@gmail.com

[1] Neuroscience Graduate Program, University of Southern California, Los Angeles, CA 90033, USA

[2] Department of Neurology, University of Southern California, 1333 San Pablo St, MCA-241, Los Angeles, CA 90033, USA

[3] Department of Molecular Microbiology and Immunology, Keck School of Medicine, University of Southern California, Los Angeles, CA 90033, USA

[4] Molecular and Cellular Biology Graduate Program, Department of Biological Sciences, University of Southern California, Los Angeles, CA 90033, USA

Introduction

Monocarboxylate transporters (MCTs) are a class of central nervous system (CNS) proteins that mediate the movement of small molecules involved in metabolism and cell signaling including L-lactate, beta-hydroxybutyrate, and other ketones. This family of transporters is composed of proteins MCT1 to MCT4, which are selectively expressed within the mammalian nervous system [1]. MCT1 is expressed in astrocytes and oligodendrocytes [2], MCT2 is localized to neurons [3, 4], MCT3 is localized to the retina and choroid plexus [5], and MCT4 is predominantly expressed by astrocytes [6, 7]. While astrocytes express both MCT1 and MCT4, their distinct subcellular localization are believed to subserve the shuttling of L-lactate

Published online: 25 November 2021

differently. MCT1 is known to localize to the vasculature and influx lactate [8–10]; in contrast, MCT4 is localized to astrocyte processes [7, 11] and serves as a major transporter to efflux L-lactate from astrocytes to neuronal synapses, formulating what is termed the astrocyte-neuron lactate shuttle (ANLS) [12]. The ANLS has been implicated in both regulating increased neuronal activity and metabolism as well as serving to regulate cell signaling and gene expression important for mediating synaptogenesis and neuroplasticity [13, 14].

The majority of studies reporting the role of the ANLS and L-lactate transport involvement in neuroplasticity, including memory and learning, have focused on the hippocampus [15]. For example, genetic knockdown of the ANLS has been repeatedly shown to impair long-term potentiation and dendritic spine density as well as spatial memory acquisition and consolidation in the rodent brain [16–19]. A more recent study has also shown that the ANLS plays a role in the prefrontal cortex, with knockdown of MCT4 resulting in a loss of a stress-induced coping response [20]. However, a major gap in knowledge is the role of MCT4 and the ANLS in mediating neuroplasticity of other cortical brain regions, including the M1 primary motor cortex. The M1 primary motor cortex is affected in many brain disorders, leading to extensive motor impairments and disability [21]. Identifying targets that may facilitate neuroplasticity may prove useful for promoting rehabilitation and restoring motor function and quality of life.

To study the potential role of MCT4 on M1 primary motor cortex–mediated behavior, we used a cell-type specific, Cre-recombinase–controlled lentiviral vector construct to selectively knockdown the expression of MCT4 in astrocytes. Following *in vitro* and *in vivo* validation, we evaluated the astrocyte-specific knockdown of MCT4 on motor behavior and pyramidal neuron synaptic structure and function. We compared mice having astrocyte-specific knockdown of MCT4 in the M1 primary motor cortex with normal controls on motor behavior on the accelerating rotarod as well as its impact on dendritic spine density and the pattern of expression of several proteins important for synaptic structure and neuroplasticity. We also examined the impact of MCT4 knockdown on neuronal activity through uptake of the ligand 2-deoxyglucose within the M1 primary motor cortex, the site of MCT4 knockdown, and a subset of anatomical sites involved in motor behavior. Overall, our findings show that astrocyte-specific MCT4 is likely important for cortical dendritic spine structure and motor learning and extends the role of the ANLS in the neuroplasticity of the M1 primary motor cortex.

Methods and Materials

Mice

Heterozygous *Aldh1l1*-CreERT2$^{+/-}$ (termed Cre^{+} mice) male mice expressing Cre-recombinase selectively in astrocytes [22] and *Aldh1l1*-CreERT2$^{-/-}$ (Cre^{-} mice) littermates were generated from in-house breeding pairs of *Aldh1l1*-CreERT2$^{+/-}$ and *Aldh1l1*-CreERT2$^{-/-}$ mice at the University of Southern California. All animals were group housed, up to five animals per cage, and had ad libitum food and water access on an inverse dark–light cycle (lights off/on 0700/1900 h). CreERT2 gene expression was assessed by PCR with primers towards CreERT2 or the wild-type sequence insert according to previously described methods [22]. Daily intraperitoneal (i.p) injections of tamoxifen (Sigma, St. Louis, MO; 20 mg/ml, dissolved in corn oil; 75 mg tamoxifen per kg body weight) were administered for 5 days to induce MCT4 shRNA gene expression (vector construction described below) in Cre^{+} mice. Cre^{-} mice also received daily injections of tamoxifen as control. All experimental procedures in animals were approved by the Institutional Animal Care and Use Committee at the University of Southern California (Protocol No. 21044) and carried out in compliance with the National Institutes of Health Guide for the Care and Use of Laboratory Animals, 8th Edition, 2011.

Plasmids and Vector Construction

MSCV (Murine Stem Cell Virus)-CreERT2 puro plasmid was a gift from Tyler Jacks (Addgene, Watertown, MA; plasmid # 22,776; http://n2t.net/addgene:22,776; RRID: Addgene_22776). *pCL-Eco* was a gift from Inder Verma (Addgene plasmid # 12,371; http://n2t.net/addgene:12,371; RRID: Addgene_12371). *pCMV-VSV-G* was a gift from Bob Weinberg (Addgene plasmid #8454; http://n2t.net/addgene:8454; RRID: Addgene_8454). *pCMV-deltaR8.2* was a gift from Didier Trono (Addgene plasmid # 12,263; http://n2t.net/addgene:12,263; RRID: Addgene_12263). The *pSico-EGFP* plasmid was a gift from Tyler Jacks (Addgene plasmid #11,578; http://n2t.net/addgene:11,578; RRID: Addgene_11578). *pSico* contains loxP segments, flanking an insert site for pre-designed short hairpin RNA (shRNA) sequences, allowing for Cre-mediated recombination. To target the mouse MCT4 gene (*Slc16a3*), novel shRNA sequences specific to *Slc16a3* were designed using the pSicoligomaker software (Ventura Laboratory, https://venturalaboratory.com/home/downloads/) and synthesized as single stranded cDNA oligonucleotides with Hpa1 and Xho1 overhangs (IDT Technologies, Coralville, IA). The

shRNA MCT4 top and bottom cDNA sequences were annealed together and cloned into the *pSico-EGFP* vector plasmid using restriction enzymes Hpa1 and Xho1. For *MSCV-CreERT2* retroviral vector, *MSCV-CreERT2*, *pCL-Eco*, and *pCMV-VSV-G* plasmids were transfected into HEK-293 T cells using calcium phosphate as previously described [23]. To construct *pSico-EGFP-sh*MCT4 lentivirus vector (termed Lenti-*pSico-EGFP-sh*MCT4), *pSico-EGFP-sh*MCT4, *pCMV delta R8.2*, and *pCMV-VSV-G plasmids* were all transfected into HEK-293 T cells. After 2 days, the supernatant containing the vector was collected and passed through a 0.45 µm filter. In addition, 100X concentrated vector was made by ultracentrifugation (100,000 × *g* for 2 h) through a 20% sucrose cushion, resuspended in 1:1 PBS (phosphate buffered saline): FBS (fetal bovine serum) and stored at − 80 °C until use.

Astrocyte Cell Line Expressing CreERT2

The C8-D1A astrocyte cell line (CRL-2541, ATCC, Manassas, VA) was purchased and maintained in DMEM-10 (DMEM with 10% fetal bovine serum and 1% penicillin/streptomycin: Genesee Scientific, San Diego, CA). C8-D1A cells were modified to express an inducible CreERT2 protein (known further as C8-D1A-CreERT2 astrocytes) by transducing C8-D1A cells with *MSCV-CreERT2* retroviral vector. CreERT2 expression was constitutively selected for using puromycin (2 µg/mL, Sigma) and maintained in DMEM-10 media.

Quantitative Real-Time PCR

Following MCT4 shRNA expression in C8-D1A-CreERT2 astrocytes, total RNA was extracted (Zymo Research, Irvine, CA), and 100 ng of RNA reverse transcribed to cDNA (PCR Biosystems, Wayne, PA) before quantitative RT-PCR was performed on an Eppendorf Mastercycler ep Realplex [24] as previously described using the following primer pairs: *Slc16a1* forward: TGTTAGTCGGAGCCTTCATTT; reverse: CACTGGTCGTTGCACTGAATA; *Slc16a3* forward: TCACGGGTTTCTCCTACGC; reverse: GCCAAA GCGGTTCACACAC; *Actb* forward: GGCTGTATTCCC CTCCATCG; reverse: CCAGTTGGTAACAATGCCATG.

Flow Cytometry

Flow cytometry was used to assess EGFP expression in C8-D1A or C8-D1A-CreERT2 astrocytes transduced with Lenti-*pSico-EGFP-sh*MCT4. The *pSico* plasmid expresses a floxed EGFP, which is excised following Cre-mediated recombination, and relative loss of EGFP expression can be used as a measure of recombination efficacy. Cells were treated with 0.25% trypsin (Genesee Scientific), fixed in 4% paraformaldehyde, and run on a FACS Canto Flow Cytometer (BD Biosciences, San Jose, CA). Living cells were first gated by forward- and side-scatter as previously published [25]; then, quantitative analysis of $EGFP^+$ cells was performed with FloJo software (BD Biosciences).

Calcium Imaging

C8-D1A-CreERT2 astrocytes were seeded in 96 well plates (25,000 cells/well) and immediately transduced with Lenti-*pSico-EGFP-sh*MCT4 (1×10^{12} viral particles/ml) and allowed to grow for 1 week. 1 µM 4-hydroxytamoxifen (4-OHT; Sigma) was added to select wells 5 days prior to imaging to allow for adequate Cre-mediated recombination and expression of MCT4 shRNA; remaining wells did not receive 4-OHT treatment as control. On imaging day, Fluo-4AM (50 µg; Biotium, Fremont, CA; Cat# 50,018) was dissolved in 50 µl Pluronic F-127 (Biotium, Cat# 59,004) and further diluted with 10 mL HBSS with 20 mM HEPES to make Fluo-4 solution. Astrocyte culture medium was removed, cells were washed with ice-cold HBSS, and 200 µl of Fluo-4 solution was added to each well and incubated at 37 °C for 45 min. Fluo-4 solution was removed, replaced with fresh HBSS + 20 mM HEPES, and the plate returned to 37 °C for an additional 20 min to allow for complete cleavage of Fluo-4. Calcium imaging was performed on a Synergy H1 Hybrid Multimode Reader (BioTek, Winooski, VT) with 494 nm excitation and 516 nm emission filters. Baseline fluorescence was recorded every 30 s for 3.5 min, and then 100 µM ATP (Sigma) was injected and mixed in all wells, and then fluorescence was recorded every 30 s for another 9 min for a total of 26 measurements (including $t = 0$). Fluorescence intensity in each well was normalized to the average baseline fluorescence and plotted across the imaging session as deltaF/F.

Stereotactic Surgery for Vector Delivery to Motor Cortex

Mice were anesthetized with 3% isoflurane and maintained at 1.5% isoflurane throughout the surgery. Cre^+ and Cre^- littermates were placed in a stereotactic frame (Stoelting, Wood Dale, IL), and their skulls were exposed with a single scalpel cut. Bore holes were drilled in the skull over the M1 primary motor cortex using stereotactic coordinates and Lenti-*pSico-EGFP-sh*MCT4 (1.0ul, 1×10^{12} genome copies/mL) was injected bilaterally using a 26-gauge syringe (701 N, Hamilton, Reno, NV) at a rate of 0.20 µl/min. Lentivirus was targeted to the M1 primary motor cortex (anterior–posterior [AP]: + 1.5 mm; medial–lateral [ML]: ± 1.8 mm; dorsal–ventral [DV]: − 1.5 mm from Bregma on the surface of the skull). The incision was closed with a single stainless-steel surgical staple (Stoelting), and mice were allowed to recover

on heating pads with Medigel (containing 1-mg carprofen, Clear H_2O, Westbrook, ME) refreshed daily for 3 days. Mice were utilized for behavioral or molecular analysis 2–3 weeks after stereotactic surgery to allow for adequate lentiviral-mediated shRNA expression, which has been previously used for astrocyte-specific genetic manipulation in vivo [26].

Immunohistochemistry of Mouse Brain Tissue

Mice were transcardially perfused with ice-cold saline and 4% PFA-PBS. Whole brains were post fixed with 4% PFA-PBS before being transferred to 30% sucrose until they sank. Brains were frozen in dry ice-cooled 2-methylbutane and sliced on a freezing cryostat in the coronal orientation at 50 µm before being stored in cryoprotectant solution at − 20 °C. Sections were processed for immunohistochemistry as previously described [24]. Briefly, sections were washed and permeabilized in TBS with 0.05% Tween-20 (TBST), nonspecific staining was blocked with blocking solution (TBST and 4% normal donkey or normal goat serum) and incubated overnight at 4 °C with SOX9 antibody (1:2000, Millipore, AB5535, RRID: AB_2239761). Sections were washed and incubated with Alexa 568-conjugated secondary antibody (1:5000, Thermo Fisher Scientific, A11011, RRID: AB_143157) then cover-slipped (Vectashield Hardset Antifade with DAPI; Vector Laboratories). All confocal images were taken on an IXB-DSU spinning disk Olympus BX-61 (Olympus America) and captured with an ORCA-R2 digital CCD camera (Hamamatsu) and MetaMorph Advanced software (Molecular Devices). Mouse brain sections were imaged for co-localization of SOX9 (an astrocyte-specific nuclear marker) and GFP (expressed by the MCT4 shRNA lentivirus) in the motor cortex to assess relative transduction of astrocytes by stereotactic lentivirus injection; the mice used for this experiment did not undergo tamoxifen-induced Cre-mediated recombination, which would result in a loss of EGFP signal and induce MCT4 shRNA expression. M1 primary motor cortex was located using anatomical landmarks and images taken in both the RFP and GFP channels throughout the M1 primary motor cortex. Images were acquired across at least three sections per mouse. Colocalization of RFP and GFP signals were analyzed using ImageJ [27], as previously detailed [24].

Western Immunoblotting

Mice were rapidly euthanized by cervical dislocation and whole brains quickly removed and the M1 primary motor cortex (1.0 mm anterior to Bregma; dorsal to the corpus callosum spanning 1.0 to 2.5 mm from midline) rapidly dissected, snap frozen on dry ice, and stored at − 80 °C. Astrocyte cell line cultures were scraped off 6-well plates with ice-cold RIPA buffer with protease and phosphatase inhibitors (MSSAFE, Sigma) and transferred to a chilled microcentrifuge tube. Cortical tissue samples were lysed in RIPA buffer with protease and phosphatase inhibitors. Cell culture and cortical samples were centrifuged at 16,000 × *g* and the soluble fraction collected for subsequent protein analysis. Total protein content was determined by BCA analysis (ThermoFisher) and 20 µg of protein resolved on a 10% Tris–Glycine gel by electrophoresis (BioRad, Hercules, CA). Total protein was transferred to nitrocellulose membranes (BioRad), blocked in OneBlock buffer (Cat# 20–314, Genesee Scientific) and probed with the following antibodies overnight at 4 °C: mouse anti-PSD95 (1:2000, Millipore, Cat# MAB1596, RRID: AB_2092365), mouse anti-synaptophysin (1:2000, Abcam, Cambridge, MA; Cat# ab8049, RRID: AB_2198854), rabbit anti-MCT1 (1:1000, Thermo Fisher Scientific, Cat# PA5-72,957, RRID: AB_2718811) rabbit anti-MCT4 (1:1000, Novus Biologicals, Littleton, CO; Cat# NBP1-81,251, RRID: AB_11033184), rabbit anti-Arc (H-300, 1:500, Santa Cruz Biotechnology, Dallas, TX; Cat# sc-15325, RRID: AB_634092), rabbit anti-Fos (9F6, 1:1000, Cell Signaling Technology, Danvers, MA; Cat# 2250), and mouse anti-beta actin (1:5000, LI-COR, Lincoln, NE; Cat# 926–42,212, RRID: AB_2756372). Membranes were washed, incubated with corresponding goat anti-mouse or goat anti-rabbit conjugated near-infrared secondary fluorescent antibodies (1:5000, LI-COR, Cat# 926–32,211, RRID: AB_621843; and Cat# 926–68,070, RRID: AB_10956588), and scanned on an Odyssey imaging system (LI-COR). Relative protein expression was quantified by optical density and normalized to beta-actin as loading control.

Golgi-Cox Staining for Dendritic Spine Density

Mice were rapidly euthanized by cervical dislocation and decapitation, and whole brains removed. Golgi-Cox staining (FD NeuroTechnologies, Columbia, MD) of mouse brains was performed according to the manufacturer's protocol as previously described [28]. Briefly, brains were impregnated for 2 weeks, frozen on dry-ice chilled 2-methylbutane, sectioned in the coronal plane in 100 µm thickness, and processed according to the manufacturer's protocol. Pyramidal neurons residing in layer 5 of the M1 primary motor cortex were identified, and 15 to 20 cells were imaged per mouse using an Olympus BX50 (Olympus America) and captured with a KAPELLA digital CCD camera (Jenoptik, Jena, Germany). Golgi impregnated cells were imaged across at least three sections per mouse, and multiple spans of dendrites were counted and analyzed per cell using FIJI and BIOQUANT software as previously described [28]. Total dendritic counts were averaged across all cells imaged per mouse.

Near-Infrared 2-Deoxyglucose Mapping

Following the final trial on the accelerating rotarod, mice were injected intraperitoneally with 10 nmol of near-infrared–conjugated 2-deoxyglucose (2DG-IR; LI-COR, Cat# 926–08,946). This 2-deoxyglucose analogue was specifically selected for rotarod-specific mapping based upon to its apparent preference for neuronal uptake, which seems to occur in an activity-dependent manner in the mouse cortex [29], although the exact mechanism underlying this relationship remains obscure. Mice were placed on the rotarod at a slow, constant speed (8 rpm) for 30 min before being euthanized, perfused, and brains removed and processed for immunohistochemistry. Slices containing structures of interest (motor cortex [AP: + 1.3 from Bregma], dorsal striatum [AP: + 0.5], motor nuclei of thalamus [AP: − 1.3], and dorsal hippocampus [AP: − 1.8]) were selected per mouse; all efforts were made to match Bregma levels across individual mice and groups. Slices were washed in PBS, mounted on gelatin-subbed microscope slides, and slides scanned using identical settings on an Odyssey near-infrared imaging system (LI-COR) before analyzing with FIJI. First, overall fluorescent intensity of matching slices in both groups were analyzed in FIJI; no differences were observed between mice or groups, indicating equal administration and uptake of the tracer. 2DG-IR positive signals were then thresholded to exclude any non-specific background, aligned to a standard mouse atlas [30], and total optical density of 2DG-IR puncta within specific anatomical regions was quantified and averaged across sections for each mouse.

Motor Behavior Testing

The impact of MCT4 knockdown in M1 was assessed with several tests of motor behavior including activity in the open field, reversal climbing on the pole test, and latency to fall from the rotarod. All behavioral assessments took place during the first half of the dark cycle (0900–1200 h). Mice were brought to the behavioral suite and allowed to acclimate to the room for 30 min before any behavior testing.

Open Field Test

Open field test was used to assess total locomotion behavior. Behavioral testing was conducted twice, once before tamoxifen administration, and once prior to motor learning on the accelerating rotarod. Mice were placed in an open field chamber (30 cm × 30 cm × 30 cm white plywood box) for 5 min, and total movement was recorded by a digital video camera at 30 frames per second. Locomotion was analyzed using the EzTrack pipeline [31], and distance was binned in 1-min intervals. Motor behavior was expressed as total distance traveled in meters.

Pole Test

Pole test was used to test speed and dexterity of the mice by assessing their ability to descend a wooden pole. Briefly, mice were placed at the top of a 50-cm wooden pole in an empty cage filled with normal bedding, and the time to descend to the base of the pole is recorded. The trial was repeated five times, with a 1-min inter-trial interval.

Accelerating Rotarod

Accelerating rotarod was used to assess motor behavior and task learning. All mice were tested for motor learning and coordination on the accelerating rotarod with slight modifications as previously described [32]. Briefly, mice were oriented to the stationary rod for 3 min before their first trial. Mice then completed two trials per day for 4 days, with a 5-min intertrial during which mice were returned to their home cage. The rotarod (3 cm diameter rod, divided into five lanes; Ugo Basile, Comerio, Italy) accelerated over the course of 300 s from 4 to 40 rpm, and speed at time of fall and latency to fall automatically recorded by magnetic trip plates. A trial ended when the mouse made a complete backward revolution, fell off, or reached the 300-s threshold. Learning curves were fit with linear regression analysis and slope defined as the learning rate and the Y-intercept of the fitted regression line defined as the initial coordination, a measure of baseline motor coordination on the accelerating rotarod [32].

Statistical Analysis

Sample sizes were calculated based on our previously published work, and all efforts were made to minimize the number of mice used. For glucose mapping, histology, and dendritic spine analysis, we used three male mice ($n = 3$) per group. For western blotting, we used five male mice ($n = 5$) per group. For behavioral experiments, we used eight male mice ($n = 8$) per group.*In vitro* experiments were conducted with at least three independent biological replicates from two independent culture preparations. All data was tested for normality using D'Agostino and Pearson test. If both groups (control and MCT4 shRNA) passed normality tests, an unpaired or paired *t*-test was used; this was the case with almost all of the data analyzed in this paper. In the case of peak calcium fluorescence and dendritic spine analysis, these data were not normally distributed and were analyzed using a Kolmogorov–Smirnov test. To compare overall performance on behavioral tasks (open field, pole test and accelerating rotarod), a 2-way ANOVA with Sidak's multiple comparisons was used. All statistical analyses were conducted using Prism (version 8.2, GraphPad) with significance denoted as $p < 0.05$.

Results

In Vitro Validation of MCT4 shRNA Knockdown Vector

To selectively knockdown MCT4 expression in astrocytes, a Cre-inducible *pSico* expression plasmid carrying a short hairpin RNA (shRNA) specific to the mouse transcript *Slc16a3* (MCT4) [33] was constructed (Fig. 1a). The shRNA sequence for this application is unique relative to previous designs examining MCT4 knockdown, as the sequence is specially designed for use in the *pSico* plasmid [33]. Two approaches were used to validate the efficacy of Cre-mediated recombination of *pSico in vitro*: (i) flow cytometry was used to examine Cre-mediated excision of EGFP; and (ii) qRT-PCR and western blotting were used to determine the level of expression of MCT4 following knockdown. To evaluate the efficacy of Cre-mediated excision of EGFP, the C8-D1A astrocyte cell line

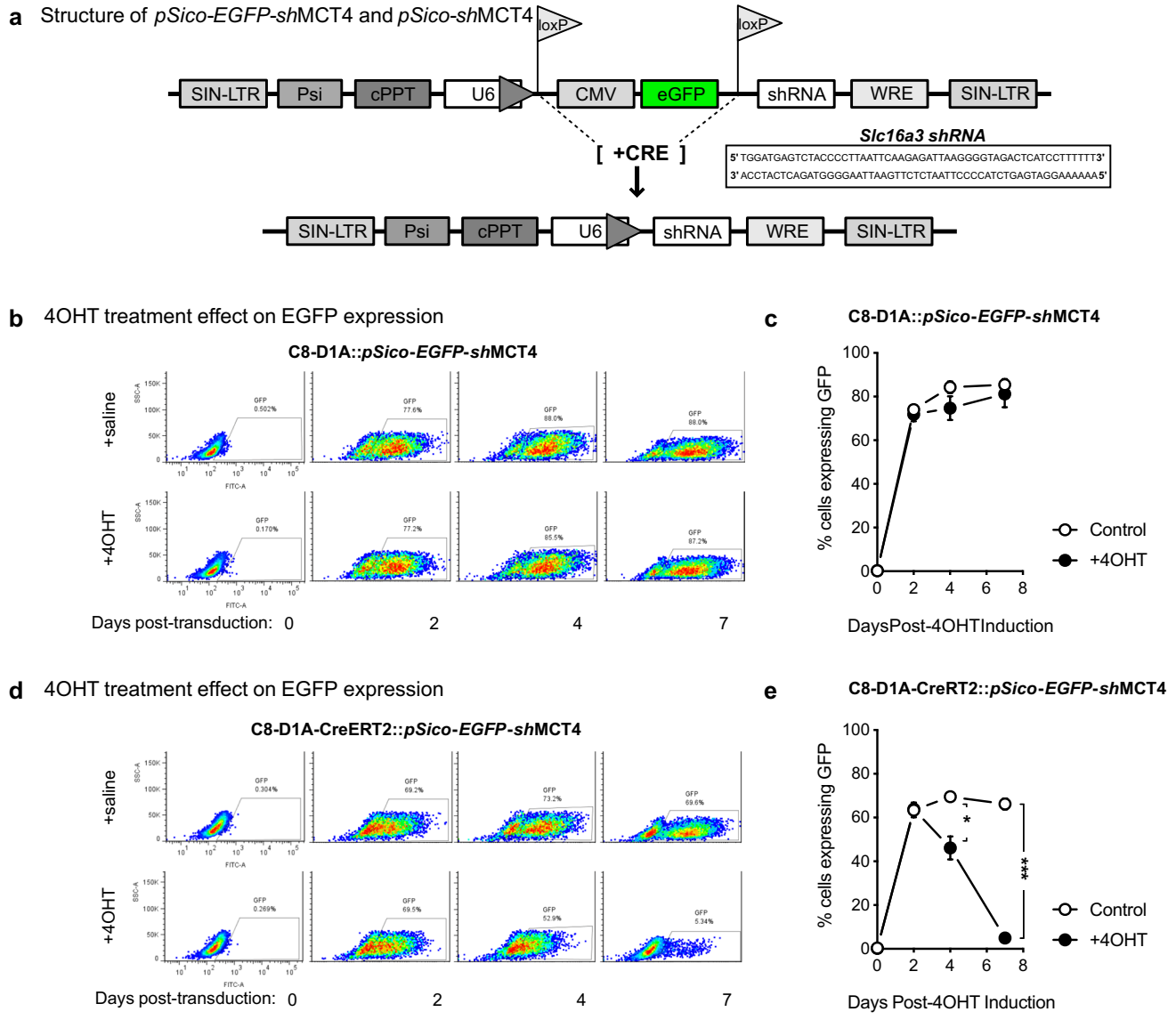

Fig. 1 *In vitro* validation of *pSico-EGFP-sh*MCT4 vector. **a** Schematic highlighting *pSico-EGFP* plasmid carrying Cre-dependent MCT4 shRNA, with MCT4 shRNA sequence detailed in inset box. **b** Representative flow cytometry plots of negative control C8-D1A astrocytic cell line transduced with *pSico* (C8-D1A::*pSico-EGFP-sh*MCT4) treated with saline or 4OHT. **c** Quantification of EGFP expression in C8-D1A::*pSico-EGFP-sh*MCT4 transduced astrocytes following 1 µM 4-OHT treatment. **d** Representative flow cytometry plots of C8-D1A-CreERT2 astrocytic cell line transduced with *pSico* (C8-D1A-CreERT2::*pSico-EGFP-sh*MCT4) treated with saline or 4OHT. **e.** Quantification of EGFP expression following 1 µM 4OHT treatment. Data are mean ± s.e.m.; * $p < 0.05$, *** $p < 0.001$, unpaired *t*-test, two-sided ($n = 3$ experiments per group)

was transduced with a retroviral vector, *MSC::CreERT2 puro* [34], in order to establish a Cre-ERT2-expressing astrocyte cell line, *C8-D1A-CreERT2*, that expresses a tamoxifen-inducible Cre recombinase. Both C8-D1A and C8-D1A-CreERT2 astrocyte cell lines were then stably transduced with lenti-*pSico-EGFP-sh*MCT4 as demonstrated by expression of GFP using flow cytometry at 2-, 4-, and 7-day post-transduction (Fig. 1b, d). Application of the tamoxifen metabolite 4-hydroxytamoxifen (4-OHT) did not result in any change in GFP expression at 2-, 4-, and 7-day post-transfection in C8-D1A cells (Fig. 1c). Induction of Cre-recombinase in C8-D1A-CreERT2 astrocytes by application of the 4-OHT resulted in a statistically significant reduction in GFP expression at day 4 (day 4: control, 69.5 ± 2.17% GFP + cells; + 4OHT, 46.1 ± 5.28% GFP + cells; unpaired two-tailed *t*-test, $t = 4.099$, $df = 4$, $p = 0.015$) and day 7 (day 7: control, 66.17 ± 2.54% GFP + cells; + 4OHT, 4.95 ± 0.91% GFP + cells; unpaired two-tailed *t*-test, $t = 22.67$, $df = 4$, $p < 0.001$) (Fig. 1e).

To evaluate the efficacy of *pSico*-mediated targeted knockdown of MCT4, C8-D1A-CreERT2 astrocytes were transduced with lenti-*pSico-EGFP-sh*MCT4. Lentiviral transduction was found to cause mild toxicity immediately following transduction, but no toxicity was observed by the time of experimentation (day 14) (Supplementary Fig. 1). Following 7 days of 4-OHT administration, the level of MCT4 transcripts and protein expression were evaluated by qRT-PCR and western blotting, respectively. *pSico-sh*MCT4 significantly decreased MCT4 transcript expression by 68 ± 7% (Cre^-, 1.0 ± 0.206; Cre^+, 0.321 ± 0.074; unpaired two-tailed *t*-test, $t = 3.102$, $df = 6$, $p = 0.021$) (Fig. 2a) but did not significantly decrease the level of MCT1 transcripts (Cre^-, 1.0 ± 0.205; Cre^+, 0.977 ± 0.099; unpaired two-tailed *t*-test, $t = 0.101$, $df = 6$, $p = 0.923$) (Fig. 2a), indicating our shRNA is highly specific to MCT4. In addition, MCT4 knockdown resulted in a 31 ± 8% decrease in the level of protein expression (Cre^-, 1.0 ± 0.044; Cre^+, 0.683 ± 0.072; unpaired two tailed *t*-test, $t = 3.743$, $df = 4$, $p = 0.02$) (Fig. 2b). To verify that MCT4 knockdown did not affect the functional capacity of transduced C8-D1A-CreERT2 astrocytes, real-time imaging with the calcium indicator Fluo-4 was used in the presence of 100 μM ATP to activate astrocyte specific P2Y1 and P2X7 receptor channels [35]. Both lenti-*pSico-sh*MCT4-transduced non-Cre expressing (Cre^-) and (Cre^+) C8-D1A-CreERT2 astrocytes responded similarly to ATP exposure, with no significant difference in calcium-mediated fluorescence change between these two groups (two-way ANOVA, MCT4 shRNA: $F_{(1, 62)} = 0.0307$, $p = 0.862$) (Fig. 2c). Interestingly, we did observe a higher peak response to ATP exposure in Cre^+ cells (Cre^-, 0.532 ± 0.03; Cre^+, 0.710 ± 0.033; Kolmogorov–Smirnov test, $D = 0.562$, $p < 0.001$) (Fig. 2d), which may be caused by residual astrocyte reactivity following lentiviral transduction [36, 37].

In Vivo Assessment of MCT4 Knockdown in M1 Cortex

The efficacy of selective MCT4 knockdown in astrocytes via lenti-*pSico-EGFP-sh*MCT4 transduction was determined using immunohistochemistry and western blotting. Lenti-*pSico-EGFP-sh*MCT4 particles were stereotaxically delivered into the primary motor cortex (M1) of mice expressing an astrocyte-specific tamoxifen-inducible Cre recombinase (termed Cre^+ or Cre^- mice) [22] (Fig. 3a). Within the M1 primary motor cortex, 42 ± 12% of SOX9-positive astrocytes were observed to be transduced, as assessed by SOX9- and EGFP-colocalization (Fig. 3b). Next, to determine the efficacy of MCT4 knockdown, both Cre^+ and Cre^- mice that had been injected with Lenti-*pSico-EGFP-sh*MCT4 were administered tamoxifen daily for 5 days, and the level of MCT4 protein was determined by western blot 10 days after the last injection. There was a significant decrease in MCT4 protein expression in Cre^+ (− 28 ± 6.1%; Cre^-, 1.0 ± 0.041; Cre^+, 0.716 ± 0.046; unpaired two tailed *t*-test, $t = 4.600$, $df = 6$, $p = 0.004$) compared to Cre^- mice with no significant change in MCT1 protein expression (+ 26 ± 33%; Cre^-, 1.0 ± 0.13; Cre^+, 1.26 ± 0.31; unpaired two tailed *t*-test, $t = 0.792$, $df = 6$, $p = 0.459$) between Cre^+ and Cre^- mice (Fig. 3c).

MCT4 Knockdown and Motor Performance

In order to examine alterations in motor performance following astrocyte-specific MCT4 knockdown in M1 primary motor cortex, Cre^+ and Cre^- mice were injected with Lenti-*pSico-EGFP-sh*MCT4. Following tamoxifen-induction of MCT4 shRNA expression, these mice were compared for motor behaviors including (i) the open field, (ii) the pole test, and (iii) the accelerating rotarod. There was no statistically significant difference between Cre^- and Cre^+ mice in the total distance traveled using the open field (Cre^-, 11.27 ± 0.54 m; Cre^+, 10.4 ± 0.61 m; unpaired two tailed *t*-test, $t = 1.064$, $df = 14$, $p = 0.305$) (Fig. 4a, b), and no statistically significant difference in time to descend a 50-cm pole (Cre^-, 3.24 ± 0.16 s; Cre^+, 3.53 ± 0.20 s; unpaired two tailed *t*-test, $t = 1.134$, $df = 14$, $p = 0.276$) (Fig. 4c). However, using the accelerating rotarod, Cre^+ mice showed a significantly worse overall performance as measured by latency to fall and terminal speed than Cre^- mice (latency to fall, two-way ANOVA, MCT4 shRNA: $F_{(1,112)} = 11.90$, $p < 0.001$; terminal speed, two-way ANOVA, MCT4 shRNA: $F_{(1,112)} = 8.644$, $p = 0.004$) (Fig. 4d, e). In addition, Cre^+ mice showed significantly slower learning rate (slope RPM/trial) compared to Cre^- mice (Cre^-, 2.58 ± 0.43 RPM/trial; Cre^+, 1.34 ± 0.33

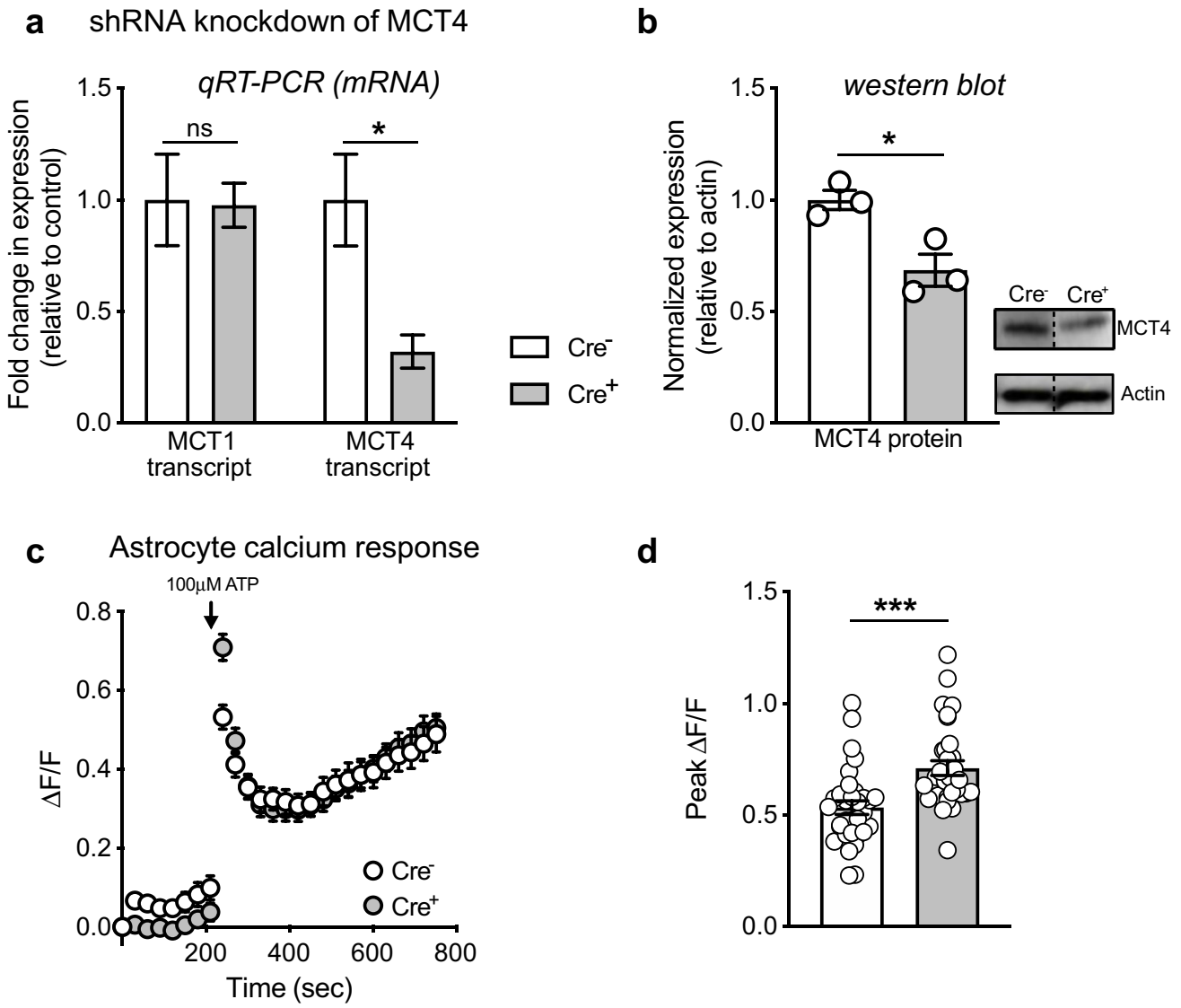

Fig. 2 *pSico-EGFp-sh*MCT4 causes loss of MCT4 expression in C8-D1A-CreERT2 astrocytes. **a** Loss of MCT4 (*Slc16a3*) mRNA and protein expression following activation of shRNA expression. Data are mean ± s.e.m.; *n.s.*, $p > 0.05$, * $p < 0.05$, unpaired *t*-test, two-sided ($n = 3$ replicates per group). **b** Loss of MCT4 protein expression following activation of shRNA expression. Data are mean ± s.e.m.; * $p < 0.05$, unpaired *t*-test, two-sided ($n = 3$ replicates per group). Bands shown are representative from the same experiment. **c** MCT4 knockdown does not affect overall ATP-mediated calcium response in astrocytes (measured with Fluo-4). Data are mean ± s.e.m. Some error bars are too small to be displayed ($n = 32$ wells across 3 experiments per group). **d** MCT4 knockdown enhances peak ATP-mediated calcium response in astrocytes (measured with Fluo-4). Data are mean ± s.e.m. ***, $p < 0.001$, Kolmogorov–Smirnov test ($n = 32$ wells across 3 experiments per group)

RPM/trial; simple linear regression, $F_{(1,\ 124)} = 4.604$, $p = 0.034$) (Fig. 4f).

MCT4 knockdown Reduces Dendritic Spine Density in M1

To determine the effect of MCT4 knockdown on neuronal dendritic structure on M1 primary motor cortex pyramidal neurons, Golgi-Cox impregnation was used to label neurons following tamoxifen-induced MCT4 knockdown (Fig. 5a). There was a significant decrease in dendritic spine density and spine width in Cre^+ mice compared to Cre^- mice (Cre^-, 0.736 ± 0.019 spines/μm; Cre^+, 0.588 ± 0.029 spines/μm; Kolmogorov–Smirnov test, $D = 0.351$, $p < 0.001$) and dendritic spine width (Cre^-, 1.056 ± 0.013 μm; Cre^+, 0.988 ± 0.018 μm; Kolmogorov–Smirnov test, $D = 0.143$, $p < 0.001$) (Fig. 5b). Comparing Cre^- to Cre^+ mice, there was no significant cellular density changes in M1 primary motor cortex using Nissl staining (Cre^-, 1719 ± 17.8 μm; Cre^+, 1724 ± 30.3 μm;

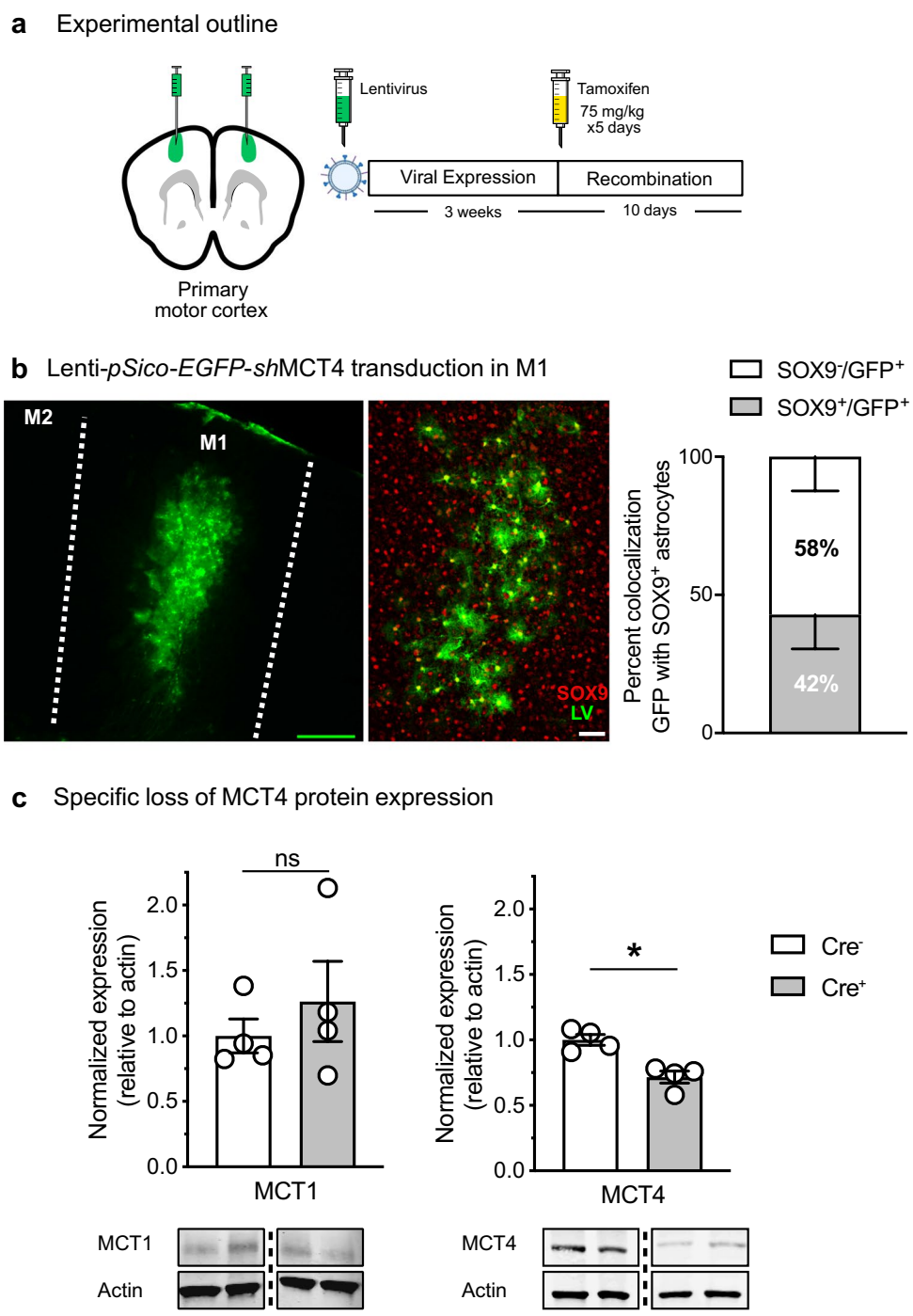

Fig. 3 In vivo validation of Lenti-*pSico-EGFP-sh*MCT4 to knockdown astrocytic MCT4. **a** Experimental schematic and timeline for in vivo application of Lenti-*pSico-EGFP-sh*MCT4. **b** Example micrograph showing localization of lentivirus to M1 primary motor cortex (M1) in mice, and Lenti-*pSico-EGFP-sh*MCT4 (LV) localizes with astrocytic nuclear marker SOX9, with ~ 42% of all transduced cells being astrocytes. **c** Activation of MCT4 shRNA decreases expression of MCT4 protein but not MCT1 protein in M1 primary motor cortex. Data are mean ± s.e.m. *n.s.*, $p > 0.05$; ** $p < 0.01$, unpaired *t*-test, two sided ($n = 5$ mice per group). Bands shown are select representative lanes

unpaired two tailed *t*-test, $t = 0.111$, df = 36, $p = 0.912$) (Fig. 5c).

MCT4 Knockdown Reduces Synapse-Specific Protein Marker Expression

Comparing Cre^+ to Cre^- mice, there was no significant difference in synaptophysin protein expression (Cre^-, 1.0 ± 0.06; Cre^+, 0.82 ± 0.082; unpaired two tailed *t*-test, $t = 1.741$, df = 8, $p = 0.120$) (Fig. 6a). There was a significant decrease in PSD95, Arc, and cFos protein expression in Cre^+ mice compared to Cre^- mice (PSD95: Cre^- 1.0 ± 0.07, Cre^+ 0.79 ± 0.05; unpaired two tailed *t*-test, $t = 2.474$, df = 8, $p = 0.039$; Arc: Cre^- 1.0 ± 0.09, Cre^+ 0.75 ± 0.04; unpaired two tailed *t*-test, $t = 2.549$, df = 8, $p = 0.034$; cFos: Cre^- 1.0 ± 0.9, Cre^+ 0.65 ± 0.04; unpaired two tailed *t*-test, $t = 3.591$, df = 8, $p = 0.007$) (Fig. 6b–d).

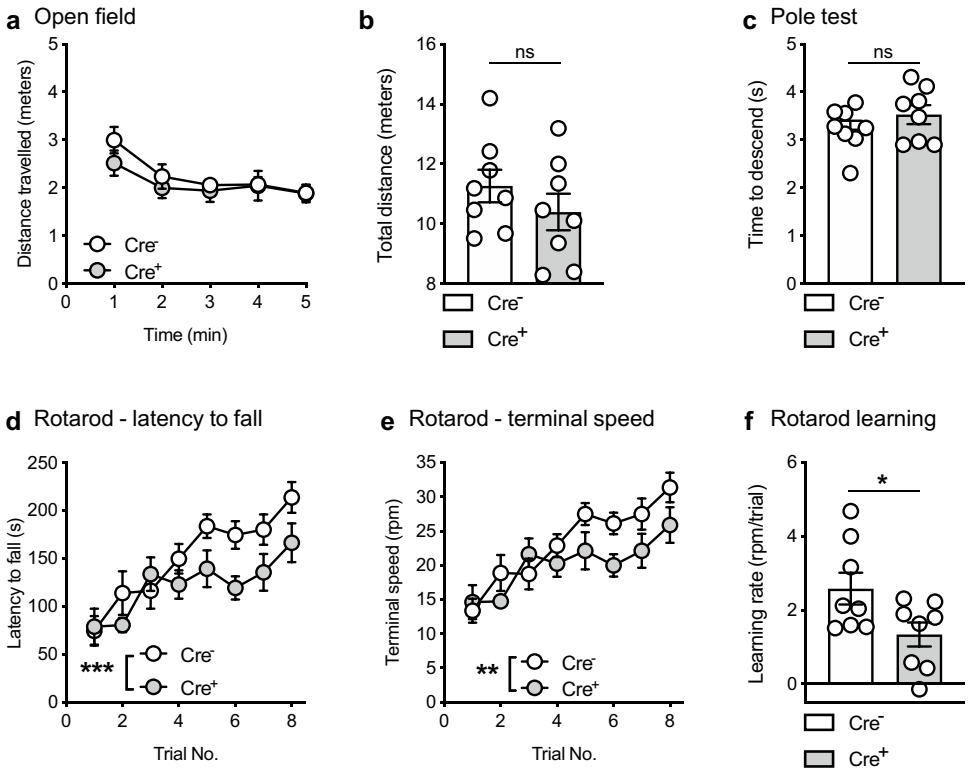

Fig. 4 Astrocyte-specific knockdown of MCT4 impairs motor learning without affecting locomotion or motor coordination. **a** Locomotion as measured across a 5-min session in the open field. Data are mean ± s.e.m. **b** MCT4 knockdown in motor cortex does not affect total locomotion. Data are mean ± s.e.m.; ns, $p > 0.05$ ($n = 8$ mice per group; unpaired t-test, two sided). **c** MCT4 knockdown does not affect time to descend on the pole test. Data are mean ± s.e.m.; ns, $p > 0.05$ ($n = 8$ mice per group; unpaired t-test, two sided). **d–e** MCT4 knockdown in motor cortex decreases overall performance on the accelerating rotarod, assessed by **d** latency to fall and **e** terminal speed. Data are mean ± s.e.m. ***, $p < 0.001$, **, $p < 0.01$ shRNA effect ($n = 8$ mice per group: 2-way repeated-measures ANOVA with Bonferroni correction). **f** MCT4 knockdown in motor cortex diminished learning rate (calculated as slope of the accelerating rotarod learning curve) on the accelerating rotarod. Data are mean ± s.e.m.; *, $p < 0.05$ ($n = 8$ mice per group; unpaired t-test, two sided)

MCT4 Knockdown Reduces 2-Deoxyglucose Uptake

Given that Cre$^+$ mice showed significantly worse motor performance (as measured by latency to fall and terminal speed) compared to Cre$^-$ mice on the accelerating rotarod, 2DG-IR was used to examine differences in neuronal activation within M1 primary motor cortex and associated subcortical motor regions (dorsal striatum and ventral thalamus) while performing on the accelerating rotarod (Fig. 7a). There was a significant decrease in 2DG uptake in the M1 primary motor cortex of Cre$^+$ mice compared to Cre$^-$ mice (unpaired t-test, $t = 4.994$, df = 29, $p < 0.001$) (Fig. 7b). There was also a significant decrease in 2DG uptake in the dorsal striatum and motor thalamus (ventroanterior and ventroposterior nuclei) of Cre$^+$ mice compared to Cre$^-$ mice (dorsal striatum: unpaired two tailed t-test, $t = 2.498$, df = 32, $p = 0.018$; motor thalamus: unpaired two tailed t-test, $t = 2.161$, df = 33, $p = 0.038$) (Fig. 7b, c). There was no significant difference in 2DG uptake between Cre$^-$ and Cre$^+$ mice in the non-motor region dorsal hippocampus (unpaired two tailed t-test, $t = 1.614$, df = 33, $p = 0.116$, Fig. 7d).

Discussion

Monocarboxylate transporters, MCT1 through 4, have been shown to play a key role in cellular signaling and neuroenergetics through the transport of small molecules involved in metabolism and cell signaling including L-lactate, beta-hydroxybutyrate, and other ketones important for promoting neuroplasticity [12]. MCT4 is an astrocyte-specific monocarboxylate transporter, a constituent of the astrocyte-neuron lactate shuttle (ANLS), that plays a crucial role in regulating changes in neuronal activity and metabolism through the transport of L-lactate [13, 14, 38–40]. In the last decade, MCT4 as part of the ANLS has also been implicated in neuroplasticity and learning. For example, in the hippocampus, knockdown of MCT4 has been shown to impair both long-term memory and synaptic integrity [17, 18]. However, the

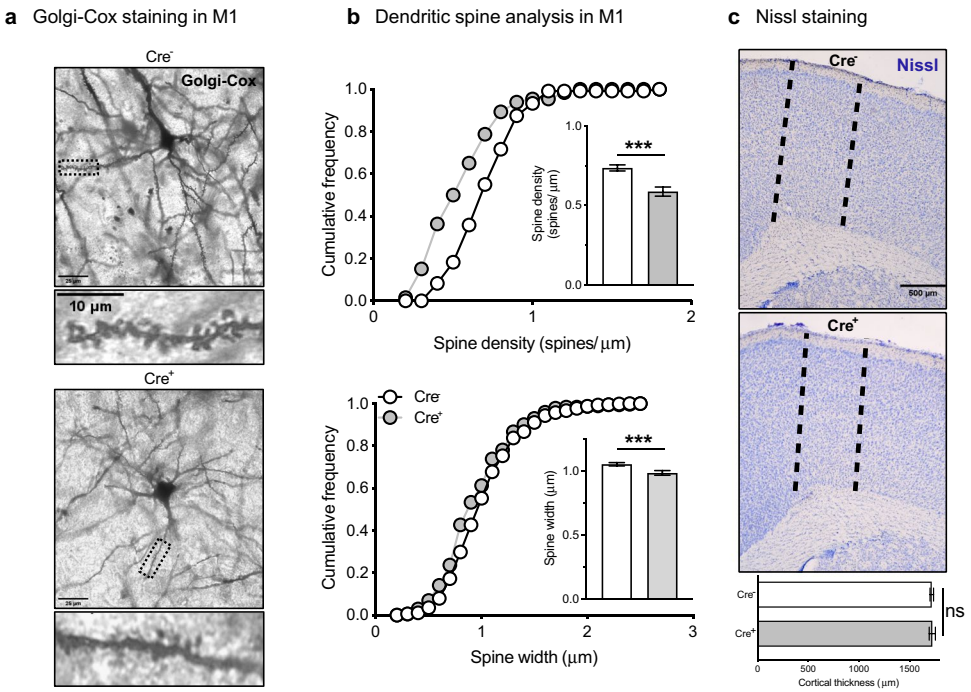

Fig. 5 Loss of astrocytic MCT4 causes cortical dendritic spine loss. **a** Representative layer 5 pyramidal neuron in M1 primary motor cortex of control (top) and MCT4 shRNA (bottom) mouse filled via Golgi-Cox impregnation, with example dendritic branches highlighted. **b** MCT4 knockdown causes decrease in dendritic spine density (top) and dendritic spine width (bottom). Data are mean ± s.e.m.; *** $p < 0.001$ ($n = 3$ mice per group; Kolmogorov–Smirnov test). **c** Representative images of Nissl-stained motor cortex from control and MCT4 shRNA mice; dashed lines represent approximate anatomical borders for the M1 primary motor cortex. MCT4 knockdown in M1 primary motor cortex does not change cortical thickness, reflecting no change in cellular density. Data are mean ± s.e.m. ($n = 3$ mice per group)

role of astrocyte-specific MCT4 in facilitating neuroplasticity and motor learning of the M1 primary motor cortex remains a gap in knowledge. In our study, we found that selective knockdown of astrocyte-specific MCT4 in the M1 primary motor cortex resulted in the impairment of motor performance (accelerating rotarod) and motor learning. Astrocyte-specific MCT4 knockdown also led to the reduction of neuronal dendritic spine density, including loss of synaptic proteins PSD-95 and Arc and decreased expression of the neuroplasticity gene cFos. Astrocyte-specific MCT4 knockdown was also associated with reduced 2DG uptake within the vector targeted M1 primary motor cortex as well as associated subcortical motor regions of the dorsal striatum and ventral thalamus, but not non-motor regions such as the hippocampus. Overall, these findings support the hypothesis that astrocyte-specific MCT4 plays a critical role in neuroplasticity of the M1 primary motor cortex.

We found that the selective knockdown of MCT4 in astrocytes resulted in decreased motor performance and learning, as defined by the decreased performance rate (slope) over eight trials, on the accelerating rotarod. Similar to our findings in the M1 primary motor cortex, others have shown that MCT4 plays a role in learning and memory in the hippocampus. For example, seminal work utilizing antisense oligonucleotides to knockdown MCT4 in the hippocampus resulted in a significant loss of retention of long-term memory in the inhibitory avoidance task [18]. These findings have been complemented with a viral vector approach to knockdown MCT4, where it was also shown to play a distinct role in memory acquisition using the Morris water maze [17]. In addition to the hippocampus, MCT4 has been shown to play an important role in modulating hypothalamus-related behaviors, including feeding behaviors [41]. Similar to our findings in the M1 primary motor cortex, MCT4 has also been shown to play a role in neuroplasticity of other cortical brain regions, including the prefrontal cortex, where knockdown of MCT4 led to loss of a passive coping response following stress exposure [20]. To the best of our knowledge our study is the first to demonstrate the potential role of MCT4 in mediating motor learning behaviors of the M1 primary motor cortex.

In addition to impairments in motor learning, we also found that knockdown of MCT4 in M1 primary motor cortex was associated with decreased neuronal spine density and spine width of layer 5 pyramidal neurons. Pyramidal neurons from layer 5 are the major projection neurons of the motor cortex [42]. Reduction in dendritic spine morphology was associated with a significant reduction in the expression

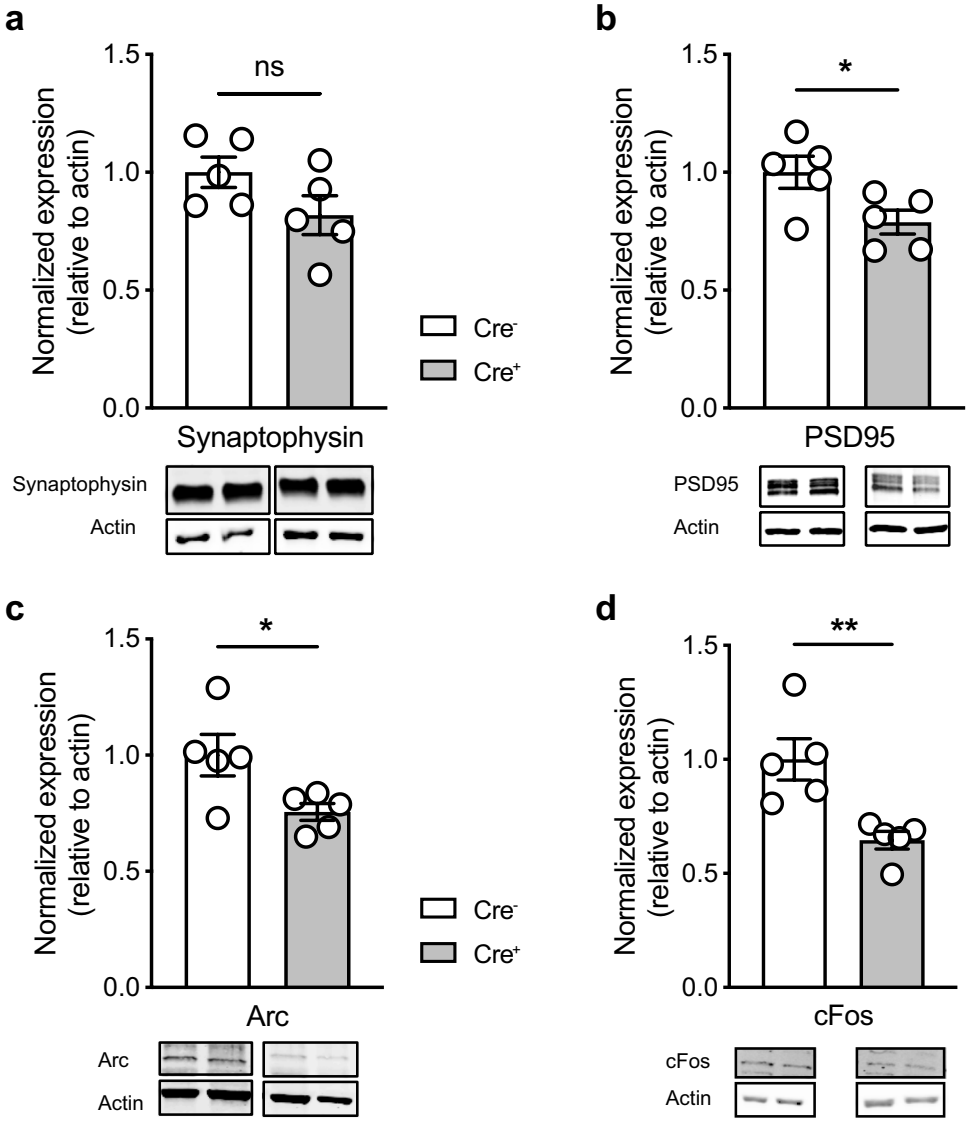

Fig. 6 Loss of astrocytic MCT4 decreases plasticity-related protein expression. **a** MCT4 knockdown does not significantly decrease expression of pre-synaptic protein synaptophysin. Representative bands from western blots of M1 primary motor cortex from control (left) and MCT4 shRNA (right) mice. Data are mean ± s.e.m. ns, $p > 0.05$ ($n = 5$ mice per group: unpaired *t*-test, two-sided). **b** MCT4 knockdown decreases expression of post-synaptic protein PSD95. Representative bands from western blots of M1 primary motor cortex from control (left) and MCT4 shRNA (right) mice. Data are mean ± s.e.m. * $p < 0.05$ ($n = 5$ mice per group: unpaired *t*-test, two sided). **c** MCT4 knockdown decreases expression of Arc (activity-regulated cytoskeletal-associated protein). Representative bands from western blots of M1 primary motor cortex from control (left) and MCT4 shRNA (right) mice. Data are mean ± s.e.m. * $p < 0.05$ ($n = 5$ mice per group: unpaired *t*-test, two sided). **d** MCT4 knockdown decreases expression of cFos. Representative bands from western blots of M1 primary motor cortex from control (left) and MCT4 shRNA (right) mice. Data are mean ± s.e.m. * $p < 0.05$ ($n = 5$ mice per group: unpaired *t*-test, two sided). All western blot quantifications are normalized relative to each lane's β-actin intensity, then normalized such that the mean of the control group is equal to 1

of both PSD-95 and Arc proteins. PSD-95 is a scaffolding-associated protein that maintains dendritic spine structure while Arc is an activity-regulated cytoskeletal structural protein that is also involved in regulating dendritic spine morphology and synaptic function. Together these two proteins participate in distinct phases of spinogenesis, maintenance, and remodeling [43]. Interestingly, Arc-expressing neuronal ensembles are associated with changes in motor learning and performance [44], suggesting a central role for Arc activity in modulating motor behaviors and synaptic structures. Specifically, studies have shown that increases in Arc mRNA expression correlates with successful learning in a pellet retrieval task in healthy rodents [45]. Similarly, in our study, we found that a reduction of Arc and PSD95 protein

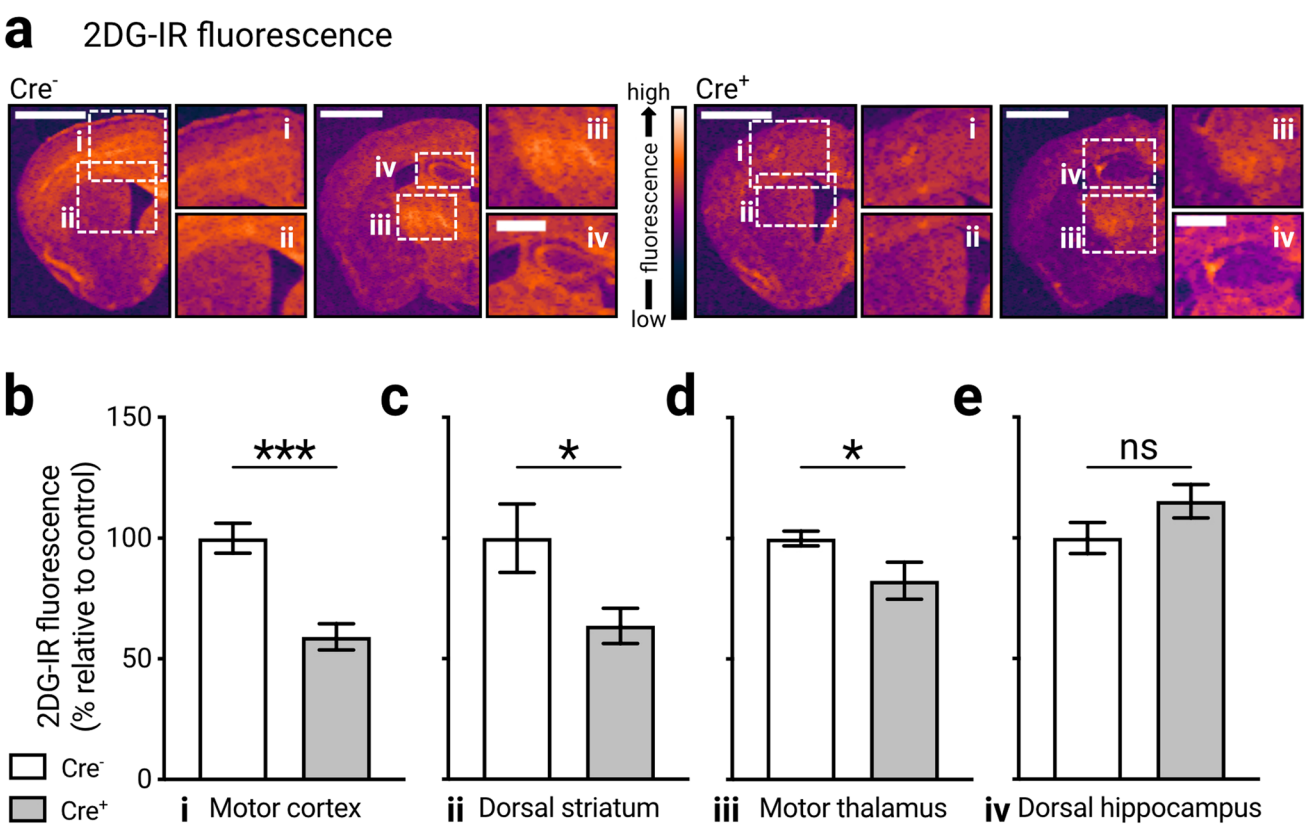

Fig. 7 Astrocytic MCT4 knockdown causes task-specific decrease in near-infrared 2-deoxyglucose uptake in motor-related brain regions. **a** Representative images of near-infrared analog of 2-deoxygluocse (2DG-IR), pseudocolored to detail gradient of fluorescent uptake and select regions of interest, including M1 primary motor cortex (i); dorsal striatum (ii); motor thalamus (focusing on ventroanterior and ventroposterior nuclei) (iii); and dorsal hippocampus (iv). All efforts were made to match high-quality, representative images between groups. Scale bars are 2 mm in hemi-sections and 1 mm in cropped regions of interest. **b–e** MCT4 knockdown in M1 primary motor cortex causes decreases in 2DG-IR uptake in motor-related regions: **b** M1 primary motor cortex; **c** dorsal striatum; and **d** motor thalamus, but not in **e** dorsal hippocampus. Data are mean ± s.e.m. and are normalized such that the mean of the control group is equal to 100%. * $p < 0.05$, *** $p < 0.001$, ns, $p > 0.05$. ($n = 3$ mice per group; unpaired *t*-test, two sided)

expression following astrocyte-specific MCT4 knockdown was correlated with deficits in motor learning rate on the accelerating rotarod (Supplementary Fig. 2). Interestingly, transgenic heterozygous or homozygous Arc knockout mice have also previously demonstrated failure to improve in balance and foot placement using the accelerating rotarod [46]. While the mechanisms by which astrocyte-specific MCT4 knockdown modulates dendritic spine density remain unknown, one possible explanation may be through activity-dependent genes involved in neuroplasticity, including Arc and cFos. MCT4 plays an important role in the shuttling of L-lactate from astrocytes to neurons through the ANLS. L-lactate production and transport has been shown to regulate Arc expression and dendritic spine density and volume in the hippocampus [18, 19]. Additionally, lactate promotes the expression of cFos in primary neuronal cultures and in the somatosensory cortex [13, 39], and cFos activity is associated with learning [47, 48]. Findings from our MCT4 knockdown studies showing a reduction in Arc and cFos expression provide further support for the potential role of L-lactate and MCT4 in contributing to immediate early gene expression and synaptic plasticity in the M1 primary motor cortex [12].

Using the fluorescent near-infrared 2DG analog (2DG-IR), knockdown of astrocyte-specific MCT4 in the M1 primary motor cortex resulted in a significant decrease in 2DG-IR uptake in the M1 primary motor cortex, along with reduced 2DG-IR uptake in related motor regions of the dorsal striatum and ventral thalamus [49]. However, there was no change in 2DG-IR uptake in non-motor regions such as the hippocampus. It is important to note that the molecular mechanisms of 2DG-IR uptake does not reflect typical fast transport of glucose through glucose transporters followed by phosphorylation, typically used as a valid surrogate marker of brain activity [50, 51]. Based on the purported preferential 2DG-IR uptake by neurons in an activity-dependent manner [29], and despite a lack of clear mechanism explaining this relationship, it was used here

only for the purpose of mapping task-specific brain activity during the rotarod. Interpretation of data arising from its use should be limited to this aspect. The mechanism by which knockdown of astrocyte-specific MCT4 in motor cortex impacts activity in subsequent associated motor regions is unknown. However, considering that pyramidal neurons in M1 primary motor cortex are known to project to the striatum and thalamus [42], it is possible that diminished activity in M1 primary motor cortex may be associated with diminished activity in associated brain regions. The potential role that astrocyte-specific MCT4 may play in regulating neuronal activity is complex and may include several different mechanisms, including the transport of L-lactate and the role of the ANLS. The ANLS is known to be coupled with synaptic activity, especially excitatory glutamatergic neurotransmission [52]. Previous works by our lab and others have shown L-lactate may influence BDNF expression, and BDNF is known to be a key modulator of glutamatergic receptor expression and synaptic activity [38, 53, 54]. Taken together, our findings support the potential role of MCT4 in regulating neuronal activity in M1 primary motor cortex and associated motor regions. Future studies will further explore the impact of modulating astrocyte-specific MCT4 on excitatory glutamatergic neurotransmission utilizing neurophysiological approaches including the evaluation of long-term potentiation, in vivo imaging of neuronal activity with fluorescent calcium indicators, and the application of whole-brain glucose mapping methods utilizing autoradiography and statistical parametric mapping [55].

In conclusion, our study supports a role for astrocyte-specific MCT4 and the ANLS in motor learning and neuroplasticity of the M1 primary motor cortex. Lactate shuttling through the ANLS can regulate the expression of genes important for synaptic structure and function, such as Arc and cFos [18, 56]. We found that astrocyte-specific MCT4 knockdown was associated with changes in synaptic structure and Arc and cFos expression in the M1 primary motor cortex, thus extending the potential role of the ANLS in neuroplasticity of the M1 primary motor cortex. In addition to its role in regulating gene expression, lactate is known as a major neuroenergetics molecule that regulates neuronal activity and metabolism [12, 14]. Interestingly, knockdown of MCT4 impacted activity in the M1 primary motor cortex and associated motor regions, which suggests that regional changes in ANLS may have widespread functional consequences in activity of associated brain networks. Given our findings, targeting of astrocyte-specific MCT4 may serve to enhance neuroplasticity and promote motor performance and rehabilitation in a number of neurological disorders, including neurodegenerative disorders such as Parkinson's disease.

Supplementary Information The online version contains supplementary material available at https://doi.org/10.1007/s12035-021-02651-z.

Acknowledgements The authors would like to thank Dr. Enrique Cadenas and Dr. Daniel Holschneider for their critical scientific insight and guidance on this project. The authors would also like to thank the contributions from friends of the PD Research Program at USC. Special thanks to Jakowec and Petzinger lab members for their helpful discussions.

Author Contribution AJL, GMP, and MWJ conceived, designed, and managed the study. AJL performed stereotaxic surgeries, and AJL and SHK performed behavior, tissue processing, and molecular analysis. GNL and NAJ performed cloning, cell-line modification, and lentiviral preparation, and AJL, GNL, and NAJ performed *in vitro* experiments. AJL, GMP, and MWJ performed statistical analysis of all data. AJL prepared figures for publication. AJL, GMP, and MWJ wrote the manuscript, and all authors contributed to editing and review. AJL, GMP, and MWJ were responsible for acquisition of funding support.

Funding This work was supported by the Achievement Rewards for College Scientists, Los Angeles Founder Chapter (AJL); Don Roberto Gonzalez Family Foundation (GMP); Parkinson's Foundation (GMP); US Army Medical Research and Material Command Parkinson Research Program, Grant/Award Numbers: W81XWH18-0665 (GMP), W81XWH18-00443 (MWJ).

Data Availability The data that support the findings of this study are available from the corresponding author upon reasonable request.

Code Availability Not applicable.

Declarations

Ethics Approval All experimental procedures in animals were approved by the Institutional Animal Care and Use Committee at the University of Southern California (Protocol No. 21044) and carried out in compliance with the National Institutes of Health Guide for the Care and Use of Laboratory Animals, 8th Edition, 2011.

Consent to Participate Not applicable.

Consent for Publication Not applicable.

Competing Interests The authors declare no competing interests.

References

1. Pérez-Escuredo J, Van Hée VF, Sboarina M, Falces J, Payen VL, Pellerin L, Sonveaux P (2016) Monocarboxylate transporters in the brain and in cancer. Biochimica et Biophysica Acta (BBA) - Molecular Cell Research 1863(10):2481–2497. https://doi.org/10.1016/j.bbamcr.2016.03.013
2. Lee Y, Morriso, BM, Li Y, Lengacher S, Farah MH, Hoffman PN, … Rothstein JD (2012) Oligodendroglia metabolically support axons and contribute to neurodegeneration. Nature 487(7408): 443–448. https://doi.org/10.1038/nature11314
3. Pellerin L, Halestrap AP, Pierre K (2005) Cellular and subcellular distribution of monocarboxylate transporters in cultured brain cells and in the adult brain. J Neurosci Res 79(1–2):55–64. https://doi.org/10.1002/jnr.20307
4. Bergersen LH, Magistretti PJ, Pellerin L (2005) Selective postsynaptic co-localization of MCT2 with AMPA receptor GluR2/3

subunits at excitatory synapses exhibiting AMPA receptor trafficking. Cereb Cortex 15(4):361–370. https://doi.org/10.1093/cercor/bhh138
5. Daniele LL, Sauer B, Gallagher SM, Pugh EN, Philp NJ (2008) Altered visual function in monocarboxylate transporter 3 (Slc16a8) knockout mice. Am J Physiol Cell Physiol 295(2):C451–C457. https://doi.org/10.1152/ajpcell.00124.2008
6. Rosafio K, Pellerin L (2014) Oxygen tension controls the expression of the monocarboxylate transporter MCT4 in cultured mouse cortical astrocytes via a hypoxia-inducible factor-1??-mediated transcriptional regulation. Glia 62(3):477–490. https://doi.org/10.1002/glia.22618
7. Bergersen LH (2015) Lactate transport and signaling in the brain: potential therapeutic targets and roles in body—brain interaction. J Cereb Blood Flow Metab 35(2):176–185. https://doi.org/10.1038/jcbfm.2014.206
8. Pierre K, Pellerin L (2005) Monocarboxylate transporters in the central nervous system: distribution, regulation and function. J Neurochem 94(1):1–14. https://doi.org/10.1111/j.1471-4159.2005.03168.x
9. Pierre K, Pellerin L, Debernardi R, Riederer B, Magistretti P (2000) Cell-specific localization of monocarboxylate transporters, MCT1 and MCT2, in the adult mouse brain revealed by double immunohistochemical labeling and confocal microscopy. Neuroscience 100(3):617–627. https://doi.org/10.1016/S0306-4522(00)00294-3
10. Chiry O, Pellerin L, Monnet-Tschudi F, Fishbein WN, Merezhinskaya N, Magistretti PJ, Clarke S (2006) Expression of the monocarboxylate transporter MCT1 in the adult human brain cortex. Brain Res 1070(1):65–70. https://doi.org/10.1016/j.brainres.2005.11.064
11. Bergersen L, Wærhaug O, Helm J, Thomas M, Laake P, Davies AJ, … Ottersen OP (2001) A novel postsynaptic density protein: the monocarboxylate transporter MCT2 is co-localized with δ-glutamate receptors in postsynaptic densities of parallel fiber-Purkinje cell synapses. Exp Brain Res 136(4): 523–534. https://doi.org/10.1007/s002210000600
12. Magistretti PJ, Allaman I (2018) Lactate in the brain: from metabolic end-product to signalling molecule. Nat Rev Neurosci 19(4):235–249. https://doi.org/10.1038/nrn.2018.19
13. Yang J, Ruchti E, Petit J-M, Jourdain P, Grenningloh G, Allaman I, Magistretti PJ (2014) Lactate promotes plasticity gene expression by potentiating NMDA signaling in neurons. Proc Natl Acad Sci 111(33):12228–12233. https://doi.org/10.1073/pnas.1322912111
14. Barros LF (2013) Metabolic signaling by lactate in the brain. Trends Neurosci. https://doi.org/10.1016/j.tins.2013.04.002
15. Alberini CM, Cruz E, Descalzi G, Bessières B, Gao V (2018) Astrocyte glycogen and lactate: new insights into learning and memory mechanisms. Glia 66(6):1244–1262. https://doi.org/10.1002/glia.23250
16. Harris RA, Lone A, Lim H, Martinez F, Frame AK, Scholl TJ, Cumming RC (2019) Aerobic glycolysis is required for spatial memory acquisition but not memory retrieval in mice. eneuro 6(1):ENEURO.0389-18.2019. https://doi.org/10.1523/ENEURO.0389-18.2019
17. Netzahualcoyotzi C, Pellerin L (2020) Neuronal and astroglial monocarboxylate transporters play key but distinct roles in hippocampus-dependent learning and memory formation. Prog Neurobiol 194:101888. https://doi.org/10.1016/j.pneurobio.2020.101888
18. Suzuki A, Stern SA, Bozdagi O, Huntley GW, Walker RH, Magistretti PJ, Alberini CM (2011) Astrocyte-neuron lactate transport is required for long-term memory formation. Cell 144(5):810–823. https://doi.org/10.1016/j.cell.2011.02.018
19. Vezzoli E, Calì C, De Roo M, Ponzoni L, Sogne E, Gagnon N, … Magistretti PJ (2020) Ultrastructural evidence for a role of astrocytes and glycogen-derived lactate in learning-dependent synaptic stabilization. Cereb Cortex 30(4): 2114–2127. https://doi.org/10.1093/cercor/bhz226
20. Yin Y-N, Hu J, Wei Y-L, Li Z-L, Luo Z-C, Wang R-Q, … Gao T-M (2021) Astrocyte-derived lactate modulates the passive coping response to behavioral challenge in male mice. Neurosci Bull 37(1): 1–14. https://doi.org/10.1007/s12264-020-00553-z
21. Underwood CF, Parr-Brownlie LC (2021) Primary motor cortex in Parkinson's disease: functional changes and opportunities for neurostimulation. Neurobiol Dis 147:105159. https://doi.org/10.1016/j.nbd.2020.105159
22. Srinivasan R, Lu TY, Chai H, Xu J, Huang BS, Golshani P, … Khakh BS (2016) New transgenic mouse lines for selectively targeting astrocytes and studying calcium signals in astrocyte processes in situ and in vivo. Neuron 92(6): 1181–1195. https://doi.org/10.1016/j.neuron.2016.11.030
23. Llewellyn GN, Seclén E, Wietgrefe S, Liu S, Chateau M, Pei H, Perkey K, Marsden MD, et al. (2019) Humanized mouse model of HIV-1 latency with enrichment of latent virus in PD-1+and TIGIT+ CD4 T cells. J Virol 93:e02086–18. https://doi.org/10.1128/JVI.02086-18
24. Lundquist AJ, Parizher J, Petzinger GM, Jakowec MW (2019) Exercise induces region-specific remodeling of astrocyte morphology and reactive astrocyte gene expression patterns in male mice. J Neurosci Res 97(9):1081–1094. https://doi.org/10.1002/jnr.24430
25. Rogers GL, Chen H-Y, Morales H, Cannon PM (2019) Homologous recombination-based genome editing by Clade F AAVs is inefficient in the absence of a targeted DNA break. Mol Ther 27(10):1726–1736. https://doi.org/10.1016/j.ymthe.2019.08.019
26. Skupio U, Tertil M, Bilecki W, Barut J, Korostynski M, GoldaS, … Przewlocki R (2020) Astrocytes determine conditioned response to morphine via glucocorticoid receptor-dependent regulation of lactate release. Neuropsychopharmacology 45(2): 404–415. https://doi.org/10.1038/s41386-019-0450-4
27. Schindelin J, Arganda-Carreras I, Frise E, Kaynig V, Longair M, Pietzsch T, … Cardona A (2012) Fiji: an open-source platform for biological-image analysis. Nature Methods 9(7): 676–682. https://doi.org/10.1038/nmeth.2019
28. Toy WA, Petzinger GM, Leyshon BJ, Akopian GK, Walsh JP, Hoffman M V, … Jakowec MW (2014) Treadmill exercise reverses dendritic spine loss in direct and indirect striatal medium spiny neurons in the 1-methyl-4-phenyl-1,2,3,6-tetrahydropyridine (MPTP) mouse model of Parkinson's disease. Neurobiol Dis 63: 201–209. https://doi.org/10.1016/j.nbd.2013.11.017
29. Lundgaard I, Li B, Xie L, Kang H, Sanggaard S, Haswell JDR, … Nedergaard M (2015) Direct neuronal glucose uptake heralds activity-dependent increases in cerebral metabolism. Nat Commun 6(1): 6807. https://doi.org/10.1038/ncomms7807
30. Dong HW (2008) The Allen reference atlas: a digital color brain atlas of the C57Bl/6J male mouse. John Wiley & Sons Inc., Hoboken
31. Pennington ZT, Dong Z, Feng Y, Vetere LM, Page-Harley L, Shuman T, Cai DJ (2019) ezTrack: An open-source video analysis pipeline for the investigation of animal behavior. Sci Rep 9(1):19979. https://doi.org/10.1038/s41598-019-56408-9
32. Rothwell PE, Fuccillo MV, Maxeiner S, Hayton SJ, Gokce O, Lim BK, … Südhof TC (2014) Autism-associated neuroligin-3 mutations commonly impair striatal circuits to boost repetitive behaviors. Cell 158(1): 198–212. https://doi.org/10.1016/j.cell.2014.04.045
33. Ventura A, Meissner A, Dillon CP, McManus M, Sharp PA, Van Parijs L, … Jacks T (2004) Cre-lox-regulated conditional RNA

interference from transgenes. Proc Natl Acad Sci 101(28): 10380–10385. https://doi.org/10.1073/pnas.0403954101
34. Kumar MS, Pester RE, Chen CY, Lane K, Chin C, Lu J, … Jacks T (2009) Dicer1 functions as a haploinsufficient tumor suppressor. Genes Dev 23(23): 2700–2704. https://doi.org/10.1101/gad.1848209
35. Agulhon C, Petravicz J, McMullen AB, Sweger EJ, Minton SK, Taves SR, … McCarthy KD (2008) What is the role of astrocyte calcium in neurophysiology? Neuron. https://doi.org/10.1016/j.neuron.2008.09.004
36. Ding S, Fellin T, Zhu Y, Lee S-Y, Auberson YP, Meaney DF, … Haydon P G (2007) Enhanced astrocytic Ca2+ signals contribute to neuronal excitotoxicity after status epilepticus. J Neurosci 27(40): 10674–10684. https://doi.org/10.1523/JNEUROSCI.2001-07.2007
37. Shigetomi E, Saito K, Sano F, Koizumi S (2019) Aberrant calcium signals in reactive astrocytes: a key process in neurological disorders. Int J Mol Sci 20(4):996. https://doi.org/10.3390/ijms20040996
38. Lundquist AJ, Gallagher TJ, Petzinger GM, Jakowec MW (2021) Exogenous L lactate promotes astrocyte plasticity but is not sufficient for enhancing striatal synaptogenesis or motor behavior in mice. J Neurosurg 99(5):1433–1447. https://doi.org/10.1002/jnr.24804
39. Margineanu M B, Mahmood H, Fiumelli H, Magistretti PJ (2018) L-lactate regulates the expression of synaptic plasticity and neuroprotection genes in cortical neurons: a transcriptome analysis. Front Mol Neurosci 11:375. https://doi.org/10.3389/fnmol.2018.00375
40. Bélanger M, Allaman I, Magistretti PJ (2011) Brain energy metabolism: focus on astrocyte-neuron metabolic cooperation. Cell Metab 14(6):724–738. https://doi.org/10.1016/j.cmet.2011.08.016
41. Portela LV, Brochier AW, Haas CB, de Carvalho AK, Gnoato JA, Zimmer ER, … Muller AP (2017) Hyperpalatable diet and physical exercise modulate the expression of the glial monocarboxylate transporters MCT1 and 4. Mol Neurobiol 54(8):5807–5814. https://doi.org/10.1007/s12035-016-0119-5
42. Oswald MJ, Tantirigama MLS, Sonntag I, Hughes SM and Empson RM (2013) Diversity of layer 5 projection neurons in the mouse motor cortex. Front Cell Neurosci 7:174. https://doi.org/10.3389/fncel.2013.00174
43. Peebles CL, Yoo J, Thwin MT, Palop JJ, Noebels JL, Finkbeiner S (2010) Arc regulates spine morphology and maintains network stability in vivo. Proceedings of the National Academy of Sciences 107(42):18173–18178. https://doi.org/10.1073/pnas.1006546107
44. Cao VY, Ye Y, Mastwal S, Ren M, Coon M, Liu Q, … Wang KH (2015) Motor learning consolidates arc-expressing neuronal ensembles in secondary motor cortex. Neuron 86(6):1385–1392. https://doi.org/10.1016/j.neuron.2015.05.022
45. Hosp JA, Mann S, Wegenast-Braun BM, Calhoun ME, Luft AR (2013) Region and task-specific activation of Arc in primary motor cortex of rats following motor skill learning. Neuroscience 250:557–564. https://doi.org/10.1016/j.neuroscience.2013.06.060
46. Ren M, Cao V, Ye Y, Manji HK, Wang KH (2014) Arc regulates experience-dependent persistent firing patterns in frontal cortex. J Neurosci 34(19):6583–6595. https://doi.org/10.1523/JNEUROSCI.0167-14.2014
47. Kleim JA, Lussnig E, Schwarz ER, Comery TA, Greenough WT (1996) Synaptogenesis and FOS expression in the motor cortex of the adult rat after motor skill learning. J Neurosci 16(14):4529–4535. https://doi.org/10.1523/JNEUROSCI.16-14-04529.1996
48. Adamsky A, Kol A, Kreisel T, Doron A, Ozeri-Engelhard N, Melcer T, … Goshen I (2018). Astrocytic activation generates de novo neuronal potentiation and memory enhancement. Cell 174(1), 59-71.e14. https://doi.org/10.1016/j.cell.2018.05.002
49. Bosch-Bouju C, Hyland BI, Parr-Brownlie LC (2013) Motor thalamus integration of cortical, cerebellar and basal ganglia information: implications for normal and parkinsonian conditions. Front Comput Neurosci 7:163. https://doi.org/10.3389/fncom.2013.00163
50. Barros LF, Weber B (2018) CrossTalk proposal: an important astrocyte-to-neuron lactate shuttle couples neuronal activity to glucose utilisation in the brain. J Physiol 596(3):347–350. https://doi.org/10.1113/JP274944
51. Zimmer ER, Parent MJ, Souza DG, Leuzy A, Lecrux C, Kim HI, … Rosa-Neto P (2017) [18F]FDG PET signal is driven by astroglial glutamate transport. Nat Neurosci 20(3):393–395. https://doi.org/10.1038/nn.4492
52. Pellerin L, Magistretti PJ (1994) Glutamate uptake into astrocytes stimulates aerobic glycolysis: a mechanism coupling neuronal activity to glucose utilization. Proc Natl Acad Sci 91(22):10625–10629. https://doi.org/10.1073/pnas.91.22.10625
53. Müller P, Duderstadt Y, Lessmann V, Müller NG (2020) Lactate and BDNF: key mediators of exercise induced neuroplasticity? J Clin Med 9(4):1136. https://doi.org/10.3390/jcm9041136
54. El Hayek L, Khalifeh M, Zibara V, Abi Assaad R, Emmanuel N, Karnib N, … Sleiman SF (2019) Lactate mediates the effects of exercise on learning and memory through SIRT1-dependent activation of hippocampal brain-derived neurotrophic factor (BDNF). Nat Neurosci 39(13):2369–2382. https://doi.org/10.1523/JNEUROSCI.1661-18.2019
55. Wang Z, Myers KG, Guo Y, Ocampo MA, Pang RD, Jakowec MW, Holschneider DP (2013) Functional reorganization of motor and limbic circuits after exercise training in a rat model of bilateral Parkinsonism. PLoS ONE 8(11):e80058. https://doi.org/10.1371/journal.pone.0080058
56. Descalzi G, Gao V, Steinman MQ, Suzuki A, Alberini CM (2019) Lactate from astrocytes fuels learning-induced mRNA translation in excitatory and inhibitory neurons. Commun Biol 2(1):247. https://doi.org/10.1038/s42003-019-0495-2

Current Research in Neurobiology 3 (2022) 100039

Contents lists available at ScienceDirect

Current Research in Neurobiology

journal homepage: www.sciencedirect.com/journal/current-research-in-neurobiology

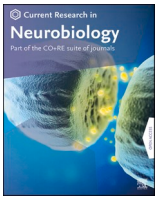

A mind in motion: Exercise improves cognitive flexibility, impulsivity and alters dopamine receptor gene expression in a Parkinsonian rat model

Wang Zhuo [c,1], Adam J. Lundquist [b,1], Erin K. Donahue [b], Yumei Guo [c], Derek Phillips [b], Giselle M. Petzinger [a,b], Michael W. Jakowec [a,b,2], Daniel P. Holschneider [a,b,c,*,2]

[a] Department of Neurology, University of Southern California, 1333 San Pablo St., Los Angeles, CA, 90033, USA
[b] Neuroscience Graduate Program, University of Southern California, Los Angeles, CA, 90089, USA
[c] Department of Psychiatry and the Behavioral Sciences, University of Southern California, 1333 San Pablo St., Los Angeles, CA, 90033, USA

A B S T R A C T

Cognitive impairment, particularly deficits in executive function (EF) is common in Parkinson's disease (PD) and may lead to dementia. There are currently no effective treatments for cognitive impairment. Work from our lab and others has shown that physical exercise may improve motor performance in PD but its role in cognitive function remains poorly eludicated. In this study in a rodent model of PD, we sought to examine whether exercise improves cognitive processing and flexibility, important features of EF. Rats received 6-hydroxydopamine lesions of the bilateral striatum (caudate-putamen, CPu), specifically the dorsomedial CPu, a brain region central to EF. Rats were exercised on motorized running wheels or horizontal treadmills for 6–12 weeks. EF-related behaviors including attention and processing, as well as flexibility (inhibition) were evaluated using either an operant 3-choice serial reaction time task (3-CSRT) with rule reversal (3-CSRT-R), or a T-maze task with reversal. Changes in striatal transcript expression of dopamine receptors (*Drd1-4*) and synaptic proteins (*Synaptophysin, PSD-95)* were separately examined following 4 weeks of exercise in a subset of rats. Exercise/Lesion rats showed a modest, yet significant improvement in processing-related response accuracy in the 3-CSRT-R and T-maze, as well as a significant improvement in cognitive flexibility as assessed by inhibitory aptitude in the 3-CSRT-R. By four weeks, exercise also elicited increased expression of *Drd1*, *Drd3*, *Drd4, synaptophysin, and PSD-95* in the dorsomedial and dorsolateral CPu. Our results underscore the observation that exercise, in addition to improving motor function may benefit cognitive performance, specifically EF, and that early changes (by 4 weeks) in CPu dopamine modulation and synaptic connectivity may underlie these benefits.

1. Introduction

Parkinson's disease (PD) is a chronic, progressive neurodegenerative disorder that diminishes the quality of life in over 630,000 people in the USA, which is projected to double by year 2040 as our population ages (Dorsey et al., 2013; Kowal et al., 2013). An early non-motor feature of PD is cognitive impairment, particularly deficits in executive function (EF), which includes processing information and cognitive flexibility (e.g., set-shifting, reversal learning) (Dirnberger and Jahanshahi, 2013; Parker et al., 2013). In PD, deficits in the fronto-striatal circuit represent a common pathophysiology (Robbins and Cools, 2014). The importance of the striatum in EF, also termed the basal ganglia (BG) or caudate nucleus-putamen (CPu), is based on a large rodent and human literature (see review (Macdonald and Monchi, 2011)). For example, in individuals with PD, resting state functional magnetic resonance imaging, as well as positron emission tomographic neuroimaging, have demonstrated hypo-activation in a number of cortical and sub-cortical (basal ganglia) regions impacting the EF network (Kim et al., 2019; Apostolova et al., 2020; Stögbauer et al., 2020; Hirano, 2021).

Rodent studies have specifically implicated the role of the dorsomedial CPu (dmCPu) in EF, and its importance in set shifting and reversal learning (O'Neill and Brown, 2007; Baker and Ragozzino, 2014; Grospe et al., 2018), particularly when selection requires competing responses and discounting more salient stimuli (Cools, 2006; Thoma et al., 2008; Yehene et al., 2008; van Schouwenburg et al., 2010). It has been proposed that deficits in reversal learning may be due to prominent projection fibers to the dmCPu from the medial prefrontal cortex, including anterior cingulate and prelimbic cortices (Voorn et al., 2004), as well as a broader cortico-striatal-thalamic circuit (Chudasama et al., 2001; Brown et al., 2010; Wang et al., 2019). Although the pathophysiological changes in the dmCPu that underlie EF changes in PD are complex, loss of synaptic integrity, including synaptophysin and PSD95, and dopamine (DA) neurotransmission, including DA loss and altered

* Corresponding author. Department of Psychiatry and the Behavioral Sciences, University of Southern California, 1975 Zonal Ave., KAM 400, MC9037, Los Angeles, CA, 90089-9037, USA.
E-mail address: holschne@usc.edu (D.P. Holschneider).
[1] These authors contributed equally.
[2] Co-senior authors.

https://doi.org/10.1016/j.crneur.2022.100039
Received 18 September 2021; Received in revised form 6 February 2022; Accepted 24 April 2022
Available online 1 May 2022

Abbreviations:

Actb	Actin-beta
ANOVA	Analysis of variance
AP	anterior-posterior
BG	Basal ganglia
CPu	Caudate putamen (striatum)
DA	Dopamine
DAR-D1-4	Dopamine receptors 1-4
dlCPu	Dorsolateral striatum
Dlg4	Gene coding for discs large MAGUK scaffold protein 4, also known as PSD-95
dmCPu	Dorsomedial striatum
Drd1-4	Genes for dopamine receptors 1-4
DT	Dual task
EDTA	ethylenediaminetetraacetic acid
EF	Executive function
Fisher's LSD	fisher's Least Significant Difference test
HPLC	High-performance liquid chromatography
ITI	Intertrial interval
L1-L3	3-CSRT learning levels 1-3
L1R-L3R	3-CSRT-R reversal learning levels 1-3
ML	Medial-lateral
MPTP	1-methyl-4-phenyl-1,2,3,6-tetrahydropyridine
NaOH	Sodium hydroxide
ns	nonsignificant
PD	Parkinson's disease
PFA/PBS	Paraformaldehyde/phosphate buffered saline
PSD-95	Postsynaptic density protein
RT-PCR	Reverse transcription polymerase chain reaction
SEM	standard error of the mean
SNC	Substantia nigra compacta
SNR	Substantia nigra reticulata
Syp	Synaptophysin
TH	Tyrosine hydroxylase
TO	Time out
vlCPu	Ventrolateral striatum
vmCPu	Ventromedial striatum
3-CSRT	3-choice serial reaction time task
3-CSRT-R	3-choice serial reaction time task with reversal
6-OHDA	6-hydroxydopamine

DA receptor expression, are reported to have a certain contribution (Salame et al., 2016). Dopamine receptors, comprised of D1-like receptors (DAR-D1 and D5R), D2-like receptors (DAR-D2, DAR-D3, and DAR-D4) play a central role in learning and EF-related cognitive processing and flexibility (Wang et al., 2019; Sala-Bayo et al., 2020).

A public health priority is to identify cost-effective therapies to combat progressive cognitive impairment in PD, which is not addressed by current therapies (Burn et al., 2014). There is significant evidence utilizing short-term clinical studies showing that different types of exercise may improve motor performance in PD, including aerobic exercise (treadmill walking, cycling), resistance exercise (strength or weight training), balance training (yoga, stepping), and multifaceted exercise (Tai Chi, dancing) (Alberts et al., 2011; Intzandt et al., 2018). Fewer studies have examined the impact of exercise on long-term cognitive function in PD patients. Even less is known regarding the molecular underpinnings of exercise-related benefits in PD-related EF impairment. Indeed, the long-term effects of chronic exercise on cognition remains controversial (Sanders et al., 2020; Schootemeijer et al., 2020; Brown et al., 2021). There is a need for research into the causality of the relationship between physical activity, cognitive performance and insights regarding exercise-induced repair mechanisms. Using the 6-hydroxydopamine (6-OHDA) lesioned model of PD, targeting specifically the dmCPu, this study sought to test the hypothesis that daily exercise improves EF-related cognitive processing and flexibility and that these benefits may be due to improved basal ganglia synaptic integrity and DA neurotransmission.

2. Methods

2.1. Animals

Wistar rats (male, 8–9 weeks of age) were purchased from Envigo Corporation (Placentia, CA, USA). Housing was under standard vivarium conditions in pairs on a 12-hr light/12-hr dark cycle (dark cycle 6 p.m. to 6 a.m.). All cages included a plastic pipe (10 cm diameter, 15 cm length) as an enrichment object. Rats had ad libitum access to food and water, except during food restriction as described in the behavioral studies. All experimental protocols were approved by the Institutional Animal Care and Use Committee of the University of Southern California, a facility approved by the Association for Assessment and Accreditation of Laboratory Animal Care, as well as by the Animal Use and Care Review Office of the US Department of the Army, and in compliance with the National Institutes of Health Guide for the Care and Use of Laboratory Animals, 8th Edition, 2011.

2.2. Experimental design overview

Groups included 6-OHDA lesioned (Lesion) or naïve (Non-Lesion) rats. We originally chose the naïve rat control over the sham-lesioned control, as we felt that examining the exercise effects in 'normals' had greater relevance to clinical translation of the effects of exercise in normal human subjects. Rats underwent food restriction as described below, beginning 2 weeks after lesion surgery. Starting 2 weeks after lesion surgery, rats were subjected to exercise in motorized running wheels with either (i) a smooth surface (termed aerobic exercise), (ii) a complex motorized running wheel with alternating rungs removed, (iii) on a horizontal treadmill, or (iv) sedentary (non-exercise). The sections below detail the experimental approaches, including the cognitive testing (Fig. 1) using the operant 3-CSRT with rule reversal (Section 2.6, Experiment 1) and T-maze with rewarded matching-to-sample (Win-Stay) and reversal (Win-Shift) (Section 2.7., Experiment 2) to evaluate executive function, as well as a striatal transcript analysis for dopamine receptors (DAR-) D1 through D4 and the synaptic genes PSD-95 and synaptophysin (Section 2.8., Experiment 3).

2.3. Rat model of bilateral, dorsomedial striatal dopamine-depletion (Wang et al., 2020)

We targeted the dorsomedial quadrant of the striatum (dmCPu) as past work has shown that this region in rodents is critical for reversal learning (O'Neill and Brown, 2007; Baker and Ragozzino, 2014; Grospe et al., 2018), with alterations in the rostromedial striatum presumably resulting in deficits in frontostriatal processing (Voorn et al., 2004). In brief, rats received stereotaxic injection of 6-OHDA at 4 striatal injection sites (2 in each hemisphere) (Sigma-Aldrich Co., St. Louis, MO, USA, 10 μg/site dissolved in 2 μL of 0.1% L-ascorbic acid/saline, 0.4 μL/min) targeting the bilateral dmCPu (AP: + 1.5 mm, ML: ± 2.2 mm, DV: 5.2 mm, and AP: + 0.3 mm, ML: ± 2.8 mm, DV: 5.0 mm, relative to bregma), which is the primary striatal sector targeted by the medial prefrontal cortex (Voorn et al., 2004) and critical for flexible shifting responses (O'Neill and Brown, 2007; Baker and Ragozzino, 2014; Tait et al., 2017; Grospe et al., 2018). After injection, the needle was left in place for 5

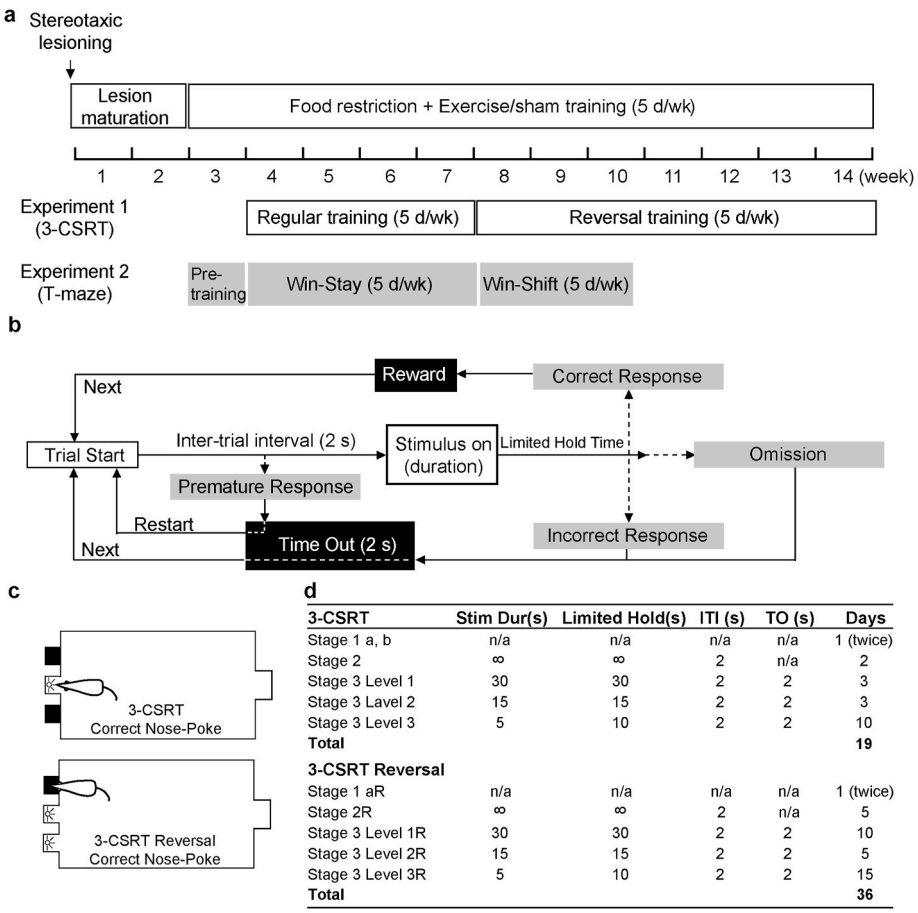

d

3-CSRT	Stim Dur(s)	Limited Hold(s)	ITI (s)	TO (s)	Days
Stage 1 a, b	n/a	n/a	n/a	n/a	1 (twice)
Stage 2	∞	∞	2	n/a	2
Stage 3 Level 1	30	30	2	2	3
Stage 3 Lavel 2	15	15	2	2	3
Stage 3 Level 3	5	10	2	2	10
Total					**19**
3-CSRT Reversal					
Stage 1 aR	n/a	n/a	n/a	n/a	1 (twice)
Stage 2R	∞	∞	2	n/a	5
Stage 3 Level 1R	30	30	2	2	10
Stage 3 Level 2R	15	15	2	2	5
Stage 3 Level 3R	5	10	2	2	15
Total					**36**

Fig. 1. Experimental protocol for operant training, T-maze, and exercise. (a) Timeline of experiments 1 and 2. **(b)** Protocol for the 3-choice serial reaction time task (3-CSRT) and reversal learning (3-CSRT-R). Gray shaded cells depict choices made by the rat. Black shaded cells depict consequences of those choices. Adapted from Asinof and Paine (2014) (Asinof and Paine, 2014)**. (c)** Acquisition of the 3-CSRT and 3-CSRT-R. **(d)** Progressive training schedule.

min before being slowly retracted (1 mm/min). Non-Lesion rats were used for controls. To prevent noradrenergic effects of the toxin, rats received desipramine (Sigma Aldrich, 25 mg/kg i.p.) before surgery (Roberts et al., 1975). Carprofen (2 mg in 5 g tablet, p. o., Bio-Serv, Flemington, NJ, USA) was administered for one day preoperatively and for two days postoperatively for analgesia. Exercise was initiated 2 weeks thereafter when lesion maturation was complete (Sauer and Oertel, 1994; Yuan et al., 2005). To verify the striatal target of 6-OHDA lesion, brains from a subset of rats were collected for immunohistochemical staining for tyrosine hydroxylase protein and HPLC analysis of DA.

2.3.1. *Tyrosine hydroxylase (TH) immunostaining*

TH immunostaining data were collected as previously reported and described quantitatively from lesioned and non-lesioned rats (Wang et al., 2020). Rats were anesthetized, subjected to transcardial perfusion with ice-cold saline followed by ice-cold 4% PFA/PBS. Brains were removed, transferred to the same fixative for 24 h, immersed in 20% sucrose for 48 h, frozen and cryo-sectioned at 25 μm thickness throughout the entire anterior-posterior extent of the brain. Selective sections spanning the 6-OHDA lesion in both the striatum and midbrain were subjected to TH-immunostaining using a primary antibody solution (1:2500 anti-tyrosine hydroxylase, Cat #AB152, Millipore-Sigma, Billerica, MA, USA), then visualized using a secondary antibody solution (1:5000 IRDye 800CW Goat anti-mouse Cat #926–3221, LI-COR, Lincoln, NE, USA). Images of tissues at the levels of the striatum representing the site of the 6-OHDA lesioning targeting the dmCPu and mid-ventral mesencephalon showing the midbrain dopaminergic neurons were obtained using a LI-COR Odyssey CLx (for internal landmarks, please see (Wang et al., 2020)).

2.3.2. *HPLC analysis of striatal dopamine*

Neurotransmitter concentrations in experiments 1 and 2 were determined according to an adaptation of Mayer and Shoup (1983) (Mayer and Shoup, 1983). Striatal tissue sections were dissected and immediately frozen on dry ice and stored at −80 °C until analysis. Tissues were sampled from coronal sections spanning bregma AP +2.00 to 0.00 mm, including tissue bordered ventrally by the anterior commissure, dorsally by the corpus callosum, medially by the lateral ventricle, and ±5.0 mm laterally from the midline) (Kintz et al., 2013; Lundquist et al., 2019). Striatal blocks were further sub-dissected to four quadrants, using the dorsal-ventral and medial-lateral divisions detailed previously (Voorn et al., 2004) to collect tissue from the dorsomedial striatum (dmCPu), dorsolateral striatum (dlCPu), ventromedial (vmCPu), and ventrolateral quadrants (vlCPu). For analysis, tissues were homogenized in 0.4 N perchloric acid, proteins were separated by centrifugation, and the supernatant used for HPLC analysis by electrochemical detection on an ESA HPLC system (ESA, Chelmsford, MA, USA) consisting of an ESA Model 582 pump, ESA Model 542 autosampler, ESA Model 5600 Detector and separation column (MD-150 × 3.2 mm). Data analysis employed the CoulArray for Window Application program (ESA Biosciences, Chelmsford, MA, USA). The protein pellet was resuspended in 0.5 N NaOH and total protein concentration determined using the BCA detection method (Pierce, Rockford, IL, USA). Striatal DA was expressed as nanograms DA per milligram protein.

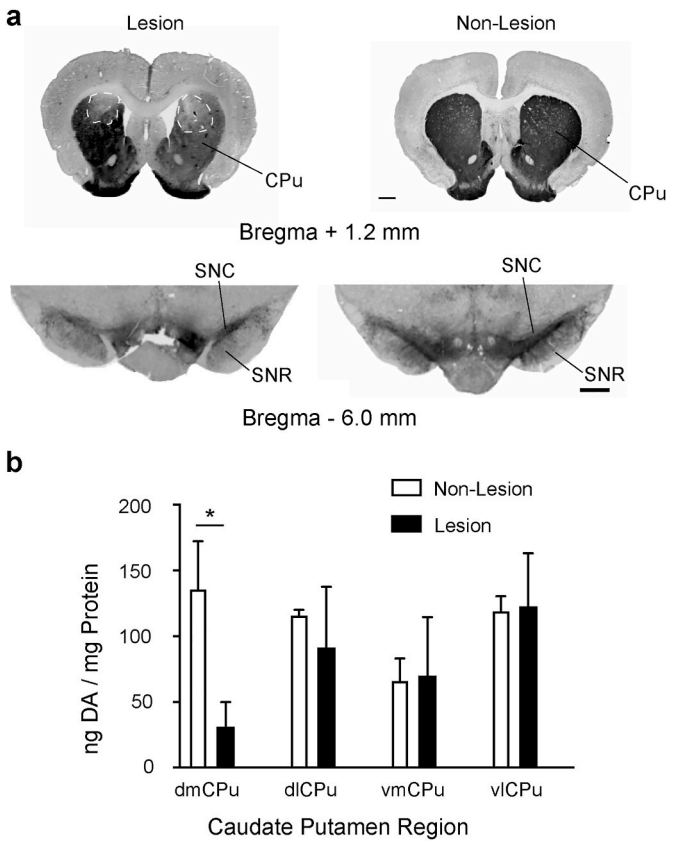

Fig. 2. Immunostaining for tyrosine hydroxylase to determine the degree and anatomical site of lesion. (a) Representative images of coronal sections reveal bilateral loss in tyrosine hydroxylase immunoreactivity in the dorsomedial striatum (bregma AP +1.20 mm anterior to bregma) and midbrain showing immunostaining of the substantia nigra pars compacta (SNC) and substantia nigra reticulata (SNR, bregma AP -6.0 mm). Scale bar = 0.5 mm. (b) HPLC analysis of striatal DA from tissues collected from coronal slice (bregma AP +2.00 to 0.00 mm) from Non-Lesion and Lesion rats in striatal tissue quadrants (dorsomedial dmCPu, dorsolateral dlCPu, ventromedial vmCPu, and ventrolateral vlCPu).

2.4. Food restriction

Food restriction was started 2 weeks after surgery and maintained throughout the 3-CSRT (Experiment 1) and T-maze (Experiment 2) behavioral studies. Rats were brought to 85% of their baseline body weight in one week and allowed to gain 5 g in body weight per week thereafter, with ad libitum access to water. Rats were fed between behavioral testing that took place in the morning and exercise that took place in the afternoon. Body weights were recorded Monday-Friday, with meal size individually adjusted on a daily basis, including weekends.

2.5. Exercise on running wheels and treadmill

2.5.1. Exercise on complex or smooth running wheels

Rats assigned to the skilled exercise group were trained in enclosed, motorized, running wheels (35.6 cm diameter, Lafayette Instrument, Lafayette, IN, USA) with irregularly spaced rungs, termed 'complex' running wheel, which demand the constant adaptation of stride length. A pseudo random pattern of rung spacing was achieved by repeating a pattern OOOOXOX, where O indicates a rung, and X a missing rung, resulting in inter-rung distance of either 1.3 or 2.6 cm). Exercise was initiated 2 weeks after lesion surgery using our prior methods (Wang et al., 2015a,b) and lasted a total of 30 min/day (4 bouts, 5 min/bout, 2-min inter-bout interval), 5 consecutive days/week (Mon - Fri). Starting time point was based on published literature reporting that bilateral striatal 6-OHDA lesions elicits TH losses at the level of the SN that reaches a plateau after 2 weeks (Yuan et al., 2005; Blandini et al., 2007), with DA losses plateauing at 2 weeks (Ben et al., 1999), and with nigral cell losses variably reported as plateauing (Yuan et al., 2005) or decreasing thereafter to 4 weeks post-injury (Blandini et al., 2007). Rats were subjected to 1 week of individually adjusted, performance-based speed adaptation to reach a plateau speed of 5 m/min, a speed achievable by most 6-OHDA lesioned rats in the complex wheel following 1 week of exercise (Wang et al., 2013, 2015). Titration of speed has been described in detail in our prior publication (Wang et al., 2013). Non-Exercise rats were left in a stationary running wheel for 30 min/day. Running speeds for the Non-Lesion, control rats were matched to speeds achievable by lesion rats in the complex wheel (5 m/min maximum). An additional group of lesion rats was trained in motorized running wheels identical to those described above, except that these wheels had regularly placed rungs and an inner plastic 'smooth' floor covering the metal rungs and were termed 'smooth' running wheel as previously reported (Wang et al., 2013, 2015). The modification made foot placement easier for lesioned rats, and therefore minimized the 'motor skill' factor. Speeds for the smooth running wheels were matched to those of the complex running wheels.

2.5.2. Exercise training on horizontal treadmill

A separate group of rats were trained on a motorized, 10-lane horizontal treadmill (lane width 10 cm, length 94 cm, wall height 20 cm, custom made) for 65 min a day, 5 days per week (Mon - Fri) starting two weeks after stereotaxic surgery. Each exercise session consisted of a 15-min warm-up, 15-min running, 5-min break, 15-min running, and 15-min cool-down. The warm-up and cool-down speed started at 4 m/min and went up to 10 m/min by 2 weeks, while the running speed started at 6 m/min and went up to 30 m/min in 4 weeks. The rats were exercised at 10 and 30 m/min for the remaining 10 weeks. A researcher prompted the rats to stay on the treadmill and run by lightly brushing the rear end of any rat that fell back with a brush. After several days of exercise, rats typically will stay on the treadmill running.

2.6. Operant training

2.6.1. Groups

In Experiment 1, rats with bilateral, dmCPu 6-OHDA lesions were exposed to exercise in either: (i) motorized, complex running wheel (Lesion/Complex Wheel, $n = 12$), (ii) motorized smooth running wheel (Lesion/Smooth Wheel, $n = 4$), or (iii) motorized horizontal treadmill (Lesion/Treadmill, $n = 6$). The control group of rats included 6-OHDA lesion, non-exercise rats (Lesion/Non-Exercise, $n = 12$) or Non-Lesion, non-exercise rats (Non-Lesion/Non-Exercise, $n = 12$). The Non-Lesion group consisted of both non-exercise (n = 6) and complex running wheel (n = 6) and since they showed no significant differences in operant training outcomes they were pooled (Supplementary Fig. S1).

Whereas in our original design sample size was balanced across all groups to access modality-specific effects of exercise, we were not able to complete all experiments due to local restrictions and university-mandated euthanasia of rats during the height of the Covid-19 pandemic. These rats were excluded from analysis. Because preliminary analysis showed the exercise effects to be modest (Supplementary Fig. S2), we pooled the three exercise groups to form a single Lesion/Exercise group ($n = 22$) in this report.

2.6.2. Three-choice serial reaction time nose-poke task with reversal (Fig. 1)

We chose a 3-CSRT paradigm with an added rule reversal feature, called 3-CSRT-reversal (3-CSRT-R), to examine cognitive flexibility. Detailed methods are provided in our prior publication (Wang et al., 2020). In brief, rats were food restricted and randomized to receive

complex wheel exercise, simple wheel exercise, treadmill exercise, or no exercise. Exercise was initiated 1 week prior to operant training, during which time they were handled on a daily basis and given 5 sucrose pellets per day in their home cage (45 mg/pellet, chocolate flavor, #F0025, Bio-Serv, Frenchtown, NJ, USA). Exercise was continued for 12 weeks. Each modular test chamber (MedAssociates, St. Albans, VT, USA) was housed in a sound attenuating cubicle, and consisted of grid floor, house light, 3-bay nose-poke wall, pellet trough receptacle, receptacle light, head entry detector, and a PC-controlled smart controller. Rats were trained to associate nose poking into an illuminated aperture with receiving a single sucrose pellet reward. Rats were familiarized with the test chamber and nose-poke and reward retrieval behavior were shaped in pretraining lasting 1 week as previously described (Wang et al., 2020). Thereafter, during the regular phase of 3-CSRT training, the rats were trained following a progressive schedule with a fixed ratio 1 schedule response-reward task (up to 90 trials or 30 min each session per day, 5 days/week, 16 sessions). The walls, nose-poke apertures, food receptacle, and grid floor were wiped with 70% isopropyl alcohol between rats.

For each trial, the light stimulus was turned on in a pseudo-randomly chosen nose-poke aperture (Fig. 1b). The stimulus stayed on for a set duration or until a nose-poke (correct or incorrect) was detected. The rat received a food reward following a correct nose-poke within the set limited hold duration, which was set to be the same as the stimulus duration or slightly longer for short stimulus durations. Following reward retrieval and a 2-s intertrial interval (ITI), the next trial was started. If an incorrect nose-poke was detected, the rat received a 2-s time out (TO), during which the chamber light was turned off. If no nose-poke was detected within the limited hold duration, an omission was recorded, with a 2-s TO. After each TO, the chamber light was turned on, and after a 2-s ITI, the next trial was started. If a nose-poke was detected during the ITI, a premature response was recorded without incrementing the trial number, and the rat received a 2-s TO. Any nose-pokes following a correct response and before reward retrieval were recorded as repetitive responses. Rats were trained through 3 difficulty levels with progressively shortened stimulus durations. We chose to control the number of training days for each level across rats to facilitate between-group comparison. This was selected based on our prior work showing that lesion rats can reach a performance level comparable to that of Non-Lesion rats at this difficulty level (Wang et al., 2020). Differences in reversal learning can thus be interpreted as differences in cognitive flexibility, rather than differences based on incomplete learning. The final stimulus duration was set at 5 s, reflecting a moderate level of difficulty.

During the rule-reversal phase of 3-CSRT-R training (Fig. 1c), the stimulus was switched from a lit aperture among dark apertures to a dark aperture among lit apertures. The animal was trained progressively to learn to nose-poke the dark aperture to receive reward (25 sessions, 1 session/day, 5 days/week).

For 3-CSRT and 3-CSRT-R the following behaviors were captured (Asinof and Paine, 2014): (i) nose-poke accuracy = (number of correct responses)/(number of correct + number of incorrect responses) * 100%, a primary measure of operant learning; to account for modest differences in 3-CSRT acquisition, we normalized nose-poke accuracy during the reversal phase by accuracy at the end of acquisition (L3, Day 10, Fig. 3); (ii) number of omissions, a measure of attention; (iii) premature responses, a measure of impulsivity and response inhibition, (iv) correct nose-poke latency = average time from onset of stimulus to a correct response, a measure of attention and cognitive processing speed; and (v) reward retrieval latency = average time from correct response to retrieval of sugar pellet, a measure of motivation.

2.7. T-maze

2.7.1. Groups

In Experiment 2, rats (n = 7) with 6-OHDA lesions were exercised for 6 ½ weeks in the complex wheel. Controls included lesion, non-exercise rats (Lesion/Non-Exercise, $n = 6$), and Non-Lesion, non-exercise controls (Non-Lesion/Non-Exercise, $n = 9$).

2.7.2. T-maze with rewarded matching-to-Sample and reversal

Cognition testing of EF in rats was adapted from methods from our work (Stefanko et al., 2017) and that of others (Deacon and Rawlins, 2006). Rats were food restricted and randomized to exercise in the complex wheel or non-exercise. One week prior to T-maze training, rats were handled on a daily basis and given 5 dustless, chocolate-flavored sucrose pellets per day in their home cage (45 mg/pellet, #F0025, Bio-Serv, Frenchtown, NJ, USA). The T-maze was constructed as a cross maze of black, opaque Plexiglas. Arms (15.2 cm width, 50.8 cm length, 35.2 cm height) could be sealed off by guillotine doors (15.2 cm width x 35.2 cm height) to prevent entry to an enclosed central platform (15.2 cm width, 15.2 cm length, 35.2 cm height). Two opposing arms were designated as the branch arms, with one of the remaining two arms randomized to be designated the stem arm with its opposite arm sealed during the 'T-maze' testing. A partition extended across the central platform and 6.4 cm into the chosen stem arm, allowing entry into either of the open branch arms. Arm entry was defined as having all four paws in the arm. If a rat failed to mobilize within 90 s, it was removed from the maze, to be exposed again 10 min later. Uneaten sucrose pellets and fecal pellets were removed from the maze between trials, and the maze wiped with 70% isopropyl alcohol solution.

T-Maze acclimatization occurred over 3 days during which time rats were allowed to explore the maze. Initially the floor of the maze was baited with individual sucrose pellets, followed by baiting of both maze arms, followed by baiting of both food cups. Rats were trained for 3 days in a forced trial paradigm, in which food reward was available only in one arm (randomized), with the other branch arm blocked (10 trials with a 5-s intertrial interval in the morning and again in the afternoon). Thereafter, they were trained in a 'Win-Stay' paradigm (sample run→choice trial, 10 trials twice per day, 5-s intertrial interval, x 20 days), in which rats had to choose the same arm during a choice trial (both arms open) that had previously been rewarded on the preceding sample trial (one arm closed). Sample trials were randomized across both arms. Thereafter, during implementation of a rule reversal, rats were exposed to a 'Win-Shift' strategy, in which the rat was only rewarded in the choice run if it entered the branch arm opposite the one chosen in the sample run (sample run→choice trial, 10 sequences twice per day, 5-s intertrial interval, x 13 days). The number of correct entries into the bated choice arm were recorded for each trial.

2.8. Quantitative RT-PCR for striatal dopamine receptor and synaptic gene expression

In Experiment 3, two additional groups of 6-OHDA-lesioned rats were exercised in the complex running wheel (Lesion/Complex Wheel, $n = 6$) or smooth running wheel (Lesion/Smooth Wheel, $n = 6$) for 4 weeks before being euthanized for transcript analysis. Since there were no statistically significant differences in gene expression between the Smooth wheel and the Complex wheel groups, the gene expression data from the two exercise modalities were pooled to form a single composite Exercise group (n = 12), similar to the approach in Experiment 1. Final group analyses included Non-Lesion/Non-Exercise (n = 6), Lesion/Non-Exercise (n = 6), and Lesion/Exercise (n = 12). The pattern of expression of several genes including *Syp* (synaptophysin, Gene ID 24804), *Dlg4* (discs large MAGUK scaffold protein 4, also known as PSD95, Gene ID 29495), *Drd1* (DAR-D1, Gene ID 24316), *Drd2* (DAR-D2, Gene ID 24318), *Drd3* (DAR-D3, Gene ID 29238), and *Drd4* (DAR-D4, Gene ID 25432) were examined. Immediately after the final exercise session, rats were sacrificed via decapitation and whole brains were extracted. Fresh tissue was rapidly micro-dissected in blocks from the CPu (dmCPu, dlCPu, vmCPu, vlCPu as described in section 2.3.2). Tissues were submerged in an RNA stabilization solution (pH 5.2) at 4 °C, containing in

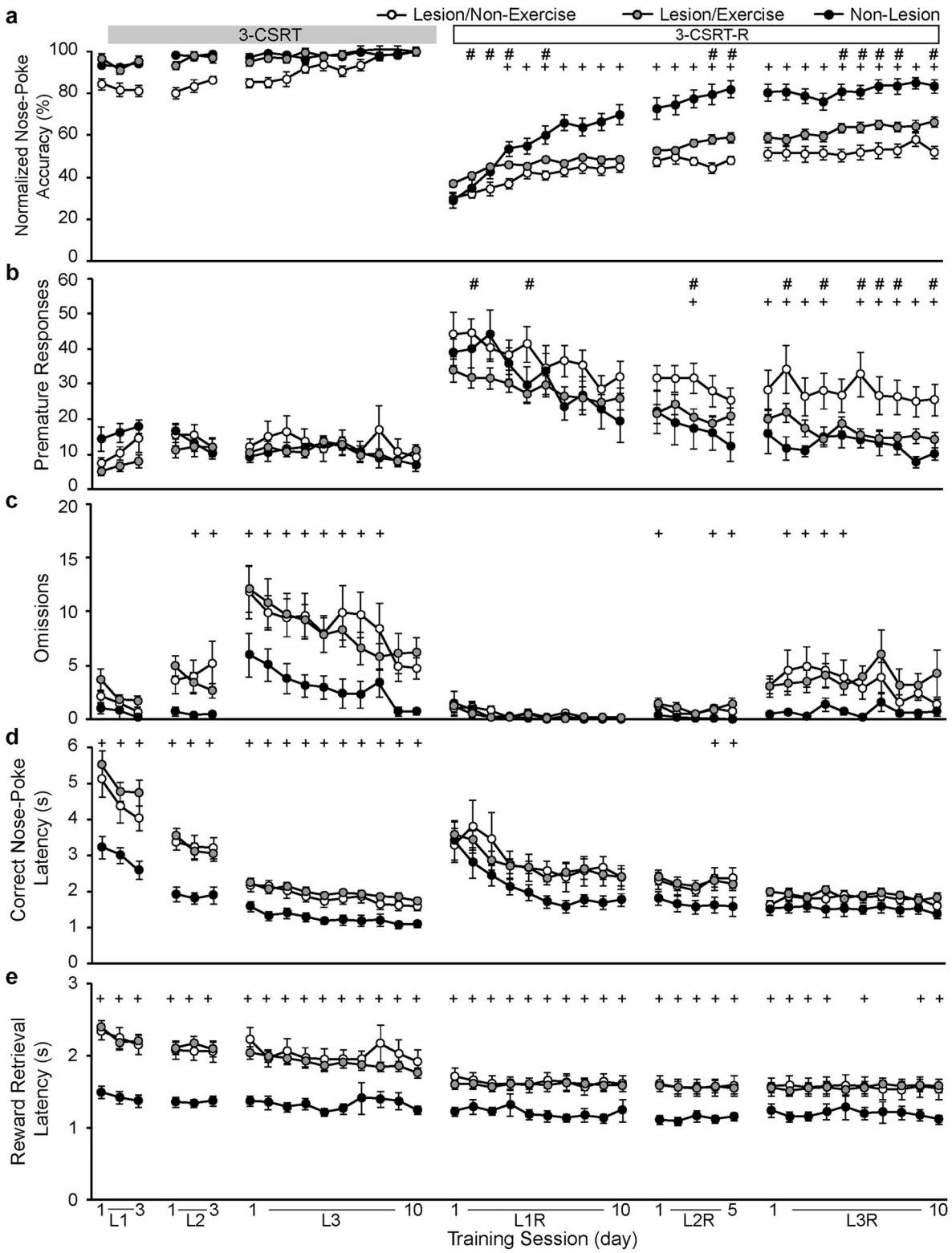

Fig. 3. Effects of exercise and lesion on the 3-choice serial reaction time task (3-CSRT) acquisition and reversal learning (3-CSRT-R). Shown are group mean ± SEM of **(a)** normalized nose-poke accuracy, **(b)** premature responses, **(c)** omissions, **(d)** correct nose-poke latency, and **(e)** reward retrieval latency for Non-Lesion ($n = 12$), Lesion/Non-Exercise ($n = 12$) and Lesion/Exercise group ($n = 22$). Results show that exercise elicits a significant, modest improvement in response accuracy in the 3-CSRT-R, as well as a robust improvement in inhibitory aptitude in the 3-CSRT-R in lesioned rats. #: $p < 0.05$ Lesion/Exercise vs. Lesion/Non-Exercise; +: $p < 0.05$ Lesion/Non-Exercise vs. Non-Lesion, Fisher's LSD multiple comparisons test. Data were also analyzed with two-way ANOVA with repeated measures (results listed in Supplementary Table S1). The Non-Lesion group consisted of both non-exercise (n = 6) and complex running wheel (n = 6), and since they showed no significant differences in operant training outcomes they were pooled (Supplementary Fig. S1).

mM: 3.53 ammonium sulfate, 16.66 sodium citrate, and 13.33 EDTA (ethylenediaminetetraacetic acid), transferred to a sterile tube containing 300 μl TRI-reagent (Cat. No. 11–330T, Genesee Scientific, San Diego, CA, USA), and homogenized with a mechanical pestle before centrifuging at 13,000×*g* for 3 min. Supernatant was removed to a new tube and 250 μl of chloroform was added and tubes vigorously shaken twice for 10 s, followed by 3 min of rest on ice and centrifugation at 13,000×*g* for 18 min at 4 °C. The upper aqueous layer was carefully removed to a new tube, an equal volume of 100% ethanol was added, and the sample was thoroughly mixed before RNA purification using the Zymo Direct-zol RNA Miniprep (Cat. No. 11–330, Genesee Scientific) according to the manufacturer's instructions. RNA was eluted in 35 μl of DNAse/RNAse free water before spectrophotometric analysis of RNA purity and concentration. Complementary DNA (cDNA) was synthesized from 1 μg isolated RNA using the qPCRBIO cDNA Synthesis Kit (Cat. No. PB30.11–10, PCR Biosystems, Wayne, PA, USA) following manufacturer's guidelines before being diluted 1:5 in DNAse/RNAse free water and stored at −20 °C. Gene expression changes were measured with quantitative RT-PCR (qRT-PCR) as previously described (Lundquist et al., 2019, 2021). Briefly, qRT-PCR was run with 2 μl of cDNA and qPCRBIO SyGreen master mix (Cat. No. PB20.11–01, PCR Biosystems) on an Eppendorf Mastercycler Ep Realplex (Eppendorf, Hauppauge, NY, USA) using a program of 15 min at 95 °C, followed by 40 cycles of 15 s at 94 °C, 30 s at 55 °C, and 30 s at 72 °C. Data was collected and normalized on Eppendorf Realplex ep software. Standard delta-CT analysis (Livak and Schmittgen, 2001) was used to quantify fold changes in gene expression in experimental groups normalized to controls, with beta-actin serving as a housekeeping gene. Primer oligonucleotide pairs are listed in Supplementary Table S7.

2.9. Statistical analysis

Data are presented as mean ± S.E.M. and analyzed using GraphPad Prism (version 8.3.0, GraphPad Software, San Diego, CA, USA).

2.9.1. 3-CSRT/3-CSRT-R

3-CSRT data were analyzed using two-way ANOVA with repeated measures for each training level, with lesion and time, or exercise and time as the factors, and with Fisher's LSD multiple comparisons test comparing groups for individual training session. In addition, to control for any possible subtle lesion-related deficits in motor and cognitive functions at the end of the 3-CSRT acquisition phase, we also examined a normalized nose-poke accuracy in which the group average of accuracies during the 3-CSRT-R were normalized by the group mean accuracy on the final day of regular training (L3 of 3-CSRT). All statistical test results for main effect of lesion and exercise are included in Supplementary Table S1.

2.9.2. T-maze with reversal

The lesion effect was analyzed by a mixed model with repeated measures in 'time' and main effect being 'lesion' ($p < 0.05$). Accuracy in the Win-Stay and Win-Shift paradigms was separately analyzed by a two-way ANOVA with repeated measures in 'time' and main effect being 'exercise' ($p < 0.05$). Performance was evaluated as: (i) percent of correct responses per session during initial learning (Win-Stay) and reversal learning (Win-Shift); (ii) the number of trials an individual rat required to reach the learning criterion during the reversal phase, defined as 9 out of 10 correct choices in consecutive trials; and (iii) perseverative or regressive errors made during the reversal learning phase. Perseverative and regressive errors were defined, respectively, as the number of incorrect choices made until or after the rat chose the correct arm for 5 consecutive trials. Perseverative and regressive errors during the Win-Shift phase were separately analyzed by a two-way ANOVA with repeated measures in 'time', and main effect either being 'lesion' or 'exercise' ($p < 0.05$). Fisher's LSD multiple comparisons tests were used to compare groups for individual days.

2.9.3. Transcript and HPLC analysis

All statistical tests were carried out and graphs made in Prism 9.1 (GraphPad, San Diego, CA, USA) with statistical significance set at $p < 0.05$. No sample size calculations were performed prior to the start of the study but are based on previous publications. Unpaired, two-tailed T-tests were used for all qRT-PCR analysis between control and pooled exercise groups (smooth wheel, complex wheel). One-way ANOVA with Tukey's multiple comparisons was used for analysis of gene expression across exercise groups (non-exercise, exercise). Statistical analysis for HPLC data was carried out by using a one-way ANOVA with Dunnett's posttest comparing saline (control) treatment with 6-OHDA-lesioned groups. All statistical test results are included in Supplementary Tables S3–7.

3. Results

3.1. Assessment of 6-OHDA-lesioning on tyrosine hydroxylase expression and dopamine levels

Analysis of TH immunoreactivity demonstrated a significant reduction in TH immunostaining in the dmCPU (the stereotactic target of 6-OHDA) in lesioned rats compared to Non-Lesion rats (Fig. 2a). There were no significant differences in the dlCPu, vmCPu, and vlCPu of lesioned compared to Non-Lesion rats. Examination of TH immunostaining in the midbrain showed reduced staining of the substantia nigra from 6-OHDA-lesioned rats compared to Non-Lesion rats. Analysis of DA levels by HPLC showed a significant difference in only the dmCPu quadrant, the region targeted for stereotaxic delivery of 6-OHDA, compared to Non-Lesion rats (31.2 ± 18.7 ng vs. 136.1 ± 36.1 DA/mg Protein, $p < 0.05$). All other quadrants of CPu tissues did not show a statistically significant difference comparing Non-Lesion with lesioned tissue quadrants (Fig. 2b). These results show that lesions were limited to the dmCPu quadrant, with retrograde bilateral dopaminergic cell losses also apparent at the level of the substantia nigra.

3.2. Experiment 1: Effect of lesion and of exercise on operant training (3-CSRT/3-CSRT-R)

3.2.1. Lesion effects

During the acquisition phase of 3-CSRT (Levels L1, L2, L3), Lesion/Non-Exercise rats compared to Non-Lesion/Non-Exercise showed: (i) statistically significant lower nose-poke accuracy (Supplementary Fig. S2a $p < 0.0001$, two-way ANOVA repeated measures that diminished towards the end of L3 (L3 Day 10: Lesion/Non-Exercise 83.77 ± 2.05% vs. Non-Lesion 91.41 ± 1.10%); (ii) no differences in the number of premature responses ($p > 0.05$. Fig. 3b); (iii) significantly higher number of omissions in L2 and L3 ($p < 0.05$. Fig. 3c); (iv) significantly greater correct nose-poke latency (~0.6 s, $p < 0.005$. Fig. 3d); and (v) significantly greater reward retrieval latency (~0.6 s, $p < 0.001$. Fig. 3e). See Supplementary Table S1 for *F* and *p* values.

A reversal was introduced to evaluate cognitive flexibility. At the start of 3-CSRT-R, when the rule for correct (rewarded) response was switched from nose-poking a lit aperture to nose-poking a dark aperture, both Lesion/Non-Exercise and Non-Lesion/Non-Exercise rats showed a sudden drop in performance with decreased nose-poke accuracy to the same extent, increased correct nose-poke latency, and increased premature responses. Both groups showed improvement in these parameters with continued training. Non-Lesion/Non-Exercise improved nose-poke accuracy rapidly to a plateau of about 75% (L3R Day 10, 76.55 ± 3.21%), while Lesion/Non-Exercise rats only improved accuracy modestly to a plateau of about 40% (L3R Day 10, 43.69 ± 2.95%). Lesion/Non-Exercise rats compared to Non-Lesion controls showed: (i) statistically significant lower nose-poke accuracy ($p < 0.001$. Supplementary Fig. S2a); (ii) significantly higher number of premature responses in L3R ($p = 0.0088$. Fig. 3b); (iii) significantly higher number of omissions in phases L2R and L3R ($p < 0.05$. Fig. 3c); (iv) no differences

in correct nose-poke latency ($p > 0.05$. Fig. 3d); and (v) significantly greater reward retrieval latency (~0.5 s, $p < 0.05$. Fig. 3e).

3.2.2. Exercise effects

Lesion/Complex Wheel, Lesion/Smooth Wheel, and Lesion/Treadmill rats showed similar outcomes in the 3-CSRT task (Supplementary Fig. S2) and were pooled to form a Lesion/Exercise group ($n = 22$). Lesion/Exercise compared to Lesion/Non-Exercise rats showed a statistically significant lower number of premature responses during the reversal phase L3R ($p = 0.018$. Fig. 3b). To account for modest differences in 3-CSRT acquisition, we normalized nose-poke accuracy during the reversal phase by accuracy at the end of acquisition (L3, Day 10). Lesion/Exercise rats showed significantly higher normalized nose-poke accuracy in all reversal levels ($p < 0.05$. Fig. 3a). There were no differences in omission, correct nose-poke latency, and reward retrieval latency between the two groups (Fig. 3c–e).

3.3. Experiment 2: Effect of exercise on T-maze task with reversal

To examine the effect of dmCPu 6-OHDA lesion and exercise on cognitive flexibility, behavior in the T-Maze with reversal was tested. The groups examined were Lesion/Non-Exercise, Non-Lesion/Non-Exercise, and Lesion/Complex Wheel. During the Win-Stay phase, there was a significant effect of lesion ($F_{1,13} = 13.47$, $p = 0.0028$) and a lesion × time interaction ($F_{19,217} = 3.34$, $p < 0.0001$) in response accuracy (Fig. 4a, Supplementary Table S2). Exercise improved accuracy in lesioned rats ($F_{1,11} = 8.063$, $p = 0.016$), without exercise × time interaction. During the rule reversal Win-Shift phase, there were significant effects of lesion ($F_{1,13} = 41.83$, $p < 0.0001$) and lesion × time interaction ($F_{12,142} = 4.76$, $p < 0.0001$. Fig. 4b). Non-Lesion/Non-Exercise compared to Lesion/Non-Exercise rats reached the learning criterion significantly earlier ($p < 0.00001$. Fig. 4c) and showed fewer perseverative errors ($F_{1,13} = 4.69$, $p < 0.05$. Fig. 4d) and fewer regressive errors ($F_{1,13} = 6.76$, $p < 0.05$. Fig. 4e). During the Win-Shift phase, there was a significant effect of exercise ($F_{1,11} = 15.57$, $p = 0.0023$. Fig. 4b), but no significant exercise × time interaction. Lesion/Complex wheel compared to Lesion/Non-Exercise rats reached the learning criterion significantly earlier ($p < 0.002$. Fig. 4c) and showed fewer perseverative errors ($F_{1,11} = 7.29$, $p < 0.02$. Fig. 4d), with no significant differences in regressive errors (Fig. 4e). In summary, the T-maze detected a clear significant lesion effect during the Win-Stay paradigm, a significant difference that was accentuated during the Win-Shift phase. Lesion rats that underwent complex wheel exercise showed a greater number of correct responses compared with Non-Exercise rats. This effect showed a significant difference during the Win-Stay phase and was accentuated during the Win-Shift phase of training.

3.4. Transcript analysis

Following 6-OHDA lesioning of the dmCPu, the effects of 4 weeks of different exercise modalities – aerobic running in a smooth wheel, or skilled running in a complex wheel with irregularly spaced rungs – on synaptic plasticity (*Syp, Dlg4*) and DAR receptor gene (*Drd1, Drd2, Drd3, Drd4*) expression were examined in four quadrants of the striatum using qRT-PCR. There were no statistically significant differences in gene expression between exercise in the Smooth or Complex Running Wheel groups (Supplementary Fig. S3, Tables S3–S6). Therefore, gene expression data from the two exercise modalities were pooled to form a composite Exercise group, in parallel with the approach in Experiment 1 of the behavioral studies. Final group analyses included Non-lesion/Non-Exercise (n = 6), Lesion/Non-Exercise (n = 6), and Lesion/Exercise (n = 12) (Fig. 5). In the dmCPu, there were significant group differences in *Dlg4* (F(2,21) = 4.61, P = 0.02) and *Drd1* (F(2,21) = 10.07, $p < 0.001$), *Drd3* (F(2,21) = 10.07, P = 0.004), and *Drd4* (F(2,21) = 3.69, P = 0.04) but no significant group differences in *Syp* (F(2,21) = 2.35, P = 0.12) or *Drd2* (F(2,21) = 0.73, P = 0.49). Post hoc analysis showed a significant lesion effect on Dlg4 (PSD-95, $P = 0.04$) and an exercise effect on transcript expression of *Dlg4* ($P = 0.03$), *Drd1* ($p < 0.001$), *Drd3* ($p <$

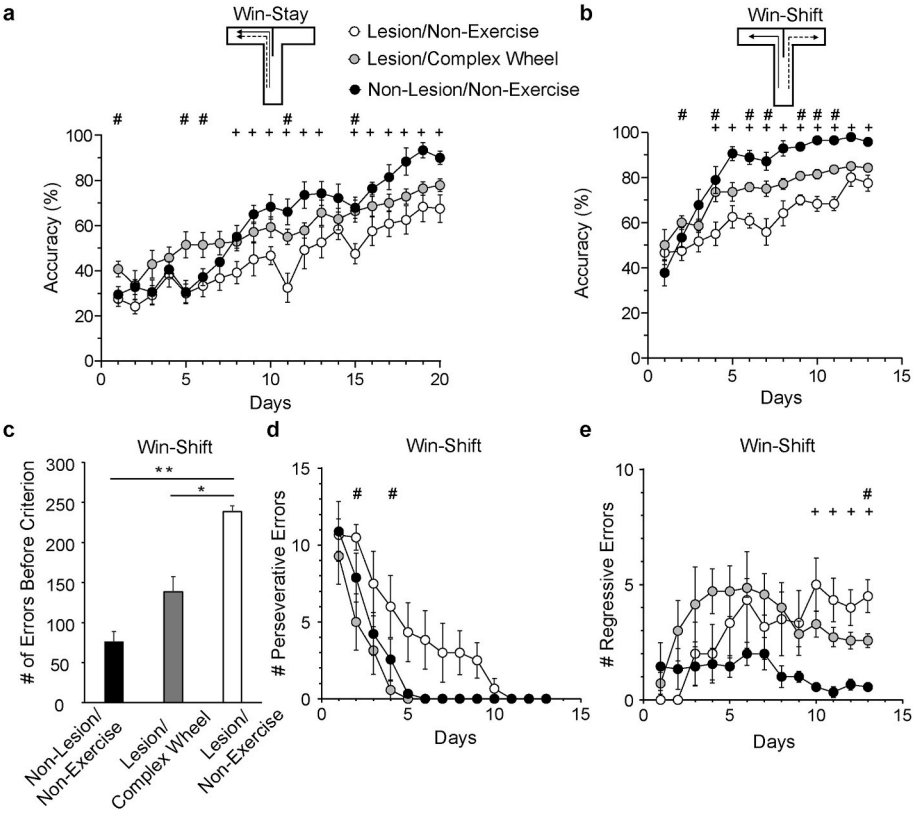

Fig. 4. Effects of lesion and exercise on T-maze learning of rewarded matching-to-sample (Win-Stay) followed by reversal (Win-Shift). **(a)** Rats were trained in a Win-Stay strategy (solid line arrow = sample trial; dashed line arrow = choice trial) for 20 days, followed by training in **(b)** Win-Shift strategy for an additional 13 days. Response accuracy (percentage of correct responses) is shown for Non-Lesion/Non-Exercise ($n = 9$), Lesion/Complex wheel ($n = 7$) and Lesion/Non-Exercise ($n = 6$). **(c)** Total number of incorrect trials performed until criterion (9 correct responses in 10 consecutive trials) was reached during the Win-Shift phase. **(d)** Perseverative errors during the Win-Shift phase. **(e)** Regressive errors during the Win-Shift phase. Mean ± SEM. Exercise improves response accuracy in the T-maze, shortens time until learning, while diminishing perseverative errors following rule reversal (Win-Shift phase). #: $p < 0.05$ Lesion/Complex wheel vs. Lesion/Non-Exercise; +: $p < 0.05$ Lesion/Non-Exercise vs. Non-Lesion/Non-Exercise, Fisher's LSD multiple comparisons test. *: $p < 0.0002$, **: $p < 0.001$ (Student's *t*-test).

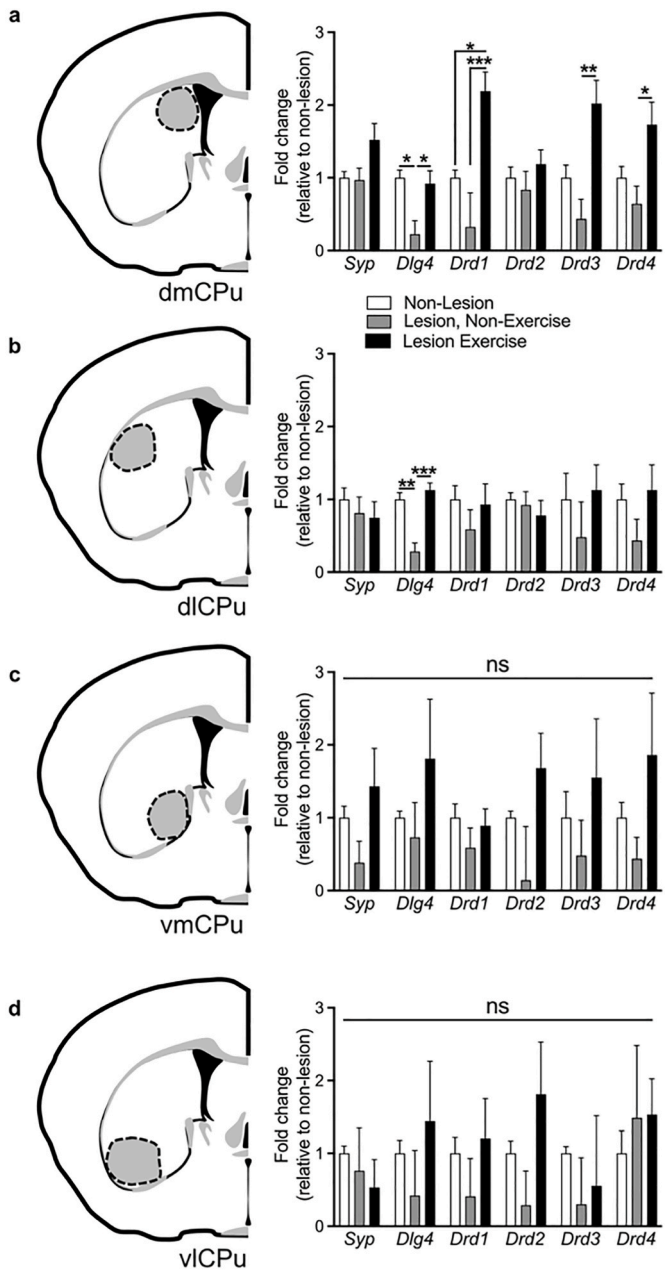

Fig. 5. Dopaminergic signaling and synaptogenic gene expression changes across caudate putamen quadrants following exercise in Lesion rats. Rat caudate putamen was divided into four quadrants for transcript analysis: **(a)** dorsomedial (dmCPu), **(b)** dorsolateral (dlCPu), **(c)** ventromedial (vmCPu), and **(d)** ventrolateral (vlCPu). Corresponding gene expression changes for four DA receptor (*Drd1, Drd2, Drd3, Drd4*) and two synaptic (*Syp, Dlg4*) genes in the exercise group (pooled complex and smooth wheel running, $n = 12$) compared to Non-Exercise controls ($n = 6$). Mean ± SEM. *$p < 0.05$, **$p < 0.01$, ***$p < 0.001$ relative to Non-Exercise control (Student's *t*-test), ns nonsignificant.

0.005), and *Drd4* (P = 0.046) (Fig. 5a). In the dlCPu, there was a significant group difference only in *Dlg*4 ($F(2,21) = 16.57$, $p < 0.001$). Post hoc analysis showed a significant lesion effect on transcript expression of Dlg4 (P = 0.001) and an exercise effect (P = 0.001). (Fig. 5b). In the ventral quadrants of the striatum (vmCPu, vlCPu), there was no statistically significant group difference in transcript expression of *Syp*, *Dlg4*, and *Drd*1, *Drd*2, *Drd*3, and *Drd*4. A complete list of statistical test results can be found in Supplementary Tables S1–S4.

4. Discussion

4.1. Effects of lesions and exercise on cognitive outcomes

Although the rate of acquisition in the 3-CSRT was slower in lesion compared to non-lesion rats, lesion rats were able to acquire a level of accuracy (84%) comparable to that of non-lesion (90%) following 16 days of exercise. This suggests a delay in memory consolidation. There were no significant group differences in premature responses, a measure of impulsive behavior, after 16 days of learning the 3-CSRT. Lesion rats compared to non-lesion rats showed a trend of higher omission rate and a statistically significant greater standard deviation of omissions, suggesting a mild deficit in attention. Consistent with prior work (Hauber and Schmidt, 1994), lesion compared to non-lesion rats had a small but significantly longer reaction time (<1 s) for reward retrieval. This difference was unlikely due to motor deficits as dmCPu lesions do not alter spontaneous locomotor activity, rotarod performance (Wang et al., 2020) or forelimb motor function (Chang et al., 1999). Furthermore, dmCPu lesions do not significantly alter appetitive preference (Wang et al., 2020). Thus, differences in reward retrieval latency (or omissions rate) likely reflect a slowing of cognitive processing and mildly impaired attention, rather than a general motor dysfunction or a lack of motivation.

In contrast to the 3-CSRT, substantial and persistent deficits were unmasked during the 3-CSRT-R phase. During the first day of the 3-CSRT-R, both lesion and non-lesion rats showed an equivalent decrease in nose-poke accuracy. Following 15 days of cognitive training, non-lesion rats rapidly improved (~80% accuracy), while lesion rats showed persistent deficits (~50% accuracy). Performance plateaued thereafter, with an additional 10 days of cognitive training showing little change to the percent accuracy measure (Fig. 3). While a delay in memory consolidation may have contributed, the plateauing of performance beginning at ~15 days for the Lesion/Non-Exercise group suggests that these deficits represent more than simply a slower rate of learning. Lesions also resulted in significant and persistent greater number of premature responses that plateaued at 15 days of cognitive training. We propose that the 3-CSRT-R task unmasked lesion-induced deficits in cognitive flexibility and response inhibition.

Qualitatively, the lesion effect on T-maze learning mirrored those in the operant task. Lesioned rats were slow to learn the Win-Stay task, and never achieved correct response rates above 70%, even after 20 days of cognitive training, while controls achieved a 90% correct response rate by 18 days (Fig. 4). Rule reversal (Win-Shift) enhanced these differences, with the lesioned rats significantly delayed in achieving the learning criterion, and never achieving more than 78% correct after 13 days of cognitive training, at a time when Non-Lesion rats showed 95% correct responses. Perseverative and regressive errors during the reversal phase were significantly greater in Lesion than in Non-Lesion rats as has previously been reported (Grospe et al., 2018).

Our studies showed that exercise in both the operant task and T-maze improved performance in lesioned rats. These results are consistent with earlier work in a rat stroke model showing that running exercise facilitates learning of a subsequent skilled forelimb task (Ploughman et al., 2007). Furthermore, exercise improved nose-poke accuracy during initial learning of the 3-CSRT task. However, as noted above, Lesion/Non-Exercise rats were able to achieve levels of accuracy equivalent to those of the controls and lesioned/exercised rats by days 14–16. The effect of exercise on cognitive improvement was most apparent during the rule shift phase (3-CSRT-R). Here, improvements in accuracy in lesion rats undergoing exercise were progressive, with improvement relative to Lesion/Non-Exercise rats maintained after 25 exercise sessions. Cognitive gains, however, were modest and significant only when exercise of all types was pooled. A greater effect of exercise in lesioned rats was seen on decreases in premature responses, a measure of behavioral impulsivity.

In the T-maze, the effect of exercise on cognitive improvement was

also most apparent during rule reversal (Win-Shift). However, unlike results in the 3-CSRT-R operant task, Lesion/Non-Exercise rats were able to match the performance of lesioned/exercised rats in the T-maze by day 12. The reason likely was that the Win-Shift T-maze task was easier to learn than the 3-CSRT-R operant task as judged by the fewer number of sessions to reach plateau levels in the T-maze. This suggests that exercise can accelerate learning, but for simpler cognitive challenges Lesion/Non-Exercise rats can 'catch up' to the performance of Lesion/Exercise rats. This is in contrast to more challenging tasks such as the 3-CSRT-R, where exercise provided a prolonged performance advantage that extended across 25 test days. Future studies can evaluate this interpretation at longer follow-up periods. Our 6-OHDA PD model assumed that dopaminergic lesions were complete at the 2-week timepoint when exercise was initiated (see section 2.5.1), with exercise-related benefits being understood in the context of neurorestoration. If lesion maturation, however, continued beyond this 2-week timepoint as some have proposed, it is possible that a component of the benefits may have been due to solely neuroprotective rather than neurorestorative mechanisms.

4.2. Changes in dopaminergic receptors and the synaptic marker PSD-95 with lesion and exercise

In these studies, we examined mRNA transcript in striatal tissues and our results showed that by 4 weeks, exercise led to increased transcript expression of both DAR-D1 and the DAR-D2-like receptors 3 and 4 in the dorsal CPu, particularly in the dmCPu, the site with the greatest degree of 6-OHDA-mediated DA-depletion. Dopamine receptors are expressed pre-synaptically within dopaminergic terminals and post-synaptically within medium spiny neurons in the CPu. Since we examined transcripts and most expression is within cell bodies and therefore post-synaptic. Changes in these receptors were concurrent with exercise-induced improvement in cognitive flexibility. In our study, cognitive flexibility was assessed through a reversal learning paradigm in which the learned association of a 'lights-on' cue and its sucrose reward was reversed when a newly presented 'lights-off' cue was associated with the same reward. Cognitive flexibility relies on the interactions of the D1- and D2-like receptors [DAR-D2, DAR-D3, and DAR-D4] (Floresco et al., 2006; Bestmann et al., 2015) at the level of the prefrontal cortex and the striatum. Although the D3-receptor is expressed at a lower level than the D2-receptor within the dorsal striatum, its role and association with the D2-receptor in reversal learning has been well established (Boulougouris et al., 2009; Groman et al., 2016; Clarkson et al., 2017). In addition to the DAR-D3, the DAR-D1 and DAR-D4 also play a role in reversal learning. For example, application of DAR-D1 agonists lead to impairment in the early phase of reversal learning (Izquierdo et al., 2006). The D4-receptor shares a similar modulatory effect on reversal learning to DAR-D1 as demonstrated by the application of a DAR-D4 antagonist and its improvement on reversal learning (Connolly and Gomez-Serrano, 2014). While the importance of the D1-receptor and the D4-receptor signaling in reverse learning has been demonstrated in the prefrontal cortex (Floresco et al., 2006), our study suggests a role of these dopamine receptors in cognitive flexibility also at the level of the dorsomedial striatum. Our results are consistent with recent reports showing that D1-receptors on medium spiny neurons in the dmCPu play an important role in reversal tasks (Wang et al., 2019).

Previous work in our lab using the MPTP model of dopamine depletion, has shown an exercise-induced increase of DAR-D2 in the dorsal CPu (Fisher et al., 2004) after six-weeks of intensive treadmill exercise. In contrast to our previous exercise studies, we found no significant increase in DAR-D2 in the dorsomedial CPu after 4-weeks of wheel running. Possible explanations for this discrepancy include differences in exercise duration, intensity, and choice of toxin and location of DA-depletion. Unlike the dorsal CPU, we found no exercise-induced effects on DA receptor transcript expression in the ventral CPu. In addition, we saw no lesion effect on dopamine receptor transcript expression within the dorsal or ventral striatum. These findings are consistent with the literature which have shown both significant and non-significant changes in the DAR-D1 and DAR-D2 after dopamine depletion, which may due to differences in lesioning paradigms [degree of lesioning, post-lesioning time point, species, toxin and mode of delivery] (Berger et al., 1991; Cadet et al., 1991).

In these studies, using qRT-PCR, we examined mRNA transcript expression in striatal tissues for PSD-95 and synaptophysin. PSD-95 is a major scaffolding protein in the postsynaptic densities of dendritic spines enriched in glutamatergic medium spiny neurons. We found that dopamine depletion in the dorsal CPu was associated with loss of PSD-95 mRNA transcripts and that exercise significantly increased PSD-95 expression in 6-OHDA lesioned rats. This finding likely reflects the increased expression of this transcript in striatal medium spiny neurons, the cells within the striatum that express this synaptic gene and proteins at post-synaptic contacts. This increase in PSD-95 is consistent with synaptogenesis and could be occurring in either or both glutamatergic and dopaminergic terminals at medium spiny neurons. Previous work in non-human primates and mice has demonstrated a significant reduction in dendritic spine density in the striatum of monkeys and mice following dopaminergic deafferentation (Villalba et al., 2009; Toy et al., 2014), with exercise eliciting a significant restoration of spine density, along with increases in synaptophysin and PSD-95 protein expression (Toy et al., 2014). We did not observe changes in synaptophysin mRNA transcripts in striatal tissues which differs in the patterns of change in protein we and others have reported. This may reflect the fact that this protein, expressed in pre-synaptic terminals is transcribes in cell bodies that reside outside of the striatum such as the cerebral cortex or thalamus. The transcriptional and translational mechanisms by which exercise may restore synaptophysin and PSD-95 expression in our model remains unknown. Prior work in the 6-OHDA model has suggested a role for Arc (activity-regulated cytoskeleton-associated protein) (Garcia et al., 2017), acting as a generalized transcription factor that can modulate dendritic spine formation and experience-dependent neuroplasticity (Peebles et al., 2010).

4.3. Translational aspects

Behavioral studies have shown that despite their slower learning-rates, PD subjects retain more or less intact motor learning (Nieuwboer et al., 2009). However, 'task-switching deficits' makes it difficult to translate learning acquired in a rehabilitation session to a real-world situation where responses must be adapted to context (Onla-or and Winstein, 2008). This inflexibility of thought and associated increased cognitive retention rates leads to errors of repetition when transferring between new categories of learning (Steinke and Kopp, 2020). We made a similar observation in our animal model. While the rate of acquisition of the 3-CSRT was delayed, lesioned rats were able to acquire a level of accuracy comparable to that of sham rats within 16 days of exercise (though not in the T-maze task). However, dramatic and persistent deficits were apparent in both the operant and T-maze tasks following the rule shift, such that lesioned rats never improved their performance much above chance levels, even after an extended period of exercise.

4.3.1. Effects of exercise on cognitive flexibility

Prior studies in naïve rodents have shown that exercise can facilitate reversal learning (Van der Borght et al., 2007; Snigdha et al., 2014; O'Leary et al., 2019). Our findings show that exercise-related improvements in cognitive flexibility can also be seen in the 6-OHDA striatal lesion model. Exercise is well known to elicit broad changes in neuroplasticity, including increases in neurogenesis (Ma et al., 2017). Increases in exercise-related neurogenesis have been reported to be associated with lower memory retention, while at the same time facilitating new learning, including reversal learning (Li et al., 2020). It has been proposed that such improved new learning may be the result of a decrease in proactive interference which usually occurs when

consolidated memories inhibit new learning (Epp et al., 2016). While in the current study, exercise effects on nose-poke accuracy of lesioned rats were modest during the reversal phase, greater effects were noted for premature responses, a measure of impulsivity and response inhibition. The decrease in premature responses is consistent with an improved ability of the exercised animal to acquire new learning, either because of a lower exercise-related recall of the prior rule set as previously proposed (Epp et al., 2016; Li et al., 2020), or possibly through facilitated suppression of the prior rule-based learning. The findings of diminished premature responses mirror a report in PD patients where 6 weeks of intermittent aerobic walking elicits significant improvement in cognitive inhibition (Flanker test) but not in set shifting (Wisconsin card sort, Trail Making tests) (Uc et al., 2014). Others have observed improvements in inhibitory aptitude (Stroop test) but not in cognitive flexibility (Trail making test) in PD patients following 3 months of intermittent aerobic cycling (Duchesne et al., 2015).

Improved cognitive flexibility may reflect underlying functional adaptation in cerebral regions of the cortico-striatal-thalamo-cortical and cortical-thalamo-hippocampal circuits (Wang et al., 2013), important in executive function and working memory. It has been suggested that motor rehabilitation programs for PD patients should include a relatively high cognitive demand, such that by engaging patients to practice task-switching, they might be able to overcome their context-dependency (Onla-or and Winstein, 2008; Petzinger et al., 2013). Surprisingly, we did not see a significant difference in cognitive outcomes in comparing different exercise modalities in lesioned rats (see Supplementary Fig. S2). This observation was valid even when exercise was undertaken for two different skill levels at comparable speeds and durations using the same exercise modality (complex versus smooth wheel running, Fig. S2). This was contrary to our expectation which, based on greater functional connectivity of the medial prefrontal-striatal circuit during acute walking in the skilled compared to the smooth wheel, had anticipated a differential cognitive effect of these different exercise modalities (Guo et al., 2017). Our findings differed from those reported in a recent meta-analysis in healthy human subjects, where there appears to be higher benefits after coordinative exercise compared to endurance, resistance and mixed exercise (Ludyga et al., 2020). In contrast, a recent systematic review of randomized controlled trials of physical exercise programs on cognitive function in PD reported that exercise-related improvements in global cognitive function, processing speed, sustained attention and mental flexibility (da Silva et al., 2018) showed the largest effect for intense treadmill exercise, not for skilled exercise (tango or cognitive exercise associated with motor exercise). However, a head-to-head comparison of different exercise modalities on cognitive function has to date not been done in PD patients. In our study, though behavioral outcomes of nose poke accuracy closely tracked across different exercise modalities, our study was insufficiently powered to detect small differences. Furthermore, we did not explore a full range of exercise durations and intensities, variables that in prior studies have shown differential efficacy across different exercise modalities (Coetsee and Terblanche, 2017; Ludyga et al., 2020), though this itself remains controversial (Sanders et al., 2020; Brown et al., 2021). Exercise was maintained for up to 12 weeks during the acquisition and testing phases of our cognitive testing. Future studies may wish to explore the effects of a broader range of exercise intensities and durations across different exercise modalities (da Costa Daniele et al., 2020).

5. Conclusion

In summary, our data adds to the expanding research reports showing the beneficial cognitive effects of physical exercise. Our prospective study demonstrates that following dopaminergic deafferentation, moderate exercise is able to provide improvements in cognitive flexibility and inhibitory aptitude, while eliciting increased expression of Drd1, Drd3, Drd4, synaptophysin, and PSD-95 in the associative and sensorimotor dorsal regions of the striatum.

Funding sources

Don Roberto Gonzalez Family Foundation (GP); Parkinson's Foundation (GP); US Army Medical Research and Materiel Command Parkinson Research Program (USAMRMC) Congressionally Directed Medical Research Programs (CDMRP), Grant/Award Numbers: W81XWH18-0665 (GMP), W81XWH18-00443 (MWJ), W81XWH18-1-0666 (DPH).

Credit authorship contribution statement

Wang Zhuo: contributed to the conception and design of the study, contributed to data acquisition, was responsible for data analysis, were responsible for statistical analyses. **Adam J. Lundquist:** contributed to the conception and design of the study, contributed to data acquisition; were responsible for data analysis, was responsible for statistical analyses. **Erin K. Donahue:** contributed to the conception and design of the study, contributed to data acquisition; was responsible for data analysis. **Yumei Guo:** contributed to the conception and design of the study, contributed to data acquisition, was responsible for data analysis, were responsible for writing and editing the manuscript. **Derek Phillips:** contributed to data acquisition. **Giselle M. Petzinger:** contributed to the conception and design of the study, was responsible for data analysis, were responsible for writing and editing the manuscript, were responsible for acquisition of funding support. **Michael W. Jakowec:** contributed to the conception and design of the study. **Daniel P. Holschneider:** contributed to the conception and design of the study, contributed to data acquisition, was responsible for data analysis, was responsible for writing and editing the manuscript, was responsible for acquisition of funding support.

Declaration of competing interest

The authors declare the following financial interests/personal relationships which may be considered as potential competing interests: Daniel Holschneider, Giselle Petzinger, Michael Jakowec reports financial support was provided by Department of Defense and by the US Army Medical Research and Materiel Command Parkinson Research Program. Giselle Petzinger reports financial support was provided by Don Roberto Gonzalez Family Foundation.

Acknowledgements

The authors would like to thank the contributions of friends of the PD Research Program at USC. Special thanks to lab members for their helpful discussions. Thank you to Dan Haase, Ryan Wang, Susan Kishi, Tyler Gallagher, and Ilse Flores who participated in the exercising of animals.

Appendix A. Supplementary data

Supplementary data to this article can be found online at https://doi.org/10.1016/j.crneur.2022.100039.

References

Alberts, J.L., Linder, S.M., Penko, A.L., Lowe, M.J., Phillips, M., 2011. It is not about the bike, it is about the pedaling: forced exercise and Parkinson's disease. Exerc. Sport Sci. Rev. 39 (4), 177–186.

Apostolova, I., Lange, C., Frings, L., Klutmann, S., Meyer, P.T., Buchert, R., 2020. Nigrostriatal degeneration in the cognitive part of the striatum in Parkinson disease is associated with frontomedial hypometabolism. Clin. Nucl. Med. 45 (2), 95–99.

Asinof, S.K., Paine, T.A., 2014. The 5-choice serial reaction time task: a task of attention and impulse control for rodents. JoVE 90, e51574.

Baker, P.M., Ragozzino, M.E., 2014. Contralateral disconnection of the rat prelimbic cortex and dorsomedial striatum impairs cue-guided behavioral switching. Learn. Mem. 21 (8), 368–379.

Ben, V., Blin, O., Bruguerolle, B., 1999. Time-dependent striatal dopamine depletion after injection of 6-hydroxydopamine in the rat. Comparison of single bilateral and double bilateral lesions. J. Pharm. Pharmacol. 51 (12), 1405–1408.
Berger, K., Przedborski, S., Cadet, J.L., 1991. Retrograde degeneration of nigrostriatal neurons induced by intrastriatal 6-hydroxydopamine injection in rats. Brain Res. Bull. 26 (2), 301–307.
Bestmann, S., Ruge, D., Rothwell, J., Galea, J.M., 2015. The role of dopamine in motor flexibility. J. Cognit. Neurosci. 27 (2), 365–376.
Blandini, F., Levandis, G., Bazzini, E., Nappi, G., Armentero, M.T., 2007. Time-course of nigrostriatal damage, basal ganglia metabolic changes and behavioural alterations following intrastriatal injection of 6-hydroxydopamine in the rat: new clues from an old model. Eur. J. Neurosci. 25 (2), 397–405.
Boulougouris, V., Castañé, A., Robbins, T.W., 2009. Dopamine D2/D3 receptor agonist quinpirole impairs spatial reversal learning in rats: investigation of D3 receptor involvement in persistent behavior. Psychopharmacology (Berl) 202 (4), 611–620.
Brown, B.M., Frost, N., Rainey-Smith, S.R., Doecke, J., Markovic, S., Gordon, N., Weinborn, M., Sohrabi, H.R., Laws, S.M., Martins, R.N., Erickson, K.I., Peiffer, J.J., 2021. High-intensity exercise and cognitive function in cognitively normal older adults: a pilot randomised clinical trial. Alzheimer's Res. Ther. 13 (1), 33.
Brown, H.D., Baker, P.M., Ragozzino, M.E., 2010. The parafascicular thalamic nucleus concomitantly influences behavioral flexibility and dorsomedial striatal acetylcholine output in rats. J. Neurosci. 30 (43), 14390–14398.
Burn, D., Weintraub, D., Ravina, B., Litvan, I., 2014. Cognition in movement disorders: where can we hope to be in ten years? Mov. Disord. 29 (5), 704–711.
Cadet, J.L., Last, R., Kostic, V., Przedborski, S., Jackson-Lewis, V., 1991. Long-term behavioral and biochemical effects of 6-hydroxydopamine injections in rat caudate-putamen. Brain Res. Bull. 26 (5), 707–713.
Chang, J.W., Wachtel, S.R., Young, D., Kang, U.J., 1999. Biochemical and anatomical characterization of forepaw adjusting steps in rat models of Parkinson's disease: studies on medial forebrain bundle and striatal lesions. Neuroscience 88 (2), 617–628.
Chudasama, Y., Bussey, T.J., Muir, J.L., 2001. Effects of selective thalamic and prelimbic cortex lesions on two types of visual discrimination and reversal learning. Eur. J. Neurosci. 14 (6), 1009–1020.
Clarkson, R.L., Liptak, A.T., Gee, S.M., Sohal, V.S., Bender, K.J., 2017. D3 receptors regulate excitability in a unique class of prefrontal pyramidal cells. J. Neurosci. 37 (24), 5846–5860.
Coetsee, C., Terblanche, E., 2017. The effect of three different exercise training modalities on cognitive and physical function in a healthy older population. Eur. Rev. Aging Phys. Act. 14, 13.
Connolly, N.P., Gomez-Serrano, M., 2014. D4 dopamine receptor-specific antagonist improves reversal learning impairment in amphetamine-treated male rats. Exp. Clin. Psychopharmacol 22 (6), 557–564.
Cools, R., 2006. Dopaminergic modulation of cognitive function-implications for L-DOPA treatment in Parkinson's disease. Neurosci. Biobehav. Rev. 30 (1), 1–23.
da Costa Daniele, T.M., de Bruin, P.F.C., de Matos, R.S., de Bruin, G.S., Maia Chaves, C.J., de Bruin, V.M.S., 2020. Exercise effects on brain and behavior in healthy mice, Alzheimer's disease and Parkinson's disease model-A systematic review and meta-analysis. Behav. Brain Res. 383, 112488.
da Silva, F.C., Iop, R.D.R., de Oliveira, L.C., Boll, A.M., de Alvarenga, J.G.S., Gutierres Filho, P.J.B., de Melo, L., Xavier, A.J., da Silva, R., 2018. Effects of physical exercise programs on cognitive function in Parkinson's disease patients: a systematic review of randomized controlled trials of the last 10 years. PLoS One 13 (2), e0193113.
Deacon, R.M., Rawlins, J.N., 2006. T-maze alternation in the rodent. Nat. Protoc. 1 (1), 7–12.
Dirnberger, G., Jahanshahi, M., 2013. Executive dysfunction in Parkinson's disease: a review. J. Neuropsychol. 7 (2), 193–224.
Dorsey, E.R., George, B.P., Leff, B., Willis, A.W., 2013. The coming crisis: obtaining care for the growing burden of neurodegenerative conditions. Neurology 80 (21), 1989–1996.
Duchesne, C., Lungu, O., Nadeau, A., Robillard, M.E., Bore, A., Bobeuf, F., Lafontaine, A. L., Gheysen, F., Bherer, L., Doyon, J., 2015. Enhancing both motor and cognitive functioning in Parkinson's disease: aerobic exercise as a rehabilitative intervention. Brain Cognit. 99, 68–77.
Epp, J.R., Silva Mera, R., Köhler, S., Josselyn, S.A., Frankland, P.W., 2016. Neurogenesis-mediated forgetting minimizes proactive interference. Nat. Commun. 7, 10838.
Fisher, B.E., Petzinger, G.M., Nixon, K., Hogg, E., Bremmer, S., Meshul, C.K., Jakowec, M. W., 2004. Exercise-induced behavioral recovery and neuroplasticity in the 1-methyl-4-phenyl-1,2,3,6-tetrahydropyridine-lesioned mouse basal ganglia. J. Neurosci. Res. 77 (3), 378–390.
Floresco, S.B., Magyar, O., Ghods-Sharifi, S., Vexelman, C., Tse, M.T., 2006. Multiple dopamine receptor subtypes in the medial prefrontal cortex of the rat regulate set-shifting. Neuropsychopharmacology 31 (2), 297–309.
Garcia, P.C., Real, C.C., Britto, L.R., 2017. The impact of short and long-term exercise on the expression of arc and AMPARs during evolution of the 6-hydroxy-dopamine animal model of Parkinson's disease. J. Mol. Neurosci. 61 (4), 542–552.
Groman, S.M., Smith, N.J., Petrullli, J.R., Massi, B., Chen, L., Ropchan, J., Huang, Y., Lee, D., Morris, E.D., Taylor, J.R., 2016. Dopamine D3 receptor availability is associated with inflexible decision making. J. Neurosci. 36 (25), 6732–6741.
Grospe, G.M., Baker, P.M., Ragozzino, M.E., 2018. Cognitive flexibility deficits following 6-OHDA lesions of the rat dorsomedial striatum. Neuroscience 374, 80–90.
Guo, Y., Wang, Z., Prathap, S., Holschneider, D.P., 2017. Recruitment of prefrontal-striatal circuit in response to skilled motor challenge. Neuroreport 28 (18), 1187–1194.
Hauber, W., Schmidt, W.J., 1994. Differential effects of lesions of the dorsomedial and dorsolateral caudate-putamen on reaction time performance in rats. Behav. Brain Res. 60 (2), 211–215.
Hirano, S., 2021. Clinical implications for dopaminergic and functional neuroimage research in cognitive symptoms of Parkinson's disease. Mol. Med. 27 (1), 40.
Intzandt, B., Beck, E.N., Silveira, C.R.A., 2018. The effects of exercise on cognition and gait in Parkinson's disease: a scoping review. Neurosci. Biobehav. Rev. 95, 136–169.
Izquierdo, A., Wiedholz, L.M., Millstein, R.A., Yang, R.J., Bussey, T.J., Saksida, L.M., Holmes, A., 2006. Genetic and dopaminergic modulation of reversal learning in a touchscreen-based operant procedure for mice. Behav. Brain Res. 171 (2), 181–188.
Kim, H., Oh, M., Oh, J.S., Moon, H., Chung, S.J., Lee, C.S., Kim, J.S., 2019. Association of striatal dopaminergic neuronal integrity with cognitive dysfunction and cerebral cortical metabolism in Parkinson's disease with mild cognitive impairment. Nucl. Med. Commun. 40 (12), 1216–1223.
Kintz, N., Petzinger, G.M., Akopian, G., Ptasnik, S., Williams, C., Jakowec, M.W., Walsh, J.P., 2013. Exercise modifies alpha-amino-3-hydroxy-5-methyl-4-isoxazolepropionic acid receptor expression in striatopallidal neurons in the 1-methyl-4-phenyl-1,2,3,6-tetrahydropyridine-lesioned mouse. J. Neurosci. Res. 91 (11), 1492–1507.
Kowal, S.L., Dall, T.M., Chakrabarti, R., Storm, M.V., Jain, A., 2013. The current and projected economic burden of Parkinson's disease in the United States. Mov. Disord. 28 (3), 311–318.
Li, C., Li, R., Zhou, C., 2020. Memory traces diminished by exercise affect new learning as proactive facilitation. Front. Neurosci. 14, 189.
Livak, K.J., Schmittgen, T.D., 2001. Analysis of relative gene expression data using real-time quantitative PCR and the 2(-Delta Delta C(T)) Method. Methods 25 (4), 402–408.
Ludyga, S., Gerber, M., Puhse, U., Looser, V.N., Kamijo, K., 2020. Systematic review and meta-analysis investigating moderators of long-term effects of exercise on cognition in healthy individuals. Nat. Human Behav.
Lundquist, A.J., Gallagher, T.J., Petzinger, G.M., Jakowec, M.W., 2021. Exogenous l-lactate promotes astrocyte plasticity but is not sufficient for enhancing striatal synaptogenesis or motor behavior in mice. J. Neurosci. Res. 99 (5), 1433–1447.
Lundquist, A.J., Parizher, J., Petzinger, G.M., Jakowec, M.W., 2019. Exercise induces region-specific remodeling of astrocyte morphology and reactive astrocyte gene expression patterns in male mice. J. Neurosci. Res. 97 (9), 1081–1094.
Ma, C.L., Ma, X.T., Wang, J.J., Liu, H., Chen, Y.F., Yang, Y., 2017. Physical exercise induces hippocampal neurogenesis and prevents cognitive decline. Behav. Brain Res. 317, 332–339.
Macdonald, P.A., Monchi, O., 2011. Differential effects of dopaminergic therapies on dorsal and ventral striatum in Parkinson's disease: implications for cognitive function. Parkinsons Dis 2011, 572743.
Mayer, G.S., Shoup, R.E., 1983. Simultaneous multiple electrode liquid chromatographic-electrochemical assay for catecholamines, indole-amines and metabolites in brain tissue. J. Chromatogr. 255, 533–544.
Nieuwboer, A., Rochester, L., Muncks, L., Swinnen, S.P., 2009. Motor learning in Parkinson's disease: limitations and potential for rehabilitation. Park. Relat. Disord. 15 (Suppl. 3), S53–S58.
O'Leary, J.D., Hoban, A.E., Murphy, A., O'Leary, O.F., Cryan, J.F., Nolan, Y.M., 2019. Differential effects of adolescent and adult-initiated exercise on cognition and hippocampal neurogenesis. Hippocampus 29 (4), 352–365.
O'Neill, M., Brown, V.J., 2007. The effect of striatal dopamine depletion and the adenosine A2A antagonist KW-6002 on reversal learning in rats. Neurobiol. Learn. Mem. 88 (1), 75–81.
Onla-or, S., Winstein, C.J., 2008. Determining the optimal challenge point for motor skill learning in adults with moderately severe Parkinson's disease. Neurorehabilitation Neural Repair 22 (4), 385–395.
Parker, K.L., Lamichhane, D., Caetano, M.S., Narayanan, N.S., 2013. Executive dysfunction in Parkinson's disease and timing deficits. Front. Integr. Neurosci. 7, 75.
Peebles, C.L., Yoo, J., Thwin, M.T., Palop, J.J., Noebels, J.L., Finkbeiner, S., 2010. Arc regulates spine morphology and maintains network stability in vivo. Proc. Natl. Acad. Sci. U. S. A. 107 (42), 18173–18178.
Petzinger, G.M., Fisher, B.E., McEwen, S., Beeler, J.A., Walsh, J.P., Jakowec, M.W., 2013. Exercise-enhanced neuroplasticity targeting motor and cognitive circuitry in Parkinson's disease. Lancet Neurol. 12 (7), 716–726.
Ploughman, M., Attwood, Z., White, N., Dore, J.J., Corbett, D., 2007. Endurance exercise facilitates relearning of forelimb motor skill after focal ischemia. Eur. J. Neurosci. 25 (11), 3453–3460.
Robbins, T.W., Cools, R., 2014. Cognitive deficits in Parkinson's disease: a cognitive neuroscience perspective. Mov. Disord. 29 (5), 597–607.
Roberts, D.C., Zis, A.P., Fibiger, H.C., 1975. Ascending catecholamine pathways and amphetamine-induced locomotor activity: importance of dopamine and apparent non-involvement of norepinephrine. Brain Res. 93 (3), 441–454.
Sala-Bayo, J., Fiddian, L., Nilsson, S.R.O., Hervig, M.E., McKenzie, C., Mareschi, A., Boulos, M., Zhukovsky, P., Nicholson, J., Dalley, J.W., Alsiö, J., Robbins, T.W., 2020. Dorsal and ventral striatal dopamine D1 and D2 receptors differentially modulate distinct phases of serial visual reversal learning. Neuropsychopharmacology 45 (5), 736–744.
Salame, S., Garcia, P.C., Real, C.C., Borborema, J., Mota-Ortiz, S.R., Britto, L.R., Pires, R. S., 2016. Distinct neuroplasticity processes are induced by different periods of acrobatic exercise training. Behav. Brain Res. 308, 64–74.
Sanders, L.M.J., Hortobágyi, T., Karssemeijer, E.G.A., Van der Zee, E.A., Scherder, E.J.A., van Heuvelen, M.J.G., 2020. Effects of low- and high-intensity physical exercise on physical and cognitive function in older persons with dementia: a randomized controlled trial. Alzheimer's Res. Ther. 12 (1), 28.

Sauer, H., Oertel, W.H., 1994. Progressive degeneration of nigrostriatal dopamine neurons following intrastriatal terminal lesions with 6-hydroxydopamine: a combined retrograde tracing and immunocytochemical study in the rat. Neuroscience 59 (2), 401–415.
Schootemeijer, S., van der Kolk, N.M., Bloem, B.R., de Vries, N.M., 2020. Current perspectives on aerobic exercise in people with Parkinson's disease. Neurotherapeutics 17 (4), 1418–1433.
Snigdha, S., de Rivera, C., Milgram, N.W., Cotman, C.W., 2014. Exercise enhances memory consolidation in the aging brain. Front. Aging Neurosci. 6, 3.
Stefanko, D.P., Shah, V.D., Yamasaki, W.K., Petzinger, G.M., Jakowec, M.W., 2017. Treadmill exercise delays the onset of non-motor behaviors and striatal pathology in the CAG140 knock-in mouse model of Huntington's disease. Neurobiol. Dis. 105, 15–32.
Steinke, A., Kopp, B., 2020. Toward a computational neuropsychology of cognitive flexibility. Brain Sci. 10 (12).
Stögbauer, J., Rosar, F., Dillmann, U., Faßbender, K., Ezziddin, S., Spiegel, J., 2020. Striatal dopamine transporters and cognitive function in Parkinson's disease. Acta Neurol. Scand. 142 (4), 385–391.
Tait, D.S., Phillips, J.M., Blackwell, A.D., Brown, V.J., 2017. Effects of lesions of the subthalamic nucleus/zona incerta area and dorsomedial striatum on attentional set-shifting in the rat. Neuroscience 345, 287–296.
Thoma, P., Koch, B., Heyder, K., Schwarz, M., Daum, I., 2008. Subcortical contributions to multitasking and response inhibition. Behav. Brain Res. 194 (2), 214–222.
Toy, W.A., Petzinger, G.M., Leyshon, B.J., Akopian, G.K., Walsh, J.P., Hoffman, M.V., Vučković, M.G., Jakowec, M.W., 2014. Treadmill exercise reverses dendritic spine loss in direct and indirect striatal medium spiny neurons in the 1-methyl-4-phenyl-1,2,3,6-tetrahydropyridine (MPTP) mouse model of Parkinson's disease. Neurobiol. Dis. 63, 201–209.
Uc, E.Y., Doerschug, K.C., Magnotta, V., Dawson, J.D., Thomsen, T.R., Kline, J.N., Rizzo, M., Newman, S.R., Mehta, S., Grabowski, T.J., Bruss, J., Blanchette, D.R., Anderson, S.W., Voss, M.W., Kramer, A.F., Darling, W.G., 2014. Phase I/II randomized trial of aerobic exercise in Parkinson disease in a community setting. Neurology 83 (5), 413–425.
Van der Borght, K., Havekes, R., Bos, T., Eggen, B.J., Van der Zee, E.A., 2007. Exercise improves memory acquisition and retrieval in the Y-maze task: relationship with hippocampal neurogenesis. Behav. Neurosci. 121 (2), 324–334.
van Schouwenburg, M., Aarts, E., Cools, R., 2010. Dopaminergic modulation of cognitive control: distinct roles for the prefrontal cortex and the basal ganglia. Curr. Pharmaceut. Des. 16 (18), 2026–2032.
Villalba, R.M., Lee, H., Smith, Y., 2009. Dopaminergic denervation and spine loss in the striatum of MPTP-treated monkeys. Exp. Neurol. 215 (2), 220–227.
Voorn, P., Vanderschuren, L.J., Groenewegen, H.J., Robbins, T.W., Pennartz, C.M., 2004. Putting a spin on the dorsal-ventral divide of the striatum. Trends Neurosci. 27 (8), 468–474.
Wang, X., Qiao, Y., Dai, Z., Sui, N., Shen, F., Zhang, J., Liang, J., 2019. Medium spiny neurons of the anterior dorsomedial striatum mediate reversal learning in a cell-type-dependent manner. Brain Struct. Funct. 224 (1), 419–434.
Wang, Z., Flores, I., Donahue, E.K., Lundquist, A.J., Guo, Y., Petzinger, G.M., Jakowec, M.W., Holschneider, D.P., 2020. Cognitive flexibility deficits in rats with dorsomedial striatal 6-hydroxydopamine lesions tested using a three-choice serial reaction time task with reversal learning. Neuroreport 31 (15), 1055–1064.
Wang, Z., Guo, Y., Myers, K.G., Heintz, R., Holschneider, D.P., 2015a. Recruitment of the prefrontal cortex and cerebellum in Parkinsonian rats following skilled aerobic exercise. Neurobiol. Dis. 77, 71–87.
Wang, Z., Guo, Y., Myers, K.G., Heintz, R., Peng, Y.H., Maarek, J.M., Holschneider, D.P., 2015b. Exercise alters resting-state functional connectivity of motor circuits in parkinsonian rats. Neurobiol. Aging 36 (1), 536–544.
Wang, Z., Myers, K.G., Guo, Y., Ocampo, M.A., Pang, R.D., Jakowec, M.W., Holschneider, D.P., 2013. Functional reorganization of motor and limbic circuits after exercise training in a rat model of bilateral parkinsonism. PLoS One 8 (11), e80058.
Yehene, E., Meiran, N., Soroker, N., 2008. Basal ganglia play a unique role in task switching within the frontal-subcortical circuits: evidence from patients with focal lesions. J. Cognit. Neurosci. 20 (6), 1079–1093.
Yuan, H., Sarre, S., Ebinger, G., Michotte, Y., 2005. Histological, behavioural and neurochemical evaluation of medial forebrain bundle and striatal 6-OHDA lesions as rat models of Parkinson's disease. J. Neurosci. Methods 144 (1), 35–45.